**Dissertation**

# Artificial bone graft substitutes for the treatment of benign and low-grade malignant bone tumours: clinical and radiological experience with Cerasorb


submitted by

**Dr. med. univ. Ulrike Wittig**


for the Academic Degree of

**Doctor of Medical Science (Dr. scient. med.)**

at the


**Medical University of Graz**

**Department of Orthopaedics and Trauma**


under the Supervision of

**Res. Prof. Priv. Doz. DDr. Susanne Scheipl**

2024

*Für Mama und Papa*

# STATUTORY DECLARATION

*I hereby declare that this is my original work and that I have fully acknowledged by name all of those individuals and organizations that have contributed to the research for this thesis. Due acknowledgement has been made in the text to all other material used. Throughout this thesis and in all related publications, I followed the "Standards of Good Scientific Practice and Ombuds Committee at the Medical University of Graz".*

*Krems, 23.07.2024* *Dr. med. univ. Ulrike Wittig eh*

# DISCLOSURE

Parts of this thesis have been published in the following article:

**Wittig US**, Friesenbichler J, Liegl-Atzwanger B, Igrec J, Andreou D, Leithner A, Scheipl S. Artificial bone graft substitutes for curettage of benign and low-grade malignant bone tumors: clinical and radiological experience with Cerasorb (1).

**Contributing authors (listed in alphabetical order)**

**Andreou Dimosthenis, Ass. Prof. Priv. Doz. Dr.**
Department of Orthopaedics and Trauma, Medical University of Graz

**Friesenbichler Jörg, Priv. Doz. DDr.**
Department of Orthopaedics and Trauma, Medical University of Graz

**Igrec Jasminka, DDr.**
Division of General Radiology, Department of Radiology, Medical University of Graz

**Leithner Andreas, Univ. Prof. Dr.**
Department of Orthopaedics and Trauma, Medical University of Graz

**Liegl-Atzwanger Bernadette, Univ. Prof. Priv. Doz. Dr.**
Diagnostic and Research Institute of Pathology, Medical University of Graz

**Scheipl Susanne, Res. Prof. Priv. Doz. DDr.**
Department of Orthopaedics and Trauma, Medical University of Graz

**All co-authors have explicitly agreed to use their data in this thesis.**
Department of Orthopaedics and Trauma, Medical University of Graz

# ACKNOWLEDGEMENTS

First of all, I would like to thank the three supervisors of this thesis, ***Res. Prof. Priv. Doz. DDr. Susanne Scheipl***, ***Ass. Prof. Priv. Doz. Dr. Dimosthenis Andreou*** and ***Univ. Prof. Priv. Doz. Dr. Bernadette Liegl-Atzwanger*** for their great support during this thesis. Special thanks go to *Res. Prof. Priv. Doz. DDr. Susanne Scheipl* for her continuous support during my dissertation, but also for her tireless support in our clinical work. Furthermore, I would like to thank *Univ. Prof. Dr. Andreas Leithner* for always providing support and a helping hand during this project, but also many other scientific projects, as well as for always being supportive regarding clinical work and providing advice for any kinds of issues. Many thanks also apply to *Univ. Prof. Priv. Doz. Dr. Bernadette Liegl-Atzwanger* as well as to her team, including *Res. Prof. Priv. Doz. DDr. Iva Brcic* and *Dr. Christian Viertler* at the Diagnostic and Research Institute of Pathology, Medical University of Graz, for their support.

I am also indebted to *Priv. Doz. DDr. Jörg Friesenbichler*, who spent a lot of time and effort on recruiting the underlying patient collective and on data collection. I used to start this thesis under his supervision, that he then transmitted to Res. Prof. Priv. Doz. DDr. Susanne Scheipl at the end of 2021, as he withdrew from the Medical University of Graz. Thank you for making this work possible and sharing your great knowledge on this topic.

Cordial thanks go to *DDr. Jasminka Igrec* from the Department of Radiology at the Medical University of Graz for playing a genuine role in the realization of this thesis by sharing her in-depth knowledge regarding oncological radiology, and for her precise description of the characteristic signs of different tumour entities on x-ray, CT and MR imaging.

Furthermore, I would like to thank the orthopaedic surgeons at the Department of Orthopaedics and Trauma at the Medical University of Graz who have performed the relevant surgical procedures and therefore offered the data underlying this thesis.

Moreover, many thanks go to my dear friends, for always being supportive and lending me an ear when I was stuck.

At last, yet most of all, I would like to thank my parents for providing their loving support and for always encouraging me to never give up. Without you and the supporting environment you offered me ever since, I would never have achieved all this, and I am extremely grateful for the values and life philosophy you taught me to live by. Thank you for always being there and lending me a helping hand – and for constantly reminding me to stay grounded and open-minded and never to lose sight of the bigger picture.

This thesis was written as part of the doctoral school "Musculoskeletal System and Oral Health" at the Medical University of Graz. No sources of funding were used. Permission to reuse tables and figures in this thesis was obtained from the respective copyright holders.

# TABLE OF CONTENTS

# LIST OF ABBREVIATIONS

| *ABBREVIATION* | *DESCRIPTION* |
|---|---|
| **ABGS** | Artificial bone graft substitute |
| **ABM** | Autologous bone marrow |
| **ACT** | Atypical cartilaginous tumour |
| **BRAF** | V-raf murine sarcoma viral oncogene homolog B |
| **CS** | Calcium sulfate |
| **CS1** | Grade 1 chondrosarcoma |
| **CT** | Computer tomography |
| **DBM** | Demineralized bone marrow |
| **EC** | Enchondroma |
| **FD** | Fibrous dysplasia |
| **FDG PET** | Fluorodeoxyglucose positron emission tomography |
| **GCT** | Giant cell tumour |
| **GNAS** | Guanine nucleotide binding protein, alpha stimulating activity polypeptide |
| **ICBG** | Iliac crest bone graft |
| **IDH** | Isocitrate dehydrogenase |
| **IGC** | Intraosseous ganglion cyst |
| **IL-6** | Interleukin-6 |
| **LC** | Langerhans cell |
| **LCH** | Langerhans cell histiocytosis |
| **MAPK** | Mitogen-activated protein kinase |
| **MRI** | Magnetic resonance imaging |
| **PMMA** | Polymethylmethacryclate |
| **RANKL** | Receptor activator of nuclear factor kappa beta ligand |
| **RDD** | Rosai Dorfman disease |
| **TCP** | Tricalciumphosphate |
| **WHO** | World Health Organization |

# LIST OF FIGURES

**Figure 13:** X-ray of a case of Rosai-Dorfman disease (RDD) of the right acetabular region.

**Figure 14:** Histopathologic image of a case of RDD.

**Figure 15:** A graphical schema of bone tumour localizations. The x-axis shows the respective tumour localization. The y-axis shows the absolute number of tumours, with the kind permission of Springer Nature, according to figure 1 in "Artificial bone graft substitutes for curettage of benign and low-grade malignant bone tumors: clinical and radiological experience with Cerasorb", Indian Journal of Orthopaedics, published online on June 22nd, 2023.

**Figure 16:** A graphical comparison of analyzed tumour entities. The x-axis shows the respective tumour entity. The y-axis shows the absolute number of tumours, with the kind permission of Springer Nature, according to figure 2 in "Artificial bone graft substitutes for curettage of benign and low-grade malignant bone tumors: clinical and radiological experience with Cerasorb", Indian Journal of Orthopaedics, published online on June 22nd, 2023.

**Figures 17a, 17b and 17c: (17a)** Postoperative x-ray of a 21-year-old male patient one day after curettage and filling of an enchondroma in the left humeral diaphysis, and **(17b)** after a pathological fracture within the curetted area that occurred after minor trauma five weeks after primary surgery. **(17c)** Follow-up radiograph following plate osteosynthesis in order to stabilize the pathological fracture five weeks after primary surgery, with the kind permission of Springer Nature, according to figures 5a, 5b and 5c in "Artificial bone graft substitutes for curettage of benign and low-grade malignant bone tumors: clinical and radiological experience with Cerasorb", Indian Journal of Orthopaedics, published online on June 22nd, 2023.

**Figures 18a, 18b and 18c: (18a)** Preoperative and **(18b)** one-day postoperative X-rays of a 15-year-old male patient after curettage and filling of a chondroblastoma in the left proximal humerus. **(18c)** An X-ray twelve months after surgery shows complete

osseous integration of the ABGS, with the kind permission of Springer Nature, according to figures 3a and 3b in "Artificial bone graft substitutes for curettage of benign and low-grade malignant bone tumors: clinical and radiological experience with Cerasorb", Indian Journal of Orthopaedics, published online on June 22nd, 2023.

**Figures 19a, 19b and 19c: (19a)** Preoperative and **(19b)** one-day postoperative X-rays of a 24-year-old female patient after curettage and filling as well as protective plate osteosynthesis of LCH in the left femur. **(19c)** An X-ray twelve months after surgery shows complete osseous integration of the ABGS.

**Figures 20a, 20b and 20c: (20a)** Preoperative and **(20b)** one-day postoperative X-rays of a 50-year-old female patient suffering from an enchondroma of the left proximal humerus. **(20c)** An X-ray 30 months after surgery shows partial osseous integration of the ABGS.

**Figures 21a, 21b and 21c: (21a)** Preoperative and **(21b)** postoperative x-ray one day after surgery of a 40-year-old female patient after curettage and filling of an enchondroma in the left distal femur with additional protective plate osteosynthesis. **(21c)** Follow-up radiograph twelve months after index surgery showing only partial osseous integration of the ABGS, with the kind permission of Springer Nature, according to figures 4a and 4b in "Artificial bone graft substitutes for curettage of benign and low-grade malignant bone tumors: clinical and radiological experience with Cerasorb", Indian Journal of Orthopaedics, published online on June 22nd, 2023.

# LIST OF TABLES

# ZUSAMMENFASSUNG

**Hintergrund/Ziel.** Gutartige und niedriggradig maligne Knochentumore werden üblicherweise mittels intraläsionaler Curettage behandelt. In weiterer Folge kann der knöcherne Hohlraum leer belassen oder mit autologen oder allogenen Knochenersatzmaterialien aufgefüllt werden. Der Einsatz künstlicher Knochenersatzstoffe im Anschluss an die Curettage von Knochentumoren erfreut sich steigender Beliebtheit, da diese im Gegensatz zu autologen Knochenersatzstoffen keine Morbidität an der Entnahmestelle mit sich bringen. Zahlreiche künstliche Knochenersatzstoffe sind verfügbar, darunter demineralisierte Knochenmatrix, Knochenersatzexpander und knochenmorphogenetische Proteine.

Das Ziel der vorliegenden retrospektiven Analyse lag darin, das ossäre Integrationsprofil des künstlichen Knochenersatzstoffs Cerasorb® (Curasan-AG, Kleinostheim, Deutschland), einem Beta-Tricalcium-Phosphat in Granulat-Form, zu evaluieren, und potenzielle damit assoziierte Komplikationen aufzuzeigen.

**Material & Methoden.** Insgesamt 55 Patient*innen, welche an gutartigen und niedriggradig malignen Knochentumoren erkrankt waren, wurden zwischen 2018 und 2021 an der Universitätsklinik für Orthopädie und Traumatologie der Medizinischen Universität Graz mittels Curettage und Auffüllung des knöchernen Hohlraums mit dem künstlichen Knochenersatzstoff Cerasorb® behandelt. Klinische Folgeuntersuchungen inklusive Röntgenaufnahmen in zwei Ebenen erfolgten sechs Wochen, drei Monate, sechs Monate und zwölf Monate postoperativ. Sämtliche Operationen wurden von erfahrenen Tumororthopäd*innen durchgeführt. Die Parameter, welche im Rahmen dieser Studie erhoben wurden, beinhalteten die Zeit bis zur knöchernen Konsolidierung, Lokalrezidiv-Raten und Komplikationen. Chirurgische Komplikationen wurden anhand des Klassifikationssystems von Goslings und Gouma analysiert. Die ossäre Integration wurde entsprechend des modizierten Neer-Scores erhoben.

**Ergebnisse.** 43 Patient*innen standen für die Nachkontrollen und die definitive Auswertung im Rahmen dieser Studie zur Verfügung. 12 Patient*innen erschienen nicht zur geplanten Kontrolluntersuchung und konnten weder telefonisch noch postalisch erreicht beziehungsweise überzeugt werden, weitere Kontrollen an der

Universitätsklinik für Orthopädie und Traumatologie der Medizinischen Universität Graz durchführen zu lassen, sodass ihre Ergebnisse im Rahmen der Studie nicht evaluiert werden konnten. Die Knochentumoren, an denen die in die Studie eingeschlossenen Patient*innen litten, umfassten Enchondrome (n=14), atypische cartilaginäre Tumoren (n=17), simple Knochenzysten (n=4), Chondroblastome (n=4), sowie je einen Fall einer fibrösen Dysplasie, eines intraossären Ganglions, einer Langerhanszell-Histiozytose und einer Rosai-Dorfman Erkrankung. Das mittlere Alter zum Zeitpunkt der Operation betrug 42 Jahre (Range 15-70 Jahre). 21 (48.9%) Patient*innen waren männlich, während 22 (51.2%) weiblich waren. Nach einem mittleren Follow-up Intervall von 14.6 Monaten (Range 3-35 Monate) nach Curettage und Auffüllung der Knochentumoren zeigten alle Patient*innen zumindest eine partielle radiologische Konsolidierung. Eine komplette ossäre Integration wurde bei 11.9% der Patient*innen beobachtet; bei 88.1% der Patient*innen war eine teilweise ossäre Integration sichtbar. Bei vier Patient*innen, von denen zwei Tumoren des distalen Femurs und zwei Tumoren der Humerus-Diaphyse aufwiesen, kam es innerhalb von sechs Wochen nach dem Primäreingriff zu Frakturen. In allen vier Fällen konnte eine komplikationslose Plattenosteosynthese durchgeführt werden. Während des Follow-up Intervalls konnten bei sämtlichen eingeschlossenen Patient*innen keine weiteren Komplikationen beobachtet werden.

**Schlussfolgerungen.** Zusammenfassend scheint es sich bei dem Beta-Tricalcium-Phosphat Cerasorb® basierend auf dieser Kurzzeitbeobachtung um einen verlässlichen Knochenersatzstoff zu handeln, der mit niedrigen Komplikationsraten einhergeht und der eine geeignete Alternative zu autologen oder allogenen Knochenersatzstoffen darstellt. Dennoch weist er eine Tendenz zur verzögerten ossären Integration auf. Die Anwendung von Cerasorb® scheint bei kleineren Läsionen mit einer Größe von unter 5 cm sicher zu sein. Aus unseren Daten ist jedoch abzuleiten, dass bei knöchernen Defekten mit einer Größe von über 5 cm eine Schutzverplattung durchgeführt werden sollte. Dies gilt unabhängig von der Lokalisation des Tumors in der oberen oder der unteren Extremität.

# ABSTRACT

**Background/Objective.** Benign and low-grade malignant bone tumours are usually treated with intralesional curettage. Subsequently, the bony cavity can be left empty or it can be filled with autologous or allogenic materials. Artificial bone graft substitutes (ABGS) for curettage of bone tumours are becoming increasingly popular, as, in contrast to autologous bone graft substitutes, they do not cause donor site morbidity. Several ABGS are available, including demineralized bone matrix, bone graft extenders, and bone morphogenic proteins.

The aim of this retrospective study was to evaluate the osseous integration profile of the ABGS Cerasorb® (Curasan-AG, Kleinostheim, Germany), a beta-tricalcium phosphate in granular form, and to determine potential associated complications.

**Methods.** 55 patients suffering from benign and low-grade malignant bone tumours were treated with curettage and refilling of the bony cavity using the ABGS Cerasorb® between 2018 and 2021 at the Department of Orthopaedics and Trauma at the Medical University of Graz. Clinical follow-up examinations with radiographies in two planes were performed six weeks, three months, six months and twelve months after surgery. All surgeries were carried out by experienced orthopaedic tumour surgeons. Parameters assessed in this study included time required for osseous consolidation, local recurrence rates, and complications. Surgical complications were reported according to the classification system by Goslings and Gouma. Assessment of osseous integration was performed according to the modified Neer score.

**Results.** Altogether, 43 patients were included in the final analysis. Twelve patients, who could not be reached via telephone or mail and persuaded to have further follow-up exams performed at the Department of Orthopaedics and Trauma at the Medical University of Graz, were lost to follow-up within the first four months after surgery. The tumour entities evaluated in this analysis included enchondromas (n=14), atypical cartilaginous tumours (n=17), simple or juvenile bone cysts (n=4), chondroblastomas (n=4), as well as one case of each fibrous dysplasia, an intraosseous ganglion, Langerhans cell histiocytosis, and Rosai-Dorfman disease. The mean age at surgery amounted to 42 years (range 15-70 years). 21 (48.9%) patients were male and 22

(51.2%) were female. After a mean follow-up period of 14.6 months (range 3-35 months), radiological consolidation following curettage was observed in all patients. Complete osseous integration was observed in 11.9% of patients; in the remaining 88.1%, osseous integration was partial. In four patients, of whom two had a tumour in the distal femur and two in the humeral diaphysis, fractures occurred within six weeks after primary surgery, and in all cases, uncomplicated plate osteosynthesis was performed. Overall, no further complications were observed in our cohort during the follow-up period.

**Conclusions.** In conclusion, based on the present short-term observation, the beta-TCP Cerasorb® is a reliable bone graft substitute with low complication rates. It is a suitable alternative to autologous or allogenic bone grafts, even though there seems to be a tendency towards delayed osseous integration. Thus, it can be safely applied in small osseous lesions with a diameter of less than 5 cm. However, our data suggest that protective plate osteosynthesis should be performed in bone defects exceeding 5 cm in their diameter, independent of tumour location in the upper or lower extremity.

# 1 BACKGROUND

## 1.1 Bone tumours

In general, bone tumours are defined by abnormal growth of cells inside the bone, forming a mass of tissue. Bone tumours can either be classified by their cell of origin, or by their dignity. Furthermore, primary and secondary tumours can be differentiated (2, 3).

The actual incidence of benign bone tumours is not clear, as many people have indolent lesions (4). Moreover, cartilaginous tumours are frequent incidental findings on MRI scans, especially knee MRIs, and are associated with an estimated prevalence of 2.8% (4). The most frequent benign bone tumours include osteochondroma and non-ossifying fibroma (4).

On the other hand, malignant bone tumours, so-called bone sarcomas, are quite rare and add up to approximately 0.2% of all neoplasms (4). The most frequently occurring primary malignant bone tumour is osteosarcoma, which is associated with one age peak during the second decade of life and one peak in people over 60 years. Ewing's sarcoma is less common and primarily occurs in patients under the age of 30 (4). Furthermore, the incidence of chondrosarcoma and chordoma rises with age from adolescence onwards (4).

Although most primary bone neoplasms develop de novo, some seem to arise from benign precursor lesions or from bone regions with prior history of disease (4). For example, Paget's disease of bone, chronic osteomyelitis, radiation injury, and pre-existing benign lesions are suspicious of precancerous conditions, for example enchondroma, osteochondroma, and synovial chondromatosis (4).

Moreover, genetic predispositions influencing the risk of bone tumour development are known (4): for instance, mutations may cause disorders that follow typical Mendelian patterns of inheritance. Moreover, single nucleotide polymorphisms (SNPs) may affect the function of proteins encoded by the genes concerned (5). Furthermore, certain genetic variants can be associated with an increased risk for bone tumour development; these may also affect therapy response and the development of other

tumours (4). Examples of such tumour syndromes include mutations in tumour protein *p53* (*TP53*), causing Li-Fraumeni syndrome, and mutations in *RB1* (Retinoblastoma protein 1) (6). Both mutations lead to a genetic predisposition for developing osteosarcoma (4). Additionally, non-inherited, postzygotic mutations may increase the risk of tumour development, for example mutations in the *IDH1* (Isocitrate dehydrogenase) and *IDH2* genes predisposing for enchondromatosis, or *GNAS* (Guanine nucleotide binding protein, alpha stimulating activity polypeptide) mutations causing polyostotic fibrous dysplasia, and other syndromes in which polyostotic fibrous dysplasia is associated with other neoplastic lesions, such as the McCune-Albright syndrome, or the Mazabraud syndrome (4).

### 1.1.1 Classification of bone tumours

In accordance with the recent WHO (World Health Organization) classification system dating from 2020, bone tumours are differentiated in accordance with their respective cell line of origin. Therefore, chondrogenic tumours, osteogenic tumours, fibrogenic tumours, vascular tumours, osteoclastic giant-cell rich tumours, notochordal tumours, other mesenchymal tumours of bone, and hematopoietic neoplasms of bone can be differentiated (4).

Furthermore, according to the WHO classification 2020, bone tumours are classified into four categories based on their biological behaviour, especially the risk for local recurrence and metastasis (4). Thus, benign, intermediate (locally aggressive), intermediate (rarely metastasizing), and malignant bone tumours are differentiated.

Most benign tumours are associated with a restricted capacity for local recurrence. If they do recur, they do so in a non-destructive manner and are cured by intralesional procedures, such as curettage and potentially additional filling with adjuvants (4). In the current WHO classification 2020, chondroblastoma, which was previously classified as intermediate (rarely metastasizing), has been added to this category. Furthermore, chondromyxoid fibroma, as well as aneurysmal bone cysts, which were previously classified as intermediate (locally aggressive), have also been added to the category of benign bone tumours (4).

Bone tumours categorized as intermediate (locally aggressive) frequently recur locally and have the potential to show an infiltrative and locally destructive growth pattern, although they do not seem to have the capacity to metastasize (4). Examples of this category include the atypical cartilaginous tumour, osteofibrous dysplasia-like adamantinoma, fibrocartilaginous mesenchymoma, and epithelioid hemangioma (4).
Bone tumours classified as intermediate (rarely metastasizing) are often locally aggressive (4). In addition, these lesions are capable of inducing distant metastases in rare cases (<2%), usually lung metastases. The most common example of this category is the giant cell tumour of bone (4).
Malignant bone tumours involve destructive growth, a higher potential of recurrence, and an increased risk of distant metastasis, with a frequency ranging from 20% to almost 100% according to the WHO classification 2020 (4). Low-grade sarcomas may have a reduced risk of metastasis of approximately 2-10%, but in case of recurrence, their grade is often advanced and therefore the risk of distant metastasis increases (4).

### 1.1.2 Grading and staging of bone tumours

As bone tumours vary concerning their biological behaviour, histological grading aims to predict the behaviour of a tumour based on its histological characteristics (4). Regarding bone sarcomas, no generally accepted grading system is available, as the French Fédération Nationale des Centres de Lutte Contre le Cancer (FNCLCC) grading system, that is generally recognized for soft tissue sarcomas, has never been validated for the classification of bone sarcomas (4, 7). The histological sub-classification of bone sarcomas frequently influences clinical behaviour and thus the grade (9). This grading system according to the histological subtype is summarized in **table 1**, as proposed in the WHO classification from 2020 (4).

**Table 1:** Grading of bone sarcomas determined by histological subtype (with kind permission of the WHO Classification of Tumours Editorial Board, according to table 3.02, page 343, in the WHO classification 2020) (4)

| GRADE | SARCOMA TYPE |
|---|---|
| **GRADE 1 (LOW-GRADE)** | • Low-grade central osteosarcoma<br>• Parosteal osteosarcoma<br>• Clear cell chondrosarcoma |
| **GRADE 2 (INTERMEDIATE-GRADE)** | • Periosteal osteosarcoma |
| **GRADE 3 (HIGH-GRADE)** | • Osteosarcoma<br>• Undifferentiated high-grade pleomorphic sarcoma<br>• Ewing sarcoma<br>• Dedifferentiated chondrosarcoma<br>• Mesenchymal chondrosarcoma<br>• Dedifferentiated chordoma<br>• Poorly differentiated chordoma<br>• Angiosarcoma |
| **VARIABLE GRADING** | • Conventional chondrosarcoma (grade 1-3)<br>• Leiomyosarcoma of bone (grade 1-3, no established grading system)<br>• Low- and high-grade malignant transformation of giant cell tumour of bone |

Additionally, for staging purposes regarding musculoskeletal tumours, Enneking et al. have introduced a staging system that has been validated by the Musculoskeletal Tumour Society (MSTS) (9, 10). The Enneking staging system has not been edited or revised since its introduction in 1980 (4). The tumour stage according to Enneking et al. is influenced by tumour grade, expansion beyond the affected surgical compartment, and the presence of metastases (9, 10). An overview of this staging system is presented in **table 2**. However, there are several limitations associated with the Enneking classification, as in clinical practice, most lesions are stage IIB (4). Moreover, the primary tumour size is not part of the classification, even though it constitutes an essential prognostic factor (4).

**Table 2:** Enneking staging system for malignant bone tumours (with kind permission of the WHO Classification of Tumours Editorial Board, according to table 3.03, page 344, in the WHO classification 2020) (4, 9, 10)

| Stage | Grade | Site | Metastases |
|---|---|---|---|
| **IA** | Low (G1) | Intracompartmental (T1) | No metastasis (M0) |
| **IB** | Low (G1) | Extracompartmental (T2) | No metastasis (M0) |
| **IIA** | High (G2) | Intracompartmental (T1) | No metastasis (M0) |
| **IIB** | High (G2) | Extracompartmental (T2) | No metastasis (M0) |
| **III** | Any (G) | Any (T) | Regional or distant metastasis (M1) |

### 1.1.3 Primary and secondary (metastatic) bone tumours

While primary bone tumours originate directly from bone cells, secondary bone tumours, so-called metastatic bone tumours, constitute cancers that spread to the bone from a primary malignancy in other areas of the body, mainly through a haematogenic path (4).

Whereas most bone tumours in children are primary bone tumours, the majority of malignant bone tumours in adults represent metastases of a tumour of a different origin (2, 3). The most common primary tumour sites from which metastases originate include lung, breast, prostate, kidney, thyroid, pancreas, and liver. Moreover, lymphoma and melanoma might metastasize into the bones (4). Regarding children, the generally rarely occurring metastases are mainly caused by neural, renal, or soft tissue and bone tumours, including neuroblastoma, rhabdomyosarcoma, Ewing's sarcoma, and osteosarcoma (4).

Secondary bone tumours may appear at any site, but they are frequently localized in long bones, such as the femur and the humerus, and in the axial skeleton. Areas of bone with increased vascularization are predominantly involved, for example the metaphysis of long bones, the pelvic bones, and the vertebrae.

The most common primary symptom of secondary bone tumours is predominantly pain. Moreover, pathological fractures might be the first symptoms (4). Sometimes, the metastasis may even represent the first clinical manifestation of the tumour of origin. In rare cases, the primary tumour cannot be identified, which is termed cancer of unknown primary (CUP) (4).

Secondary bone tumours might be lytic, sclerotic, or mixed on radiographs. Lytic metastases are usually caused by renal cell cancer, lung cancer, and thyroid carcinomas. On the other hand, sclerotic metastases mainly originate from prostate, breast, and neuroendocrine carcinomas (4). The imaging modality of choice in the diagnosis of metastatic spread is fluorodeoxyglucose positron emission tomography (FDG PET). However, FDG PET is dependent of the glucose metabolism of the primary tumour and will only yield true-positive results if the latter metabolizes FDG. Additionally, whole-body MRI may be of additional diagnostic value in selected cases (4).

In histopathological examinations, secondary bone tumours are characterized by the same or similar histological features as their primary tumour of origin (4). The most frequent primary lesions include adenocarcinomas and squamous cell carcinomas. Immunohistochemical analysis may be useful in order to confirm the tumour of origin. Furthermore, molecular diagnostics might be of prognostic relevance (4).

However, the prognosis is mainly defined by the characteristics of the primary tumour of origin (4).

### 1.1.4 Diagnosis of bone tumours

Basic diagnostic tools regarding the diagnosis of bone tumours include medical history, inspection, palpation, and functional testing. Relevant aspects of the medical history include age, pain, especially at night, duration of symptoms, weight loss, fever, anamnesis of trauma, and family history concerning oncological diseases (11, 12). An essential so-called "red flag" is persistent pain after minor trauma. During inspection, care has to be taken to detect swelling, erythema, deformity, prominent veins, and/or an asymmetrical muscular relief, as these might be indicative of a neoplastic lesion. Progressive or rigid swelling also represents a "red flag" (11). Palpation includes the

differentiation as to whether a swelling is soft or rigid, furthermore the tissue's ability to shift, overheating of the skin, reduced mobility, signs of fracture, pressure pain, as well as motor function, sensitivity, and circulation (11, 12). With regards to these aspects, "red flags" include rigid swelling with an inability to shift, and fractures after minor trauma (11, 12).

One of the most common symptoms of a benign bone tumour is intermittent aching pain (4). On the other hand, previously asymptomatic patients may suddenly suffer from a pathological fracture after minor trauma, which is caused by the weakening of a bone's structure by a neoplastic lesion (4). Common examples include pathologic fractures due to enchondromas or simple bone cysts (4). Osteoid osteomas are typically associated with night pain that is ameliorated by non-steroidal anti-inflammatory drugs. However, when localized in a periarticular region, they might also mimic monoarthritis (4). Osteochondromas characteristically appear as a painless lump, while chondroblastomas are usually associated with severe pain, but appear without specific clinical signs, as swelling and tenderness in proximity to the affected bones are the most frequent symptoms. In general, periarticular tumours may cause joint effusion and stiffness (4).

On the other hand, malignant bone tumours are usually associated with worsening non-mechanical pain, especially night pain that may interrupt sleep (13). Swelling commonly appears after the cortex is destroyed by the tumour and neoplastic tissue extends throughout the periosteum (4). Generally speaking, progressive swelling in a limb, combined with pain, particularly non-mechanical and/or night pain, always needs further investigation (4). It is apparent that these unspecific symptoms give rise to a broad variety of differential diagnoses, including metastases, primary malignant bone tumours, benign bone tumours, infection, and hematological diseases. Consequently, a diagnostic algorithm has been proposed, based on the most probable diagnosis at a certain age (14). The reason for that algorithm is that metastases are unlikely in patients younger than 35 years, whereas after the age of 35, the risk of a bone tumour being a metastasis of a known or undiagnosed carcinoma increases steadily (15). Approximately 43% of bone tumours are localized around the knee, and in patients younger than 20 years, even 56% arise around the knee joint. If pain and swelling around the knee are persistent, the possibility of a primary bone tumour should be

taken into account (4). The second most frequent localization of a primary bone tumour is the pelvis, where both Ewing's sarcoma and chondrosarcoma are most common (4). Pathological fractures are frequently associated with pre-existing pain or discomfort in the limb (4). These fractures are usually caused by minimal force, so that a neoplastic cause for the fracture needs to be considered in order to prevent inadequate internal fixation that might worsen the clinical outcome (16).

Following medical history and clinical examination, further diagnostic tools include two-planar radiographs as standard initial imaging modality, sonography, magnetic resonance imaging (MRI) with contrast enhancement, computed tomography (CT), skeletal scintigraphy, and FDG PET in combination with CT (PET-CT) or MRI (PET-MRI) (4, 17, 18, 19).

Bone tumours characteristically produce an internal matrix that may contain bone, cartilage, or fibrous tissue (4). Moreover, the matrix may be calcified, which is also called "mineralization" of the matrix (20, 21). The configuration of a tumour's margin in relation to the surrounding tissue and the periosteal reaction induced by its growth often reflect a neoplasm's biological behaviour and growth velocity. Whereas slow-growing neoplasms induce circumscribed margins with a narrow transition zone and a solid or thick periosteal reaction, aggressive, fast-growing tumours induce indistinct margins with a wide transition zone and an aggressive periosteal reaction. Examples of aggressive periosteal reactions include radiographic appearances of onion-skin, spiculated, sunburst, or hair-on-end-like patterns, as well as Codman triangles (20, 21).

Regarding plain radiographs, the Lodwick classification of lytic bone lesions is commonly used in order to distinguish between a benign or malignant appearing bone tumour (22). The classification involves four categories, including (1) the pattern of bone destruction, (2) whether or not there is a penetration of the cortex, (3) the presence of a sclerotic rim, and (4) an expanded shell (22, 23). These descriptors are the basis of the sequential categorization into the growth grades IA, IB, IC, II, and III. A higher grade is usually associated with a high velocity of tumour growth (22, 23). An overview of the Lodwick classification is presented in **table 3**.

**Table 3:** Lodwick classification of lytic bone lesions (22)

| Grade | Radiologic appearance | Examples |
|---|---|---|
| IA | • tumour limited to spongiosa<br>• sclerotic rim<br>• no penetration of cortex or periosteum | • enchondroma<br>• osteoid osteoma NOS |
| IB | • little to no sclerotic rim<br>• irregular boundaries<br>• potential affection of the cortex | • chondroblastoma<br>• giant cell tumour<br>• chondromyxoid fibroma<br>• osteoblastoma<br>• unicameral bone cyst<br>• aneurysmal bone cyst |
| IC | • fast growth<br>• potentially infiltrative growth<br>• blurred boundaries<br>• sclerotic rim rare, but possible<br>• arrosion of the cortex<br>• solid periosteal reaction possible | • aneurysmal bone cyst<br>• atypical cartilaginous tumour |
| II | • "moth-eaten" destruction<br>• blurred boundaries<br>• lack of sclerotic rim<br>• cortical destruction<br>• lifted-off periosteum | • chondrosarcoma<br>• osteosarcoma<br>• fibrosarcoma |
| III | • fast, permeative growth<br>• unclear boundaries<br>• onionskin-like alterations of the periosteum<br>• Codman triangle<br>• spiculated | • osteosarcoma<br>• Ewing sarcoma |

Regarding tumour location, certain entities preferably appear in characteristic skeletal locations (4). For example, adamantinomas and osteofibrous dysplasias mainly occur in the anterior cortex of the tibia. On the other hand, chondroblastomas, giant cell tumours, and clear cell chondrosarcomas have a predilection for the epiphysis of long bones. Moreover, osteosarcomas, chondrosarcomas, osteochondromas, and enchondromas are mainly found in the metaphyseal regions, often around the knee joints (4). Additionally, some tumour entities have a predilection for the cortex, including osteoid osteoma, the fibrous cortical defect, osteochondroma, periosteal chondroma, as well as parosteal and periosteal osteosarcoma (20, 21).

### 1.1.5 Biopsy of bone tumours

If a bone tumour is suspected following the clinical and radiological diagnostic examinations, patients should be referred to reference centres for bone sarcomas, as there is evidence that treatment in centres with a high amount of bone tumour therapies and the presence of a multidisciplinary team correlates with a beneficial outcome (19, 24, 25). According to the current ESMO guideline for bone sarcomas, the biopsy should be performed either by the surgical team that will carry out the definitive tumour resection, or by an interventional radiologist in coordination with the responsible surgeon (18). If a biopsy has been performed outside a sarcoma reference centre, an expert pathological review of the specimens in the reference centre is obligatory (4). In most tumours, a core-needle biopsy can be performed. Sometimes, however, an open biopsy is necessary (18). In case of a malignant bone tumour, the biopsy tract and channels through which drains have been placed are considered potentially contaminated, and need to be removed in the course of the definitive resection (4, 18). This is done with the aim of minimizing the risk of local recurrence. Moreover, during the biopsy, contamination of the surrounding tissue has to be avoided, and multiple samples of representative tumour areas must be harvested (18, 26, 27).
It is essential that histology specimens are analyzed by an experienced bone tumour pathologist and discussed in a multidisciplinary team involving radiologists, pathologists, orthopaedic surgeons, and oncologists (4, 18). Following histological

interpretation, the type of bone tumour is diagnosed in accordance with the current version of the WHO classification (4, 18).
After resection of the primary tumour, the size of the tumour inside the bone should be documented. Moreover, the histopathological report has to include the extent of local tumour spread, including the involvement of soft tissue and bone compartments (18). The resection margins need to be described and differentiated into clear (R0) resection margins, microscopically (R1), and macroscopically (R2) contaminated margins. If the resection margins are clear, the distance of the tumour from the nearest resection margin as well as the distance to the closest osteotomy margin needs to be measured in millimeters (18).

### 1.1.6 Principles of tumour resection

The surgical resection margins of musculoskeletal tumours are classified by Enneking (9, 10). There are three tumour zones, including the tumour itself, its capsule and a surrounding reactive zone. The four main options for limb salvage surgery include intralesional excision ("curettage"), marginal excision, wide excision, and radical resection. This applies for both bone and soft tissue tumours (9, 10, 18).
Intralesional excision, also called intralesional curettage, means excising the tumour and opening its capsule. Marginal excision describes an en-bloc excision of the tumour with its (pseudo-)capsule, even though the resection line runs through the reactive zone (9, 10, 18, 28). The problem using this technique for aggressive tumours is that skip lesions may occur outside the reactive zone. Wide excision includes removing the tumour en-bloc with an additional safe zone of healthy tissue around the tumour. Consequently, the resection line runs through healthy tissue (9, 10, 18, 28). On the contrary, radical resection comprises en-bloc resection of the tumour including its capsule, the reactive zone, and healthy tissue of the whole affected muscle compartment in soft tissue tumours, and the whole affected bone in bone tumours (9, 10, 18, 28).

## 1.2 Benign and low-grade malignant bone tumours

As this dissertation covers benign and low-grade malignant bone tumours that were treated with intralesional curettage, the following entities will be discussed extensively in this section: enchondroma, atypical cartilaginous tumour, intraosseous ganglion cyst, simple or juvenile bone cysts, fibrous dysplasia, chondroblastoma, Langerhans cell histiocytosis, and Rosai-Dorfman disease.

### 1.2.1 Chondrogenic tumours

According to the WHO classification 2020, chondrogenic bone tumours are classified as benign, intermediate (locally aggressive and/or rarely metastasizing), or malignant (4). The benign group comprises chondromas, enchondromas, osteochondromas, osteochondromyxomas, subungual exostosis, and the bizarre parosteal osteochondromatous proliferation (BPOP, Nora's lesion), furthermore chondroblastomas, and chondromyxoid fibromas (4) The latter two entities were moved from the intermediate group (WHO 2013) to the benign group according to the WHO classification 2020 (4, 29). In contrast, synovial chondromatosis was moved from the benign into the intermediate group of chondrogenic bone tumours in consideration of the locally aggressive growth pattern and the high risk for local recurrence of this entity. Atypical cartilaginous tumours (ACTs) are also part of the intermediate group of chondrogenic tumours due to their locally aggressive growth. Although the term "chondrosarcoma grade I" was replaced by the term "ACT" in the WHO classification 2013, the 2020 WHO classification uses both terms depending on the location of the neoplasm (4, 29). If the bone tumours are localized in the appendicular skeleton, including the long and short tubular bones, they are classified as ACTs and allocated to the intermediate group (4). If, however, the tumours are located in the axial skeleton, including the scapula, the pelvis and the base of the skull, they are allocated to the group of malignant chondrogenic tumours and are categorized as chondrosarcomas grade I, even though they display the same histopathologic features as ACTs (4). This differentiation is conducted to account for the differences in the biological behaviour of tumours in the axial skeleton compared to tumours in the appendicular skeleton (4).

#### 1.2.1.1 Enchondroma (EC)

Enchondromas are comparatively common bone tumours, as they account for approximately 10-25 % of all surgically removed benign bone tumours (4). However, their true incidence and prevalence is probably underestimated, as most enchondromas stay undetected and are diagnosed incidentally on radiographic images performed for other reasons (4). The prevalence of an incidental finding of an enchondroma on a knee MRI scan is approximately 2% (30). They usually show an asymptomatic course and characteristically occur in the third to fourth decade of life, with a median age at diagnosis of 36 years (31). Usually, patients with an enchondroma are younger than those suffering from a chondrosarcoma. Both sexes are equally affected (4).

Symptoms may include painless swelling, e.g. of a finger, or pathological fractures. Usually, enchondromas affect long tubular bones of the hands and feet, and are located in the medullary cavity of the meta-diaphysis (32).

Radiologically, a ring and arcs matrix mineralization is typically seen on radiographs and CT scans, but might be missing especially in younger patients, and in tumours in the small bones of the hand and feet (4). MRI scans usually show lobulated, non-sclerotic margins. Moreover, superficial scalloping, cortical thinning, and bone distension can be observed (4). In **figures 1a, 1b and 1c**, MRI scans of an enchondroma of the distal femur are shown.

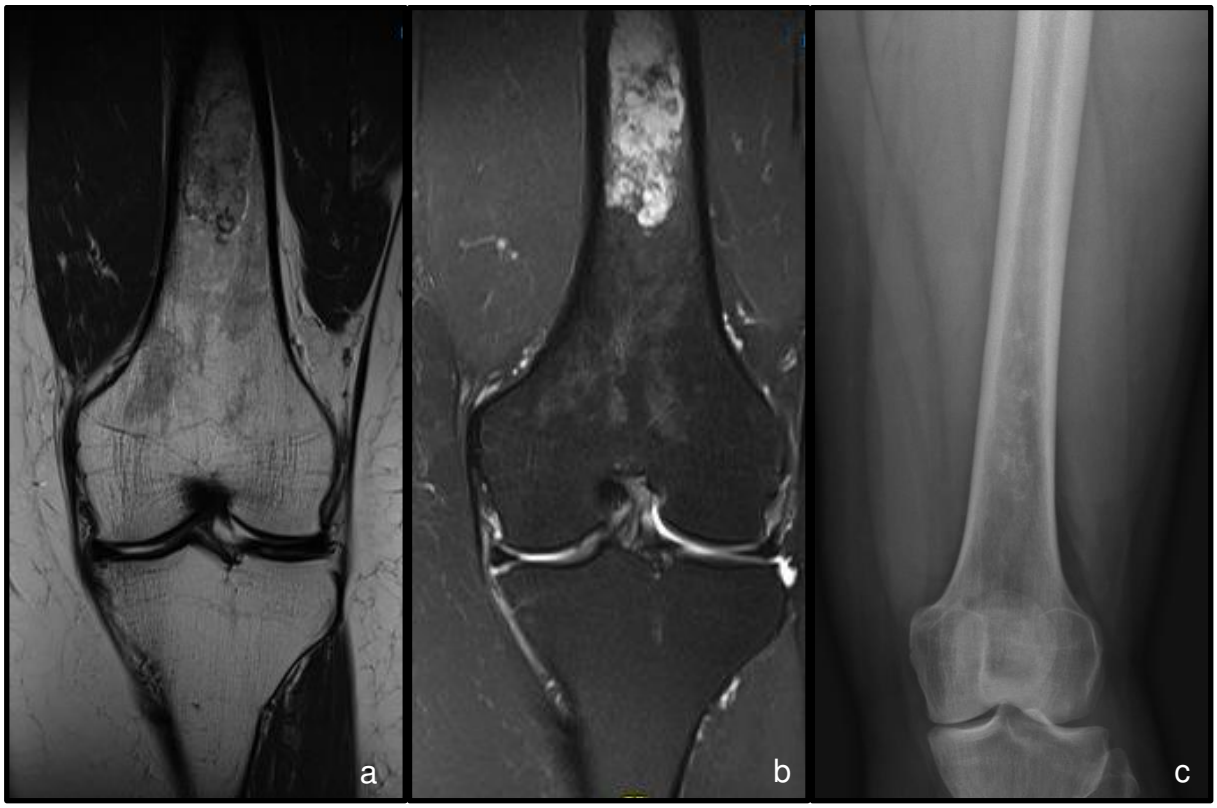


**Figures 1a, 1b and 1c: (1a)** T1-weighted and **(1b)** contrast-enhanced T2-weighted knee MRI scans, as well as **(1c)** a conventional X-ray, of an enchondroma of the distal femur of a female patient at the age of 40 years. Images show a polylobulated, partially calcified lesion in the distal diaphysis of the femur. The lesion measures 6.5 cm in its proximodistal diameter and shows a characteristically high signal on T2-sequences, indicating a high water-content of the neoplastic tissue. However, cortical thinning or scalloping cannot be observed. Moreover, there is no bone marrow edema indicating aggressive growth in contrast-enhanced sequences. Also, there are no areas suspicious of dedifferentiation. According to the Lodwick classification, conventional x-ray demonstrates little to no sclerotic rim, rather irregular boundaries, and delicate popcorn-like calcifications (22).

Regarding the etiology of enchondromas, heterozygous somatic mutations in the isocitrate dehydrogenase genes *IDH1* and *IDH2* have been detected and are thought to be involved in the pathogenesis of these neoplasms, even though the detailed mechanisms still need to be elucidated (33-36). Such mutations can be detected in 52% of sporadic enchondromas and in approximately 90% of patients suffering from

enchondromatosis (4). Isocitrate dehydrogenases usually convert isocitrate to α-ketoglutarate in the tricarboxylic acid cycle, which is involved in energy production of the cell (4). Mutations in *IDH1* and *IDH2* induce the formation of the oncometabolite D-2-HG, which causes epigenetic alterations (33-36). Studies have shown that D-2-HG is involved in the promotion of chondrogenic differentiation and the inhibition of osteogenic differentiation of mesenchymal stem cells, which constitute the presumed precursor cells of enchondroma (37, 38).

Histologically, enchondromas appear hypocellular, with a multinodular or confluent architecture. Masses of hyaline cartilage are found, and tumour cells are embedded within sharp-edged lacunar spaces (4). Cytological atypia as well as mitoses are usually not found (4). In **figure 2**, a histopathologic image of an enchondroma is presented.

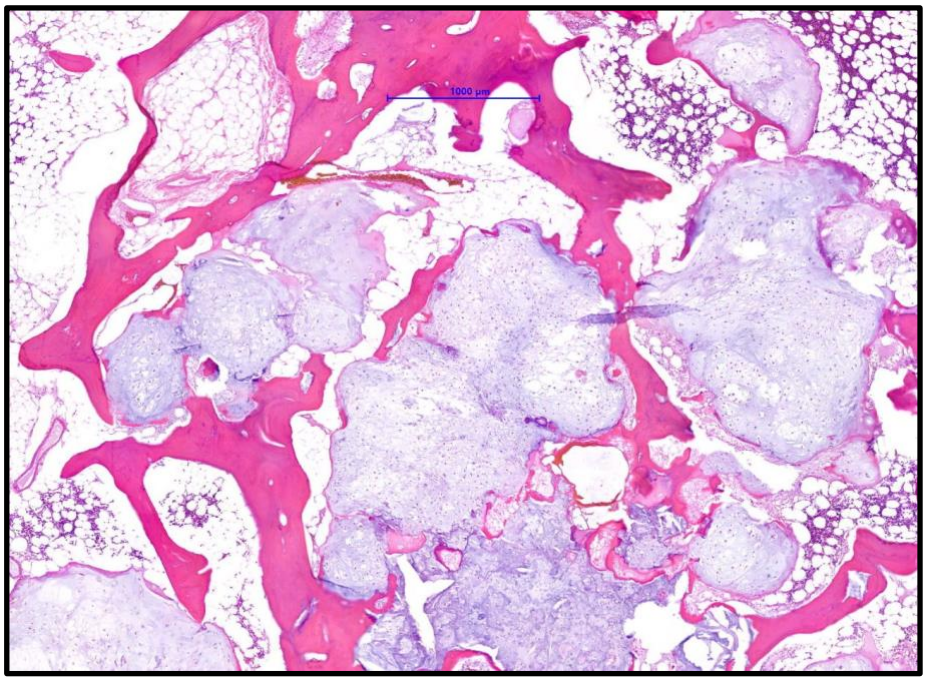


**Figure 2:** Histopathologic image of an enchondroma, with the kind permission of Univ. Prof. Priv. Doz. Dr. Bernadette Liegl-Atzwanger, Diagnostic and Research Institute of Pathology, Medical University of Graz. Enchondroma composed of hypocellular areas with lobules of hyaline cartilages surrounded by trabecular bone.

Enchondromas typically constitute solitary lesions. However, there are conditions in which multiple enchondromas are present, e.g. Ollier's disease or enchondromatosis,

or the Maffucci syndrome (39, 40). Ollier's disease is a rare, nonhereditary, often asymmetric systemic disorder with multiple intramedullary and intracortical cartilage lesions. Usually, tubular long bones are affected, which are often shortened and deformed. Ollier's disease is non-hereditary and usually becomes symptomatic early in childhood, as patients suffer from pathologic fractures, palpable masses, and limb deformity from childhood onwards (4, 39, 40). The risk for malignant transformation, particularly into higher-grade chondrosarcomas, has been reported to be approximately 5% to 30%. Furthermore, these patients have an elevated risk of developing other malignancies, including gliomas, pancreatic carcinomas, or ovarian carcinomas (40). Maffucci syndrome is also a rare, nonhereditary, typically asymmetric condition with the presence of multiple cartilaginous bone tumours. It differs from Ollier's disease due to its association with soft tissue hemangiomas and lymphangiomas, which are usually located in the same extremity that shows osseous involvement (39, 40). Within involved bones, columnar lytic lesions and matrix mineralizations are common. Bones of the hand and wrist are predominantly affected. The risk for transformation into a sarcoma, particularly into a chondrosarcoma, angiosarcoma and fibrosarcoma, has been reported to be around 20% (39, 40). Moreover, similar to Ollier's disease, patients suffering from Maffucci syndrome tend to develop other non-skeletal malignancies, such as gliomas, pancreatic carcinomas, or ovarian carcinomas (40).

The differentiation between a benign enchondroma and an atypical cartilaginous tumour/chondrosarcoma grade 1 is often challenging (41). While enchondromas are typically found in the bones of the hands and feet, chondrosarcomas are usually located in the axial skeleton (31). Radiologic characteristics of enchondromas include stippled calcifications, endosteal scalloping with areas of ossification, or a distended cortex. Apart from two-planar X-rays, the most important diagnostic tool to detect malignant features, such as bone marrow edema indicating aggressive growth, cortical destruction, soft tissue masses, as well as the multilocular appearance of cartilaginous tumours, or the involvement of flat bones, is the MRI scan (42). However, any cartilaginous lesion displaying continuous growth is suspicious of an ACT or chondrosarcoma until proven otherwise (40). The potential for malignant transformation of an enchondroma varies between 0% and 4.2% (43, 44). Multilocular

appearance, as well as conditions with multiple enchondromas, e.g. Ollier's disease or Maffuci syndrome, are among the risk factors for malignant transformation (43, 44).
In general, enchondromas do not require surgical treatment. However, if these lesions show an increase in size or if there is a risk of pathological fracture, treatment is required. Enchondromas are routinely treated by performing intralesional excision ("curettage") and consecutive filling with an autologous or allogenic bone graft or synthetic materials (31). Previous studies have indicated a certain potential of adjuvant treatment, for instance with alcohol soaking, CO2 laser ablation, or bone cementation, in order to minimize recurrence rates (45). Moreover, recent literature has described curettage without augmentation as a potential new treatment option (46). For instance, Morii et al. report similar times to bone restructuring between patients with or without augmentation after curettage (47).

#### 1.2.1.2 Atypical cartilaginous tumour (ACT)

As stated previously, locally aggressive cartilage tumours are termed atypical cartilaginous tumour (ACT) when occurring in the appendicular skeleton (long and short tubular bones), and grade I chondrosarcoma (CS1) when occurring in the axial skeleton (flat bones, including pelvis, scapula, skull base) (4). Subsequently, these tumours only differ regarding location, but not regarding histology. However, the abovementioned distinction is required, as tumours localized in the trunk are more at risk of recurrence than those in the appendicular skeleton (48).
By definition, ACT/CS1 describes a locally aggressive neoplasm composed of hyaline cartilage that develops in the medulla of bone (4). While primary tumours arise centrally within bones in the absence of a benign precursor lesion, secondary ACT/CS1s develop based on a pre-existing benign cartilaginous lesion (4).
These tumours usually originate from bones formed by endochondral ossification (4). Whereas CS1s are most frequently observed in the pelvic bones (22%) and the ribs (6%), ACTs are usually detected in the femur (31%), the humerus (11%), and the tibia (8%). Approximately 50% of central ACTs are located in the metaphysis of long bones, a third in the diaphysis, and the remaining few show a predominating epiphyseal component (4).

ACT/CS1 is mainly observed in the third to sixth decade of life, and displays an equal sex distribution (4).

Clinical symptoms include pain and/or swelling, as well as pathologic fractures, but patients may also be asymptomatic. Moreover, tumours in the skull base may cause neurological deficits (4).

On plain X-rays, ACT/CS1s appear as lytic lesions, usually displaying the characteristic cartilaginous popcorn-like calcifications (4). The geographic borders of these lesions are often less distinct compared to enchondromas (49, 50). Furthermore, cortical scalloping without breakthrough is frequently observed, although this is also seen in enchondromas (4, 51). Tumours larger than 5 cm, as well as tumours displaying cortical remodeling, deep scalloping, and/or enhancement on dynamic gadolinium chelate-enhanced MRI within 10 seconds of the start of arterial enhancement, are suspicious of ACT / CS1 (51-53). In addition, perifocal bone marrow edema in contrast-enhanced MRI sequences indicates aggressive growth. Moreover, regarding MRI scans, an intermediate signal in T1-weighted sequences, discontinuous visualization after contrast administration, a pathologic fracture, adjacent bone marrow edema, and signal alterations of the adjacent soft tissue might be indicative of an intermediate or even malignant process (53).

Even though these criteria might be indicative of an ACT/CS1, the radiological differentiation between ACT/CS1 and enchondroma might be difficult even for experienced radiologists, as there is an overlap of radiographic and MRI characteristics between enchondromas and ACT/CS1. As mentioned previously, also location matters: If cartilaginous tumours present in the phalanges, they usually constitute enchondromas, whereas cartilaginous tumours in the axial skeleton are most probably ACT/CS1 (4). In contrast, these lesions can usually be clearly distinguished from grade 2 or 3 chondrosarcomas (49, 50). In **figures 3a, 3b and 3c**, MRI scans of an ACT of the distal femur are shown.

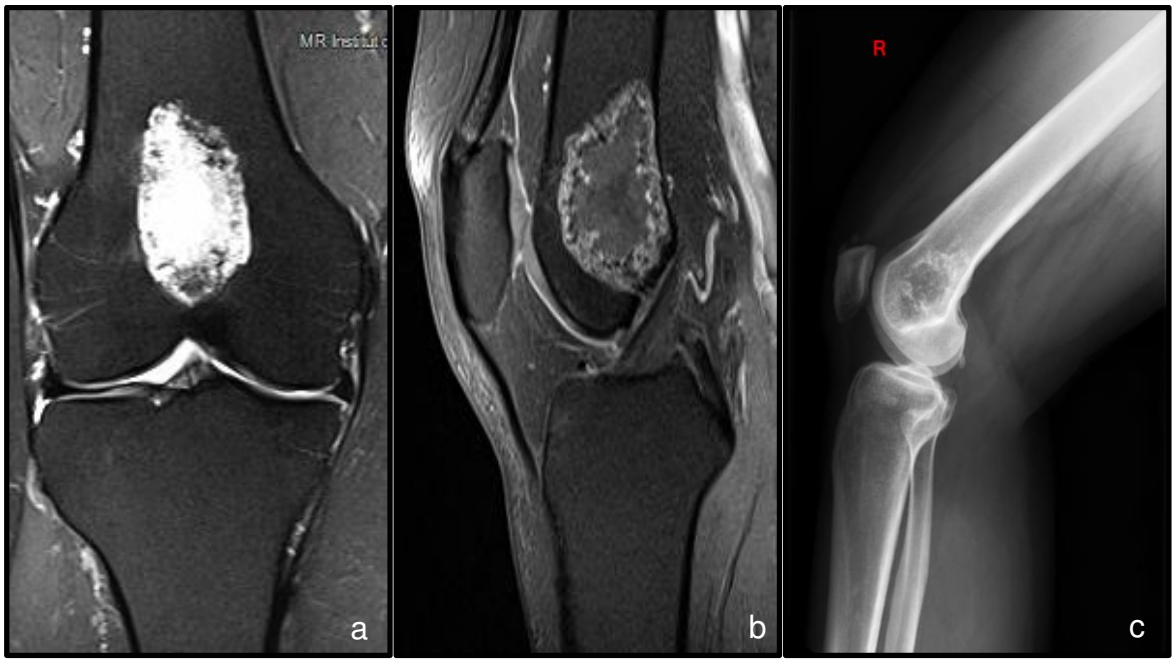


**Figures 3a, 3b and 3c: (3a)** Coronal contrast-enhanced T2-weighted and **(3b)** sagittal T2-weighted MRI scans, as well as **(3c)** a conventional X-ray, of an atypical cartilaginous tumour (ACT) of the right distal femur of a female patient at the age of 48 years. Images show a polylobulated, partially calcified lesion in the distal diaphysis of the femur with blurred boundaries according to the Lodwick classification (22). The lesion measures 4.8 cm in its proximodistal diameter and shows a characteristically high signal on T2-sequences indicating a high water-content of the neoplastic tissue. Perifocal bone marrow edema as a sign of aggressive growth cannot be observed. Furthermore, there are no areas suspicious of dedifferentiation. However, cortical thinning and scalloping are apparent in the sagittal plane in both MRI scans and X-ray regarding the dorsal cortex of the femur. Moreover, popcorn-like calcifications can be detected on the conventional X-ray.

Similar to the pathogenesis of enchondroma, somatic mutations of the *IDH1* and *IDH2* genes are reported in approximately 50% of patients with primary ACT/CS1, and in 78% of patients with secondary ACT/CS1 arising in predisposing conditions, such as Ollier's disease (32). Furthermore, cartilaginous tumours in Ollier's disease displaying an *IDH1* or *IDH2* mutation are associated with an increased risk of progression into an ACT/CS1. The overall risk of malignant transformation in Ollier's disease has been reported to be approximately 40% (4). However, the risk for patients with multiple

enchondromas that are exclusively located in the hands and feet amounts to about 15%, whereas patients with multiple enchondromas in both small and long/flat bones have a risk of 46%. Moreover, a particularly high risk for progression is associated with enchondromas localized in the pelvis (54).

Histologically, ACT/CS1 is defined by masses of hyaline cartilage matrix. Typically, a lobular growth pattern is observed, which might cause cortical thinning appearing as cortical scalloping in radiographs. Moreover, the lobules can be irregularly shaped and may vary in size (4). The characteristic encasement pattern, a deposition of bone around the tumour lobules as a sign of indolent growth, which is observed in slow-growing enchondromas, is rather uncommon in central ACT/CS1. In contrast, the tumour lobules usually penetrate and entrap the pre-existing lamellar bone trabeculae, with entrapment being defined as the presence of tumour around three sides of a normal spicule of medullary trabecular bone (4). Furthermore, the cellularity in central ACT/CS1 is slightly higher than in enchondroma. Binucleation can be observed frequently, but mitoses are absent. Necrosis may be observed (4). In **figure 4**, a histopathologic image of an ACT/CS1 is presented.

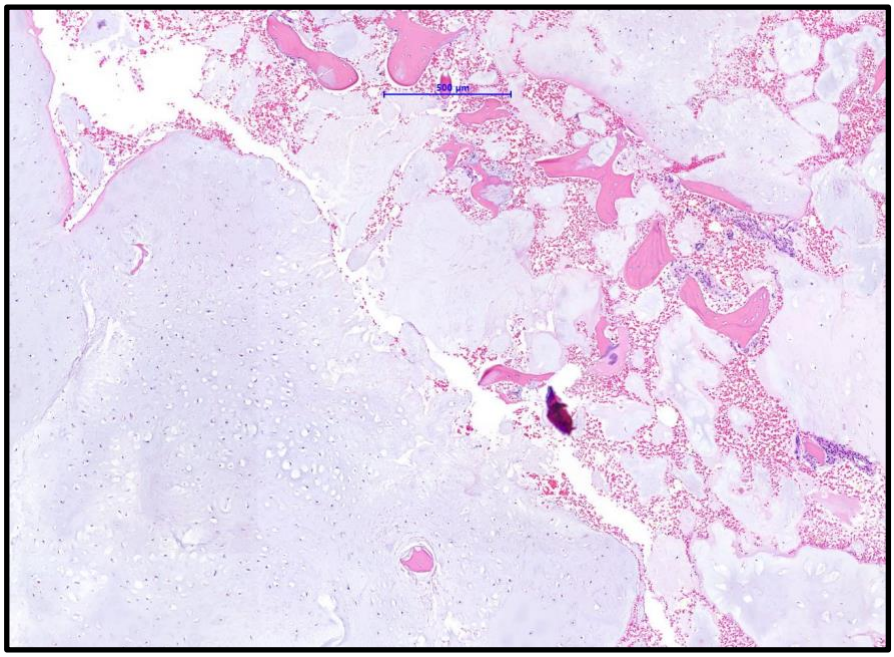

**Figure 4:** Histopathologic image of an atypical cartilaginous tumour (ACT), with the kind permission of Univ. Prof. Priv. Doz. Dr. Bernadette Liegl-Atzwanger, Diagnostic and Research Institute of Pathology, Medical University of Graz. Atypical cartilaginous

tumour composed of cartilaginous hypocellular tumour tissue with encasement of bone.

According to the WHO classification 2020, the current gold standard in treatment is curettage and local adjuvants as well as filling with auto- or allografts in long bones, and surgical excision and negative margins for tumours of the pelvis and spine, as tumours in the axial skeleton are associated with a worse outcome (4, 55). However, the gold standard treatment is currently under vivid discussion and consensus meetings are taking place in order to define profound treatment algorithms.
ACT/CS1 is associated with local recurrence rates of 7.5-11.0%, compared to 0% in enchondroma (4). Approximately 10% of the recurring ACT/CS1 progress to a higher grade.
If patients die from central ACT/CS1, death is usually due to recurrent tumours that are difficult to manage surgically owing to their location. However, overall prognosis of ACT/CS1 is excellent, as survival rates of 88-95 % have been reported (4).

### 1.2.2 Simple or solitary bone cysts

Simple or solitary bone cysts constitute benign intramedullary cysts in a fibrous membrane filled with serous or serosanguinous fluid (4). They are typically localized in the proximal humerus (50%), and the proximal femur (25%), followed by the proximal tibia and other long tubular bones (4). Other less frequently involved localizations include the calcaneus, and the pelvic bones (56). Most simple bone cysts are diagnosed within the first two decades of life. Males are affected twice as often compared to females (2:1 ratio) (4).
Simple bone cysts may be diagnosed incidentally, as they are often associated with merely mild symptoms, such as mild pain, swelling, and limitation of a joint's range of motion (56). However, they might also become clinically apparent as a consequence of a pathologic fracture presenting with pain, swelling, erythema and possible deformity (56).
When diagnosed on plain radiographs, simple bone cysts present as central, well-circumscribed, radiolucent lesions (4). The cysts can lead to bone remodeling, thinning

of the cortex, and endosteal scalloping (4). Moreover, periosteal reactions are rarely observed in the absence of a pathological fracture. The so-called "fallen fragment sign" is a pathognomonic finding in simple bone cysts and refers to fragments of cortical bone that float in the cyst fluid (4). Another pathognomonic sign is the "rising bubble sign", which describes a gas bubble inside the cyst (57). Regarding MRI, simple bone cysts show low signal intensity on T1-weighted sequences and bright, homogeneous signal intensity on T2-weighted or other fluid-sensitive sequences (4). If repetitive fractures occur, trabeculations and a multi-loculated appearance might be observed, mimicking aneurysmal bone cysts (4). Therefore, differential diagnosis includes aneurysmal bone cyst, cystic fibrous dysplasia, and calcaneal lipoma with cystic degeneration (4). In **figures 5a and 5b**, MRI scans of simple bone cysts of the distal femur and proximal tibia are shown.

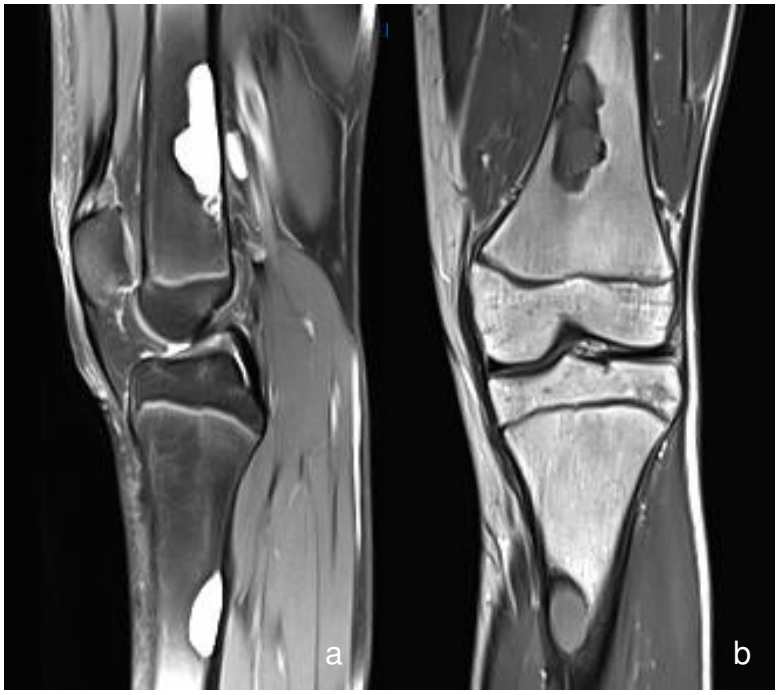


**Figures 5a and 5b: (5a)** Contrast-enhanced T2-weighted and **(5b)** T1-weighted MRI scans of a simple bone cyst of the left distal femur and proximal tibia of a male patient at the age of 15 years. Images show a well-circumscribed lesion in the distal diaphysis of the femur. The lesion measures 5.2 cm in its proximodistal diameter and shows a characteristically high signal on T2-sequences indicating a high water-content of the neoplastic tissue. Perifocal bone marrow edema as a sign of aggressive growth cannot

be observed. Furthermore, there are no areas suspicious of dedifferentiation. Moreover, cortical thinning or scalloping cannot be observed.

According to the WHO classification from 2020, the etiology and pathogenesis of simple bone cysts is yet unknown (4).
In histopathologic examinations, the wall of a simple bone cyst, which consists of a thin layer of fibrous tissue, lacks a clear lining (4). Moreover, the wall might include aspects of chronic inflammation, as well as multinucleated giant cells, hemosiderin, cholesterol clefts, reactive bone, and fibrin-like collagen deposits. Upon mineralization of these deposits, a cementum-like or ossified appearance may be observed (58). If fine-needle aspiration is performed, the fluid within these cysts is typically colorless or amber, and contains histiocytes, chronic inflammatory cells, giant cells, and high levels of prostaglandins and other enzymes (4, 56). In **figure 6**, a histopathologic image of a simple bone cyst is presented.

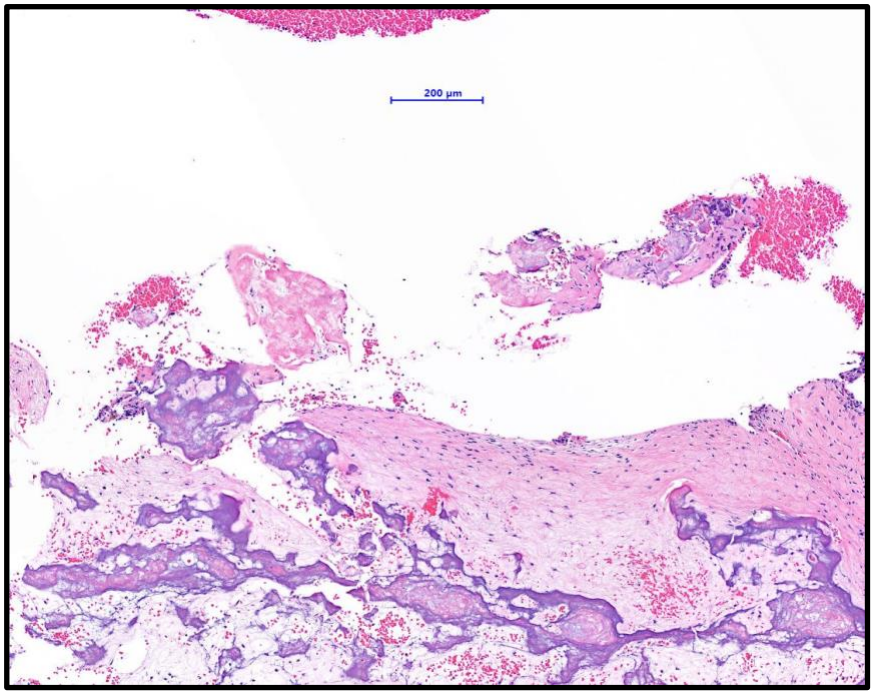


**Figure 6:** Histopathologic image of a simple bone cyst, with the kind permission of Univ. Prof. Priv. Doz. Dr. Bernadette Liegl-Atzwanger, Diagnostic and Research Institute of Pathology, Medical University of Graz. Simple bone cysts with a cyst wall composed of fibrous tissue, some multinucleated giant cells, hemosiderin, reactive bone, and fibrin-like collagen deposits.

Current treatment strategies comprise a variety of injectables, including steroids and demineralized bone marrow, furthermore decompression techniques, such as violating the wall of the cyst and draining its contents for example by needles or curettes, and the curettage of these cysts (56). Nonsurgical treatment is applied for asymptomatic simple bone cysts with no substantial loss of strength and stability in the affected bone requiring surgical intervention (59). Previous studies have reported injection techniques applying steroids, e.g., methylprednisolone, as well as autologous bone marrow (ABM), demineralized bone marrow (DBM), and osteoconductive apatitic calcium phosphate bone substitute (60, 61). The combination of ABM and DBM resulted in a higher healing rate and lower failure rate compared to steroid injections according to some publications (60, 61). Furthermore, these studies reported that patients treated with an injection of osteoconductive apatitic calcium phosphate bone substitute experienced healing rates comparable to minimally invasive surgical techniques. (60, 61)

Pathologic fractures are a common complication of simple bone cysts (4, 56). Secondary complications of large cysts and pathologic fractures are the growth arrest of the affected bone, as well as avascular necrosis (4).

However, in approximately 10% of simple bone cysts, spontaneous healing was observed after a pathologic fracture (4). If a pathologic fracture of the upper extremity occurs, immobilization for four to six weeks might be appropriate (60, 61). Surgical management is indicated in cases of pathologic fractures, particularly in the lower extremity, furthermore if a cyst displays an increase in size within the observation period, or else if cysts occur in bones with a high weight load and thus a high risk of pathologic fracture, as, for example, in the proximal femur. Surgical treatment strategies include curettage and bone grafting, decompression by injuring the wall of the cyst and draining the fluid, and osteosynthesis in case of pathologic fractures (56, 59). Local recurrence rates after various treatment methods range from 10% to 20% according to the current WHO classification (4).

### 1.2.3 Intraosseous ganglion cyst (IGC)

Intraosseous ganglion cysts (IGCs) are tumour-like, non-neoplastic pseudocysts (62). In contrast to degenerative subchondral and/or peri-articular cysts, the absence of degenerative or inflammatory arthritis is required (62). They typically occur in the subchondral regions of bones and are commonly localized in the metaphysis or epiphysis of long bones of the lower extremity, such as the tibia, furthermore in carpal and tarsal bones, and flat bones (63-65).

Symptoms of the idiopathic IGC include activity-related pain. For example, IGCs affecting the hand often present with pain in the dorsal or palmar aspect of the wrist. Moreover, periarticular swelling, sensitivity to palpation, and pathologic fracture may occur (65). However, in the majority of cases, diagnosis is made incidentally, as these lesions are often asymptomatic.

On radiography, IGCs present as well-demarcated, circular to oval, radiolucent defects without internal calcification, surrounded by a rim of sclerotic bone (65). Typically, these lesions are located close to joints (62, 63-65). Often, IGCs show signs of cortical expansion and/or thinning (65). Furthermore, an articular (i.e. communicating ganglion cyst), or a non-articular cortical defect can be present (62, 63). Occasionally, a soft tissue component can be observed if a juxta-osseous ganglion penetrates into the adjacent bone, thus resulting in a cystic bone defect (62, 63). However, periosteal reaction or other signs of aggressive growth should be absent (62, 63).

Radiological differential diagnoses particularly include subchondral bone cysts, which occur in degenerative joint disease but are otherwise indistinguishable from IGCs (62). Other differential diagnoses include various cystic bone lesions, such as solitary or aneurysmal bone cysts, furthermore giant cell tumours of bone, Brodie-abscesses, or chondroblastomas (62, 66, 67).

Histologically, IGCs are identical to their soft tissue counterpart: they contain a viscous clear mucus fluid, which is rich in glucosamine, albumin, globulin, and hyaluronic acid (68). Characteristically, IGCs do not express an epithelial or synovial lining, even though they are covered by membranous tissue resembling synovial lining (68).

The exact pathogenesis remains unknown, although synovial herniation and traumatic mucoid degeneration of connective tissue are considered as potential causative

mechanisms (64, 65, 68). Moreover, Buldu et al. reported the potential of genetic transmission, as cysts in twin sisters were observed in the same ipsilateral bones (69). Treatment is only required for large and symptomatic lesions, and consists of surgical excision with curettage and subsequent bone grafting (62). In contrast, the majority of asymptomatic IGCs will not require any treatment (62). Recurrences after surgery have been reported (62, 70, 71).

### 1.2.4 Chondroblastoma

Chondroblastoma is a rare benign, though locally aggressive bone tumour (4, 72). Chondroblastoma was first described as a cartilage-gaining giant cell tumour (GCT) by Kolodny in 1927, then characterized as an "epiphyseal chondromatous giant cell tumour" by Codman in 1931. Later, in 1942, Jaffe and Lichtenstein described it as a separate entity from GCT (72). Chondroblastoma accounts for less than 1% of all bone tumours. Males are affected twice as often as females (4). Most chondroblastomas occur in the second and early third decades of life, although they can present at any age (4, 73). The most common localizations of chondroblastomas are the epiphyses of long bones (4, 73). The most frequently affected bone is the femur, followed by the proximal tibia and the proximal humerus (4, 73). It may also occur in the talus and the calcaneus, particularly in an apophysis or close to the articular surface, as well as in the patella or in pelvic bones (especially the acetabulum) (4). Other less frequent localizations include flat bones, for example the scapula or the ribs, as well as small bones of the hand and feet, and vertebrae (4, 72, 74). Presentations in craniofacial bones are considered exceptional (4).

The time between the occurrence of first symptoms and definitive diagnosis ranges from less than one month to several years. Clinical symptoms vary with the site of disease (4). They include moderate to severe pain, combined with local tenderness, or the occurrence of a pathologic fracture. Moreover, swelling, joint effusion, and a limp might be present (72-74).

Radiologically, chondroblastoma constitutes a well-demarcated, geographic, eccentric, oval or round lytic lesion (4). Chondroblastoma is typically localized in the epiphysis or in the epiphysis and the adjacent metaphysis in close proximity to a former

growth plate (72, 73). A sharp sclerotic margin, as well as mineralization, trabeculation, cortical erosion, and expansion are found frequently (4, 72, 73). The size of chondroblastomas usually amounts to less than 5 cm (4, 72, 73). On MRI scans, chondroblastomas characteristically exhibit reactive changes outside the tumour and particularly present with a strong perifocal edema in fluid-sensitive and gadolinium-enhanced images (4, 75). In **figures 7a-7c**, an X-ray and MRI scans of a chondroblastoma of the left proximal humerus are shown.


**Figures 7a, 7b and 7c: (7a)** X-ray, **(7b)** coronal T1-weighted and **(7c)** sagittal contrast-enhanced T2-weighted **(c)** MRI scans of the left proximal humerus of a male patient at the age of 15 years. Images show a geographical lesion that is predominantly localized in the epiphysis and epi-metaphysis. The lesion measures 2.7 cm in its proximodistal diameter and shows little sclerotic rim. Perifocal bone marrow edema as a sign of aggressive growth can be observed in contrast-enhanced sequences. However, cortical thinning or scalloping cannot be observed.

Radiological differential diagnoses include GCT, primary aneurysmal bone cyst, clear cell chondrosarcoma, chondromyxoid fibroma, Langerhans cell histiocytosis, and chondroblastoma-like osteosarcoma (73, 76).

The etiology of chondroblastoma is still unknown (4). However, genetic alterations of the *H3.3* gene seem to be involved in the pathogenesis of various tumour types, including bone tumours such as chondroblastoma and GCT (4). Particularly *p.Lys36Met* substitutions were associated with chondroblastoma, and it is thought that these may provide a growth advantage for neoplastic cells (4, 77-79). Typically, these specific genetic alterations in chondroblastoma, i.e. *p.Lys36Met* substitutions, can be detected in the *H3F3B* gene on chromosome 17 (4, 77-79).

Histologically, chondroblastoma consists of layers of ovoid to polygonal cells with small singular grooved nuclei and eosinophilic cytoplasm (4). Typically, osteoclast-like giant cells and islands of eosinophilic chondroid matrix are present (4). Moreover, nuclear atypia and mitotic figures may be found (4). Pericellular calcifications are characteristically observed (4). Also, secondary aneurysmal-bone-cyst-like changes are often present (4). In **figure 8**, a histopathologic image of a chondroblastoma is shown.

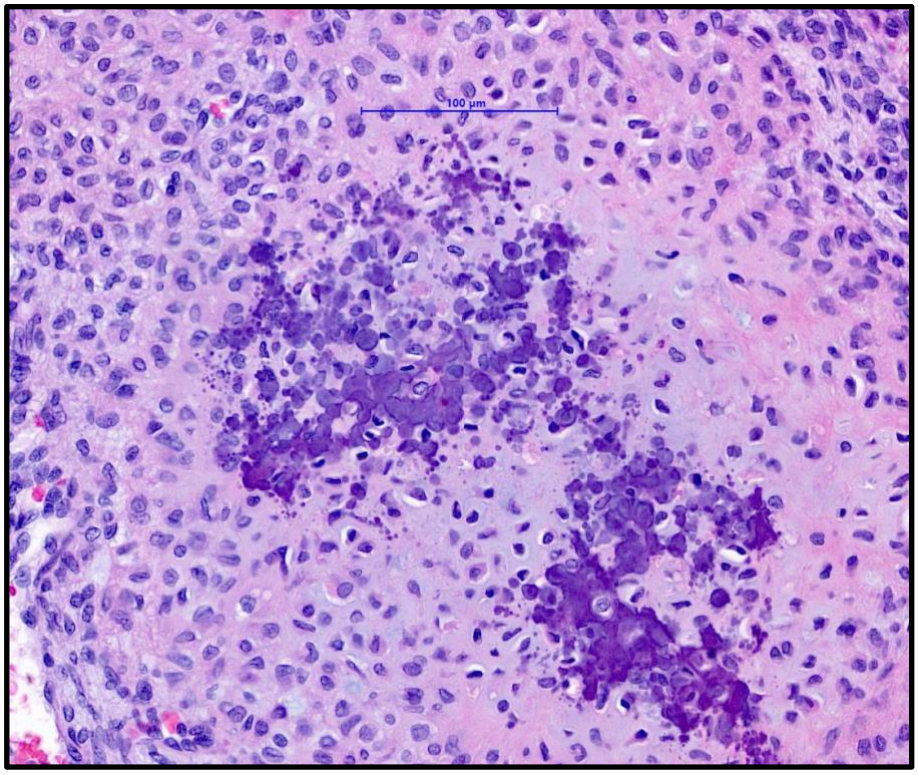


**Figure 8:** Histopathologic image of a chondroblastoma, with the kind permission of Univ. Prof. Priv. Doz. Dr. Bernadette Liegl-Atzwanger, Diagnostic and Research Institute of Pathology, Medical University of Graz. Chondroblastomas possess a

characteristic morphological profile, composed of ovoid to polygonal cells with small singular nuclei and eosinophilic cytoplasm, and osteoclast-like giant cells.

As no effective medical treatment is available and spontaneous healing has not been observed, surgical management is indicated (72, 73, 76). The treatment of choice is curettage with or without local adjuvant treatment of the surgical bed with subsequent bone grafting (4, 72, 73, 76). Importantly, surgical interferences with open growth plates and contamination of adjacent joints must be avoided (72, 73, 76). Radiofrequency ablation may be considered as an alternative to surgery in selected cases (4, 80).
It is thought that more than 80 % of chondroblastomas can be successfully treated with surgery (4). However, these tumours may recur, with recurrence rates depending on the site of the lesion and thus varying between 10% to 18% according to WHO 2020 (4, 82, 74). Exceptionally, spreading to the lungs may occur, even though these lesions are usually non-aggressive in their biological behaviour (4, 73).

### 1.2.5 Fibrous dysplasia (FD)

Fibrous dysplasia (FD) is a sporadic benign medullary fibro-osseous neoplasm that may occur multifocally and is typically characterized by distorted, poorly organized, and inadequately mineralized bone and intervening fibrous tissue (4, 81, 82). FD is typically localized in the craniofacial bones and the femur, both in monostotic and polyostotic forms (4, 81, 82). However, it might affect any bone (4, 81, 82). The monostotic form characteristically involves the femur, skull, tibia, and ribs (4). The polyostotic form typically involves the femur, pelvis, and tibia (4). FD displays an equal sex distribution and may occur in children as well as in adults (4).
FD can occur as a monostotic or polyostotic disease (4): the monostotic form, which only affects a single skeletal site, is six to ten times more common than the polyostotic form, which by definition affects more than one bone (4, 81, 82). Polyostotic FD may be restricted to one extremity or one side of the body, or it might be generalized (4). There are polyostotic manifestations that are combined with other conditions, even though these cases are rare and only account for approximately 3% of reported FD

cases (4, 83). Amongst those, McCune-Albright syndrome is defined by a combination of FD with endocrinopathies and abnormalities in cutaneous pigmentation, such as café-au-lait-like skin alterations (84). In Mazabraud syndrome, FD coincides with intramuscular myxomas (81). Infrequently, FD produces excess FGF23, which may result in osteomalacia similar to tumour-induced osteomalacia (4, 85).

Regarding its clinical presentation, FD is often asymptomatic, even though it may also cause bone pain, severe bone deformity, including leg-length discrepancies or scoliosis, and fractures (86). If FDs affect craniofacial bones, they may cause serious deformities and complications depending on the site of involvement, such as asymmetries, vision loss, or hearing impairment due to cranial nerve compression (87). Very rarely, malignant transformation is observed (4, 86, 87). Particularly polyostotic forms usually become symptomatic in childhood or adolescence, whereas monostotic manifestations typically stay asymptomatic until adulthood (4).

On plain X-rays, FD typically appears as a geographical lesion with a characteristic ground-glass matrix (4). Sometimes, cartilaginous components can be present (4). Longstanding FD may cause bone deformity, such as the so-called shepherd's crook deformity of the proximal femur, which is highly diagnostic (4, 88). Neither soft tissue extension nor periosteal reaction can be observed (4).

Polyostotic disease can be diagnosed and/or monitored using various imaging modalities, including (whole-body) MRI, CT, and bone scintigraphy (4). In **figures 9a-9c**, an X-ray, as well as a CT and MRI scan of a fibrous dysplasia of the right femoral neck are shown.

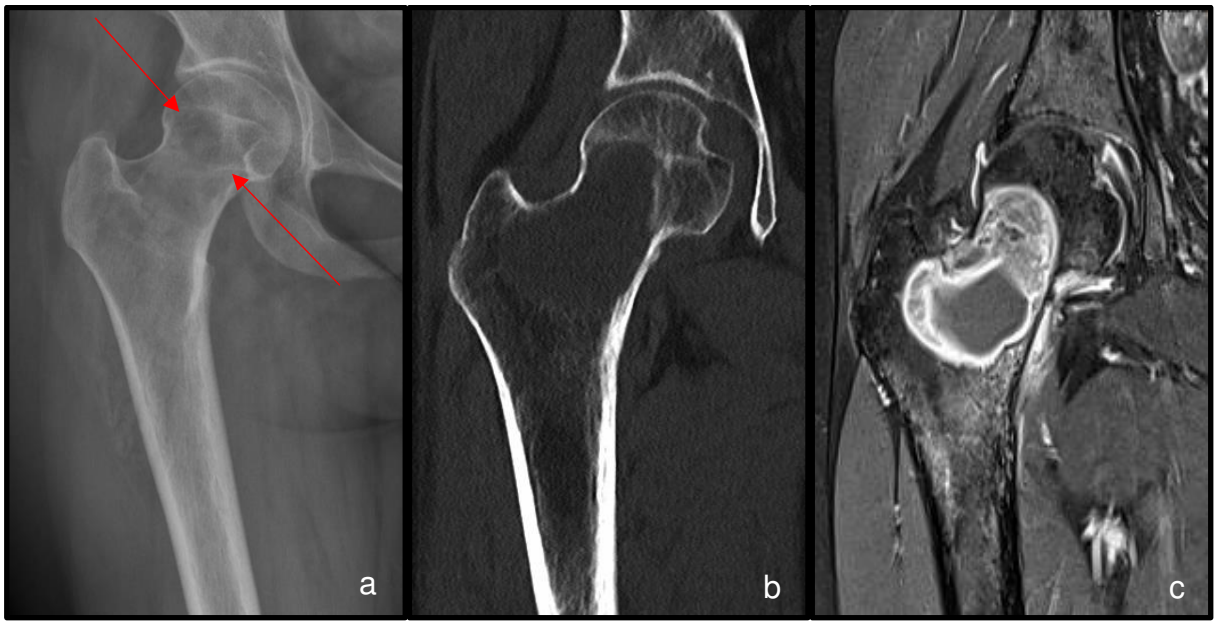


**Figures 9a, 9b and 9c: (9a)** X-ray, **(9b)** CT, and **(9c)** contrast-enhanced T2-weighted MRI scans of the right proximal femur of a female patient at the age of 29 years. Images show a lucent, geographical lesion with a ground-glass matrix. The lesion measures 5.5 cm in its proximodistal diameter and lacks a sclerotic rim. Furthermore, cortical thinning can be observed.

FD is caused by activating missense mutations in exon 8 of the *GNAS* gene on chromosome 20q13.32, which are present in 70-80 % of FD cases (4, 89-91). These *GNAS* mutations ultimately result in inhibition of the terminal maturation and differentiation of osteoprogenitor cells, resulting in the development of fibro-osseous lesions (89). Moreover, an over-production of the pro-resorptive cytokine RANKL (Receptor activator of nuclear factor kappa beta ligand) by immature osteoblasts leads to enhanced osteoclast formation and thus increased bone resorption in FD (92). Additionally, previous studies have shown that interleukin-6 (IL-6), which is emitted by mutant stroma cells in FD, might affect bone resorption linked with FD, concordant to its effect in rheumatic inflammatory diseases (93, 94). All these mechanisms possibly result in and/or contribute to the replacement of normal bone by fibro-osseous tissue in FD (89, 92-94). *GNAS* mutations have also been detected in cases of McCune-Albright syndrome (4).

Histopathologic examinations show fibrous and osseous tissues in varying proportions (4). The fibrous component consists of bland fibroblastic cells (4). Mitoses are rather

uncommon, but may be observed in case of a pathologic fracture (4). The osseous component is composed of irregular trabeculae of woven, sometimes lamellar, bone (4). Additionally, cementum-like bone deposition and calcifications may be found (4). In **figure 10**, a histopathologic image of a case of FD is shown.

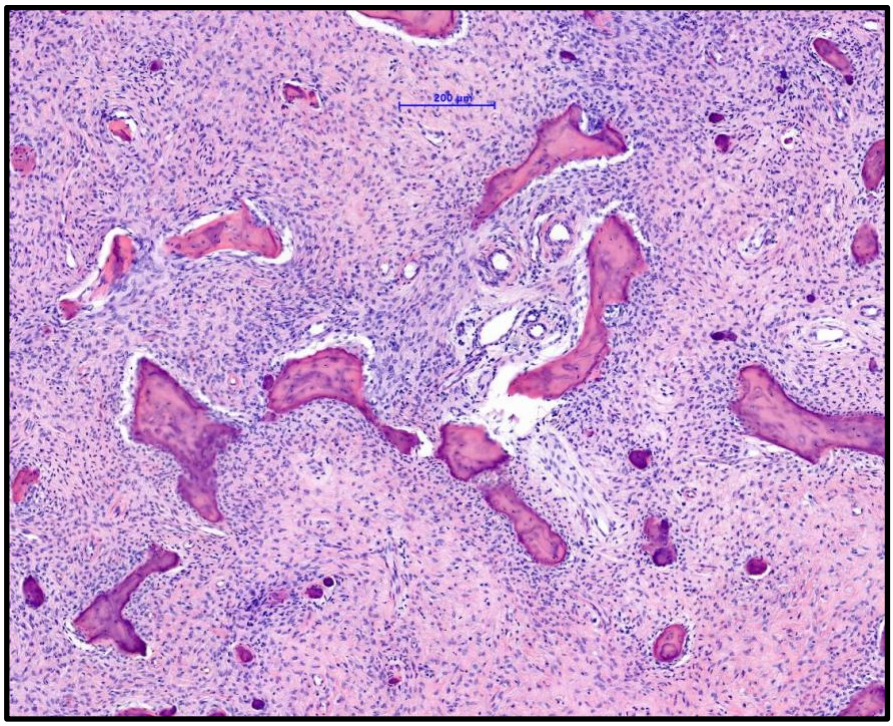


**Figure 10:** Histopathologic image of a case of fibrous dysplasia, with the kind permission of Univ. Prof. Priv. Doz. Dr. Bernadette Liegl-Atzwanger, Diagnostic and Research Institute of Pathology, Medical University of Graz. Fibrous dysplasia is composed of fibrous and osseous tissues in varying proportions. Bland fibroblastic cells are mixed with irregular bone trabeculae.

Therapeutic management of FD depends on the site of involvement and its clinical presentation (88, 95, 96). If lesions are asymptomatic, a watch-and-wait strategy can be pursued (88, 95, 96). Surgery is indicated in case of progressive deformity, painful lesions, nonunion after pathologic fracture, failure of and progression under non-surgical therapy, and malignant transformation (88, 95, 96).
Surgical treatment strategies include curettage with subsequent bone grafting, the osteosynthesis of fractures, correction of bone deformities, nerve decompression, or aesthetic corrections (88,95,96). If large lesions or extensive disease in polyostotic FD

cannot be treated surgically, pharmacologic agents targeting osteoclasts may be a therapeutic alternative in selected cases (81). In this context, studies reported that the combined oral and intravenous application of biphosphonates results in an improved cortical thickness, progressive intralesional ossification, decreased lesional diameters, pain reduction, and prevention of pathologic fractures (97-100). Moreover, denosumab, an antibody acting against RANKL, has been proposed as a treatment option in recent literature (101, 102). Denosumab has been reported to induce a decrease in lesional activity, to support osteogenic cell maturation and bone formation, and to reduce symptoms associated with FD in a recent study by Castro et al. (102). However, these treatment effects of bone resorption inhibitors, such as bisphosphonates and denosumab, are only transient and cease upon termination of the drug treatment. After treatment termination, complications such as a marked bone-turnover rebound combined with hypercalcemia may occur, as was reported by Castro et al. (102). Thus, these drug treatments might be beneficial in selected cases, but need to be handled with care and in recognition of potential side effects (100-102).
Overall, prognosis of FD is excellent in terms of survival (4, 84, 86). Nevertheless, this disease may cause skeletal deformities, leg-length discrepancies, impingement of cranial nerves, or may even be crippling, particularly in cases of severe polyostotic disease (4, 84, 86).

### 1.2.6 Langerhans cell histiocytosis

Langerhans cell histiocytosis (LCH) describes a clonal neoplastic proliferation of myeloid dendritic cells displaying a Langerhans cell (LC) phenotype (4, 103, 104).
LCH is exceptionally rare and occurs primarily in the pediatric population, with an incidence of 5 cases per 1 million in children, compared to 1 - 2 cases per 1 million in adults (4). Moreover, LCH is more common in the European and Hispanic population (4, 105). Males are affected more often compared to females (m:f = 1.2:1) (4, 105).
The extent of the disease and thus the clinical spectrum may vary: LCH can occur as a single-system or as a multisystem disease (4). In a single-system disease, LCH is confined to one organ/system (usually bone), even though it may cause unifocal or multifocal lesions in this affected system (4). Single-system LCH, which was previously

referred to as “histiocytosis X” or “eosinophilic granuloma”, particularly involves bones, such as the skull, femur, vertebrae, pelvis, ribs, or the mandibles (4, 104, 105). However, also, lymph nodes, skin, and lungs may be affected, though this is less frequently observed (4, 104, 105).

In multisystemic LCH, two or more systems are involved to a varying extent, with solid organs, such as the liver and the spleen, being more commonly affected (4, 104). Furthermore, multisystemic LCH also frequently extends into the skin, the bone, and the bone marrow (4, 104). Multisystemic LCH was previously referred to as “Hand-Schüller-Christian disease” in cases of multifocal disease, or as “Letterer-Siwe disease” in cases of disseminated visceral involvement, even though these terms are no longer recommended by the WHO (4).

With regards to clinical presentation, multifocal and disseminated disease usually occurs in younger patients compared to localized LCH (104). Single-system LCH typically affects older children or adults who present with a painful lytic lesion eroding the cortex (4). In other sites, soft-tissue masses can be indicators for solitary lesions (4). Multifocal single-system LCH is typically observed in young children, who present with multiple destructive bone lesions that are frequently associated with adjacent soft tissue masses (4, 104, 106). Multisystemic and disseminated LCH typically affects infants and causes fever, cytopenia, skin and bone lesions, and hepatosplenomegaly (4, 104, 106).

Other clinical symptoms depend upon the sites of involvement: Lesions of the spine can cause localized neck or back pain, which is often associated with a decreased range of motion, and may even result in secondary malalignment and deformities, as for instance a torticollis (106, 107). Other symptoms may be radicular nerve pain, muscular weakness, palsy, and/or bowel and bladder dysfunction (107). Cranial bone and parenchymal involvement can cause pituitary dysfunction (4, 108, 109). Consequently, secondary diabetes insipidus can arise, as well as other endocrinopathies involving for instance thyroid and growth hormones (108, 109). Extraskeletal manifestations primarily affect the skin, inducing characteristic papulosquamous granulomatous lesions of the scalp, as well as mucosal lesions in the oral cavity and the genital regions (110). Cystic lung involvement may also occur, especially in adults aged between 20 and 40, and is strongly associated with tobacco

abuse (111). Apart from the abovementioned symptoms, many more can occur, depending on the sites of involvement and the extent of disease (4, 106-111).

If bones are affected, as is the case in most patients with isolated LCH, the lesions typically occur in the diaphysis and metaphysis of long bones, but only rarely in the epiphyses (106). On conventional X-rays, LCH lesions present as radiolucent bone destructions that can either appear as well-demarcated geographical lesions or show a permeative pattern of bone involvement (104). Bony septa within the lesions may give them a bubble-like appearance (104). Periosteal reactions, endosteal scalloping, and marginal sclerosis have been observed (104, 111, 112). Radiological differential diagnoses include osteomyelitis and chondroblastoma (104). Vertebral infiltration may cause pathologic fracture and a subsequent collapse of the vertebral body, resulting in the characteristic aspect of a vertebra plana, which is especially found in children (104). Multisystemic disease needs to be ruled out by whole-body exams, that may involve CT-/MRI- and particularly FDG-PET-scans (Fluorodeoxyglucose-positron emission tomography) (104, 113).

In **figure 11**, an X-ray of a case of LCH of the left femur is shown.

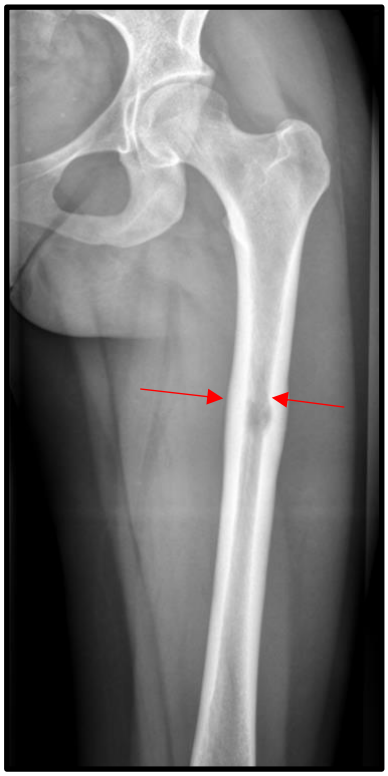

**Figure 11:** X-ray of a case of LCH in the left femoral diaphysis of a female patient at the age of 24 years. The image shows a lytic lesion that mainly involves the diaphysis or metadiaphysis of long bones. The lesion measures 2.0 cm in its proximodistal diameter and lacks a sclerotic rim. Moreover, endosteal scalloping, a periosteal reaction, and cortical thinning can be observed.

Histological appearance of LCH is defined by clusters of Langerhans cells within a reactive inflammatory cell background, including variable numbers of eosinophils, lymphocytes, and macrophages (4, 113). Multinucleated giant cells can be present (113). LCH cells show an immunohistochemical positivity for CD1a, CD207, S100, CD68, and *HLA-DR* (Human leukocyte antigen - DR isotype) (4, 105).
Activation of the mitogen-activated protein kinase (*MAPK*) pathway is considered to be essential for LCH pathogenesis (4). Activating *MAPK* mutations at different stages of myeloid differentiation have been proposed to define the extent of disease, ranging from high-risk multisystem to multilocal low-risk to unilocal LCH (4, 105, 114). *MAPK* activation is induced by various activating somatic mutations, particularly of *BRAF* (V-raf murine sarcoma viral oncogene homolog B), which can be detected in more than 85 % of LCH (4, 113-116). *BRAF p.Val600Glu (V600E)* mutations have been reported to be associated with a higher relapse risk and a worse clinical outcome (4, 117, 118). In **figure 12**, a histopathologic image of a case of FD is shown.

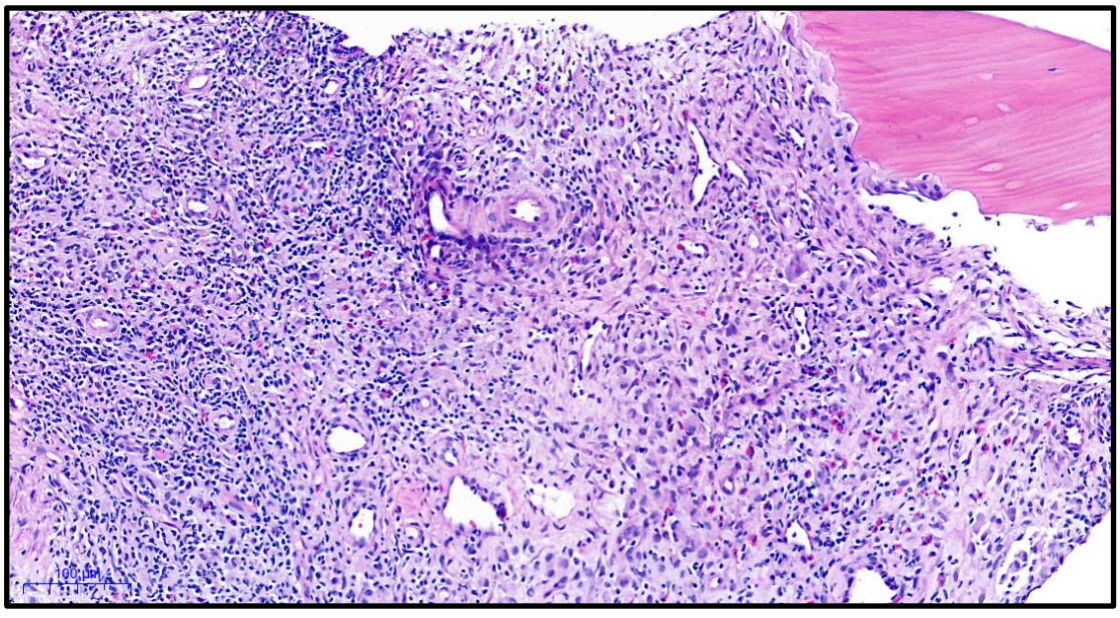

**Figure 12:** Histopathologic image of a case of LCH, with the kind permission of Res. Prof. Priv. Doz. DDr. Iva Brcic, Diagnostic and Research Institute of Pathology, Medical University of Graz. LCH possesses a characteristic morphological profile with clusters of Langerhans cells embedded in a background of reactive inflammatory cells.

Therapeutic management of LCH depends on the site(s) of involvement, the extent of the disease and the clinical symptoms. Unifocal LCH is usually curable, with 5-year survival rates exceeding 90% (4, 113). Local therapy includes surgical resection and (in bone lesions) curettage (with or without bone grafting), and should only be considered if the intervention is not severely morbid or mutilating (112). Radical excision is not recommended (104, 111). No adjuvant treatment is required after surgery (113). Remission can even occur after limited curettage or even after diagnostic biopsy without further therapy (104, 111, 113). Thus, also careful observation is an option in selected cases, as isolated lesions may show complete or partial spontaneous remissions (104, 111, 113). Isolated vertebra plana is usually treated conservatively via observation, possibly combined with a short-term immobilization for pain reduction, as invasive treatment methods are associated with potential risks and side-effects (104, 111). Intralesional corticosteroid injections (e.g., methylprednisone or triamcinolone) are an attractive alternative to surgery, depending on the location of the lesion (113, 119). Low-dose radiation therapy (e.g., 10-20 Gray) may be considered for painful, progressive lesions that are risky to access surgically, or in bone lesions if adjacent soft-tissue components are present (113, 119). Treatment regimens for multifocal and multisystemic disease, as well as for unifocal disease in locations that are not amenable to local therapies (e.g., central nervous system, pituitary gland), usually involve systemic drug treatments, including chemotherapies, bisphosphonates (particularly in cases of multifocal bone involvement), systemic corticosteroids, immunomodulatory drugs, and targeted therapeutics (particularly *BRAF*- and *MAPK*-inhibitors) (113, 120, 121). However, treatment strategies can be multimodal and need to be adapted based on the extent of disease and the sites of manifestation.

Prognosis depends on the organ involvement and the treatment response (113, 121, 122). Survival is excellent in unifocal LCH with five-year overall survival rates of >90%

(113, 121, 122). Due to evolving systemic treatment options, survival is also good for patients with multisystem/disseminated LCH: five-year overall survival rates of approximately 90% have been reported even in this population (113, 121, 122), and mortality rates of less than 20% in patients with risk-organ multisystem LCH (4, 105, 121, 122).

### 1.2.7 Rosai-Dorfman disease

Rosai Dorfman disease (RDD) constitutes a histiocytic proliferation that involves large S100-positive histiocytes with emperipolesis (4). The latter describes the enclosement of viable lymphatic cells by histiocytes (123-125). RDD is a rare disease that primarily affects lymph nodes, but may also occur at extranodal sites in approximately 40% of patients. The bone is affected in about 2-10% of cases, but primary bone involvement is comparatively rare (4, 123, 124). The syndrome can occur in any age group, however, the mean age at diagnosis is 31 years according to the WHO 2020. The sex distribution is equal (4, 124).

The main localization of primary intraosseous RDD is in the metaphysis of long bones, and the craniofacial skeleton (4). In the majority of cases (71%), a single bone is involved (4, 124).

Clinical symptoms vary depending on the site of involvement (4). In cases of bone involvement, patients usually experience pain in the area surrounding the affected bone. Pathologic fractures are rarely described (4). Moreover, this disease frequently presents with signs of cervical lymphadenopathy due to histiocytic infiltration of the expanded lymph nodes. This lymphadenopathy is usually painless and bilateral. Affected lymph nodes are small and mobile in the initial stages of disease, but become increasingly adherent with disease progression, until they finally form large multinodular masses (125). Even though cervical lymph nodes are affected in the majority of cases (87.3%), also axillary (23.7%), inguinal (25.7%), and mediastinal (14.5%) lymph nodes may be involved (126). Furthermore, extranodal manifestations may occur, which predominantly affect the head and neck region, especially the skin, nasal and paranasal cavities, subcutaneous tissue, orbit, eyelids, and bones. Organ involvement is observed in approximately 58% of patients (124). In addition to the

abovementioned symptoms, also fever, anemia, leukocytosis, neutrophilia, increased erythrocyte sedimentation rate, and hypergammaglobulinemia may be present (126, 127).

Radiologically, RDD appears as a well-defined lytic, sometimes expansive, septated mass (4). In some patients, cortical thickening and periosteal reaction are observed (4). In **figure 13**, an X-ray of a case of RDD of the right acetabulum is shown.

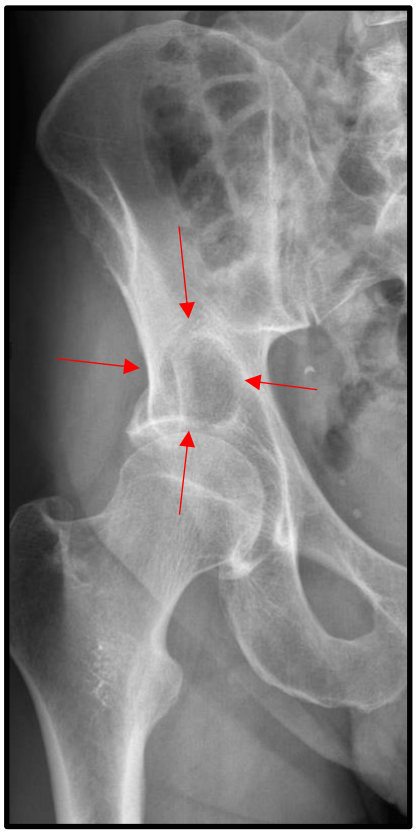

**Figure 13:** X-ray of a case of RDD in the right acetabular region of a male patient at the age of 49 years. The image shows a lytic lesion with well-defined boundaries. The lesion measures 2.8 cm in its proximodistal diameter and has a sclerotic rim. Moreover, a slight affection of the cortex can be observed.

Differential diagnoses particularly include other types of clonal histiocytic proliferations, chronic inflammatory conditions, or lymphadenopathies, for example Langerhans cell histiocytosis, osteomyelitis, Erdheim-Chester disease, Castleman's disease, dermopathic lymphadenitis, mucocutaneous lymph node syndrome, also called Kawasaki's disease, histiocytic necrotizing lymphadenopathy, also called Kikuchi's

disease, vascular transformation of lymph nodes, inflammatory pseudotumours of a lymph node, and lymphoma (4, 48, 123).

Histologically, sheets and clusters of large histiocytes with round or oval to reniform nuclei are present (4). The tumour displays indistinct margins, replaces the normal bone marrow and infiltrates the adjacent cortical bone, resulting in local bone resorption (4, 128).

The etiology of RDD is still unknown (4). However, constitutive activation of the *RAS/MAPK* pathway, which is essential for monocyte maturation, has been described in a subset of cases (4, 129). Furthermore, driver mutations in *NRAS*, *KRAS*, *MAP2K1*, *ARAF*, and *BRAF* have been detected in approximately 33-40 % (4, 130-132). Furthermore, germline mutations in *SLC29A3* and *FAS* (*TNFRSF6*) have been linked to the rare familial form of RDD (4, 130).

In **figure 14**, a histopathologic image of a case of RDD is shown.

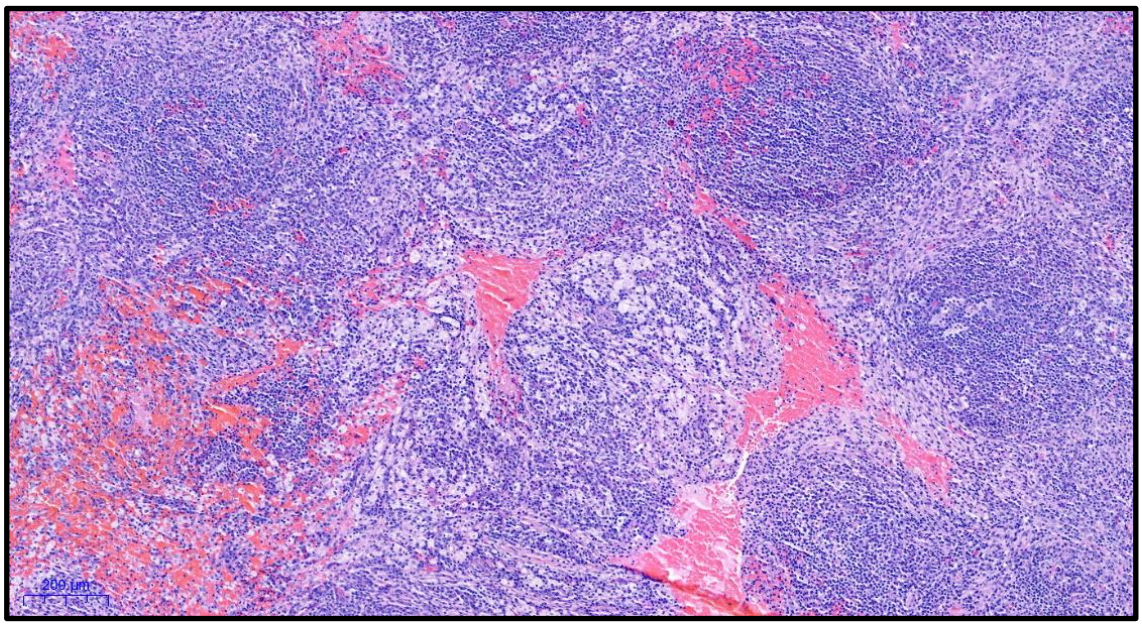


**Figure 14:** Histopathologic image of a case of RDD, with the kind permission of Res. Prof. Priv. Doz. DDr. Iva Brcic, Diagnostic and Research Institute of Pathology, Medical University of Graz. RDD possesses a characteristic morphological profile, composed of clusters of large histiocytes with round or oval to reniform nuclei that replace normal bone marrow.

Currently, no specific treatment is available for RDD (130). However, treatment is obligatory if the syndrome causes severe and potentially life-threatening symptoms, for instance airway obstruction, neurologic or ocular compressions (133, 134). Treatment options include local as well as systemic approaches, depending on the site and symptoms (133, 134). Systemic options include corticosteroids, systemic chemotherapy, and immunomodulating agents (128, 133). Local measurements comprise radiotherapy and surgery with partial or complete resection (128, 133). In general, prognosis of RDD is good (4). However, generalized lymphadenopathy, extranodal involvement of multiple organs, such as the kidneys, lungs and liver, as well as disease-associated immunologic dysregulations are associated with a poor prognosis (133).

## 1.3 Bone graft substitutes

The standard treatment regarding benign and low-grade malignant bone tumours involves intralesional curettage and subsequent filling with autologous, allogenic, or artificial bone grafts (135, 136). The aim of filling instead of leaving the bony cavity empty is mainly to achieve enhanced stability and accelerated remodeling into mature bone (135, 136). However, this remodeling might lead to radiological difficulties in identifying recurrences.
The following chapter will provide a short overview of autologous, allogenic, and artificial bone grafts.

### 1.3.1 Autologous bone grafts

Various types of bone grafts can be used, such as cortical, cancellous, corticocancellous, and vascularized bone grafts (137). Cancellous bone grafts are rich in mesenchymal stem cells and are associated with high osteogenic and osteoconductive potential, and rapid revascularization. They are used to improve fracture healing and bony union in arthrodesis and non-unions, and to fill bone defects (138, 139).

Amongst cancellous bone grafts, the iliac crest bone graft (ICBG) is the most commonly used graft. Particularly the anterior portion of the iliac crest was long considered as the gold standard for ICBG harvesting (140). However, harvesting grafts from the anterior portion of the crest is associated with more side effects compared to the grafts harvested from the posterior part of the iliac crest (140, 141). As an alternative to ICBGs, the reamer irrigator aspirator system has been introduced for the harvesting of grafts (142). This method repurposes an instrument used to drill, enlarge and/or clean the bone marrow cavity of long bones. It allows to harvest cancellous bone from bone marrow cavities, particularly the femur via an antegrade approach from the greater trochanter (142, 143). This method has been reported to be less invasive, to cause less donor site morbidity, and to harvest a greater graft volume from the intramedullary canal of long bones than obtained via ICBG (142, 143). The average graft volume harvested by RIA is approximately 40 cubic centimeters (cc), compared to around 25 cc regarding ICBG (142, 143). Altogether, RIA is associated with fewer complications than ICBG (142, 143).

In contrast to cancellous bone grafts, cortical grafts are characterized by their good mechanical stability, even though they possess only moderate osteoconductive, osteoinductive, and osteogenic properties (144). They are used less frequently compared to cancellous grafts, with their main application being segmental bone defects smaller than 5 cm (144).

On the other hand, corticocancellous bone grafts combine the advantages of both cortical and cancellous bone grafts (139-145). They provide high mechanical stability and good ingrowth (139-145). For example, corticocancellous grafts are commonly harvested from the iliac crest and used in the surgical treatment of non-unions (138, 139, 144, 145).

Vascular bone grafts are harvested with the aim to provide good vascularization to accelerate graft incorporation. The most commonly used vascularized bone graft is a vascularized fibula autograft (146).

Regardless of the harvesting method applied, autologous bone grafting causes complications and comorbidities that are often underestimated. In particular, donor site morbidities need to be considered and communicated to the patients (136). The latter include chronic local pain, sometimes accompanied by lateral femoral cutaneous nerve

lesions, and iliac wing fractures. In addition, the harvesting of autologous bone grafts bears the risk of infection and delayed wound healing, furthermore the risk of injury of neuro-vascular structures, or the development of heterotopic ossifications (137).

### 1.3.2 Bone allografts

Owing to the limitations in the available quantity of autologous bone substitutes and the associated donor-site morbidities, allograft materials are a promising alternative in orthopaedic bone reconstructions. Bone allografts are osteoconductive agents obtained from living or deceased human donors and provide a scaffold for bone formation. They can be prepared fresh or frozen. Moreover, they are available in several different forms, e.g., cortical, cancellous, and corticocancellous (147, 148). However, several concerns have been raised in context with allografts. Common concerns include their potential to induce immune reactions against the foreign tissue (immunogenicity), that may lead to an insufficient graft incorporation, furthermore issues with product sterilization, and consecutive risks of microbial contamination of donor tissues (147, 148). Studies in dogs suggested that fresh allografts were associated with elevated anti-HLA (Human leukocyte antigen) antibody levels in adjacent synovial fluids compared to frozen allografts, indicating a higher immunogenic potential of fresh compared to frozen allografts (149, 150). Apart from freezing allografts, irradiation was shown to reduce the cellularity of allograft bone, though without statistical significance (151).

Importantly, also the availability and costs of allografts need to be taken into account. Larger hospitals often have in-house tissue collections, which provide them easier access to allografts. However, tissue collections require regular controls and certifications (148). If in-house tissue collections are not available, costly allografts need to be obtained from other sources, and time until delivery needs to be considered during planning of the surgery (148).

Furthermore, a graft needs to be sterile in order to reduce the risk of transmission of infectious diseases from the donor to the recipient (147). Grafts are usually sterilized via the use of gamma-irradiation (147). A review of reconstructive procedures in tumour surgery, conducted by the Harvard University, describes infection rates of up

to 12.8% after the use of allografts (152). However, many of these patients previously underwent chemotherapy or irradiation, and thus showed an increased a priori risk of infection. Another limitation of this study was that no differentiation between irradiated and fresh-frozen allografts was performed (152). Another study demonstrates that the safety of bone allografts has noticeably increased during the past decades, as nowadays, adequate donor screening and more precise testing procedures are available (153).
Furthermore, biological aspects of allografts need to be considered, in particular the risk of delayed union or non-union at the graft-host interface due to the allogenic tissue (154, 155).

### 1.3.3 Artificial bone graft substitutes (ABGS)

Surgical adjuvants, such as ABGS, have become increasingly popular, as they are not associated with donor site morbidities as autografts are, nor do they bear a risk of transmitting infectious diseases as allografts do (136). Moreover, access to them is not restricted, and they are comparatively cheap (136). Several ABGS are currently available, including demineralized bone matrix, bone graft extenders, and bone morphogenic proteins (156-160). Demineralized bone matrix consists of proteins extracted from processed cadaver bone without minerals (156-160). Bone morphogenic proteins stimulate new bone formation by inducing osteoblastic differentiation (156-160). Bone graft extenders include ceramics (e.g., hydroxyapatite), salts (e.g., calcium sulfate (CS), tricalciumphosphate (TCP)), and synthetic products, such as polymethylmethacryclate (PMMA). They are variably moldable and consequently, they can be used to fill irregularly shaped bony defects (156-160).
Hydroxyapatite is an example of ceramics (161). It is supposed to resemble the basic component of a bone's mineral phase. Hydroxyapatite is osteoconductive and osteointegrative, but not osteoinductive or osteogenic (161).
Another commonly used ABGS is PMMA, which has been in use for over a century and is commonly referred to as “bone cement”. It consists of a polymerized ester of acrylic acid that reaches a strength comparable to native bone (162). During surgery, the rigid and transparent plastic can be prepared as a paste that subsequently

hardens. PMMA has no osteogenic or osteoinductive properties, and is only osteoconductive when prepared as a porous construct (162). PMMA yields excellent strength and might be used as temporary structural support. Furthermore, it is inert and therefore can be used for the delivery of antibiotics to infected bone areas (161). Moreover, bone cement offers the advantage of potentially earlier diagnosis of bone tumour recurrence, as it provides smooth borders to the remaining bone. In contrast, other ABGS, such as tricalcium phosphates, induce bone remodeling, so that the diagnosis of a recurrent tumour may be delayed (161, 162). Nevertheless, intraoperative preparation of the PMMA may be subject to variation and pitfalls. Also, bone cement does not resorb (161, 162). Thus, additional surgery might be required to remove the PMMA if necessary (161, 162). Due to its durability and inability to be resorbed, the bone cement itself might become a nidus for infection (161).

Calcium sulfate (CS) is an example of a salt used as a bone graft extender (161, 163). CS is osteoconductive, but not osteoinductive. Even though CS is seven times weaker than cortical bone, it offers more strength than cancellous bone grafts (161, 163). CS is available in the form of blocks, injectable material, or pellets (161, 163). The main disadvantage lies in its fast resorption, which is particularly troublesome in elderly or chronically ill patients with delayed bone healing (161, 163).

Tricalciumphosphates (TCP) are another example of salts used for bone grafting. TCPs are characterized by their biocompatibility, favorable osseous integration profile, and osteoconductive properties (164, 165). Beta-TCP is a synthetically produced inorganic substance that combines the two predominant minerals in bone, in particular calcium and phosphate (161). Cerasorb® (Curasan-AG, Kleinostheim, Germany) is an example of a pure-phase beta-TCP (166-168). In contrast to alpha-TCP, beta-TCP is thermodynamically stable in a biological environment and within a normal temperature range. Biodegradation is also faster compared to alpha-TCP. Cerasorb®'s safety profile has been investigated and demonstrated in several preclinical and clinical studies (166-168).

## 1.4 Purpose

This retrospective study intends to evaluate the osseous integration profile of the ABGS Cerasorb® (Curasan-AG, Kleinostheim, Germany), a beta-tricalcium phosphate in granular form, and to determine potential associated complications.

# 2 MATERIALS AND METHODS

## 2.1 Inclusion and exclusion criteria

We included patients with benign and low-grade malignant bone tumours, who were treated by curettage and filling with the ABGS Cerasorb® at the Department of Orthopaedics and Trauma of the Medical University of Graz, Graz, Austria between November 2018 and July 2021. The study was approved by the local ethics committee (EK 34-139 ex 21/22) (1).

Clinical files and imaging studies of these patients were retrospectively reviewed (1). Only patients with benign and low-grade malignancies, which were suspected clinically and radiologically, or histologically confirmed via biopsy, were included, as curettage and filling were not indicated in case of high-grade malignancies, as outlined in the background section of this dissertation (1).

Prior to surgery, patients were thoroughly informed about advantages and disadvantages of filling with an ABGS, and written informed consent was obtained from all of them (1). Pre-operative imaging included conventional two-planar X-rays, as well as contrast-enhanced MRI scans and, in selected cases, CT imaging. Imaging studies were analyzed by an expert tumour radiologist (1). If entity and dignity of the lesions could not be sufficiently diagnosed based on clinical and radiological information, biopsies were performed and examined by expert bone tumour pathologists (1). The decision to conduct surgery was made based on a lesion's size, its expected potential of tumour progression, and its risk of pathologic fracture. Following surgical excision, histopathological examinations of the removed tissue were performed and examined by expert bone tumour pathologists (1).

## 2.2 Surgical procedure

Surgical approaches were conducted according to oncological principles of bone tumour surgery (1). Following surgical exposure of the affected bone, the lesion was

accessed via an osseous window. Curettage was performed using sharp curettes under radiological control (1). Curettage was carried out until there was no further clinical or radiological evidence of any residual tumour tissue. The curetted tissue was sent for histopathological examination (1). All diagnostic evaluations were performed by expert bone tumour pathologists and classified according to the WHO Classification 2020 (1, 4). The ABGS (Cerasorb®) was prepared according to the manufacturer's instructions, and filled into the bone defect (1). Subsequently, the osseous window was re-attached. In 13 patients, a protective plate osteosynthesis was performed to enhance mechanical stability (1). X-rays were performed after bone grafting and/or stabilization prior to wound closure. Postoperatively, two-planar X-rays were taken at hospital discharge, as well as six weeks, three months, six months, and twelve months postoperatively, in course of routine checkups in our outpatient department (1). In case of doubt, confirmation concerning radiologic consolidation was obtained from an expert bone radiologist (J.I.) (1).

## 2.3 Patient recruitment

The ABGS Cerasorb® was first used at the Department of Orthopaedics and Trauma at the Medical University of Graz in November 2018, as prior to that time-point, a different ABGS had been used (1).

Patients who were treated with curettage and filling with Cerasorb® were identified from our internal tumour database. Patients who fulfilled the predefined inclusion criteria of this thesis were then screened via the electronic patient record of the institution (1). Datasets were checked for accuracy and completeness. Pseudonymized data were stored in a password-protected file (1). At the initial phase of recruitment, 55 potential patients with benign and low-grade malignant bone tumours treated with curettage and filling with Cerasorb® at the Department of Orthopaedics and Trauma at the Medical University of Graz between November 2018 and July 2021 were identified (1). However, twelve patients were lost for follow-up after surgery, leaving 43 patients for final analysis. These 43 patients were included in the study and retrospectively reviewed. Those patients that were lost for follow-up missed their appointments and either could not be reached via telephone or mail or could not be persuaded to have

further follow-up exams performed at the Department of Orthopaedics and Trauma at the Medical University of Graz (1).
The following patients' characteristics according to **table 4** were collected for each study participant.

**Table 4:** Details regarding evaluated patients' characteristics (1)

| Target | Details |
|---|---|
| **Age** | In years |
| **Gender** | Male; female |
| **Diagnosis** | Histopathological tumour classification according to WHO criteria |
| **Tumour size** | Maximum diameter in centimeters |
| **Therapy** | Curettage; ABGS; osteosynthesis |
| **Filling volume of ABGS** | In milliliters |
| **Follow-up interval** | In months |

## 2.4 Outcome assessment

X-rays of the operated extremity were performed six weeks, three months, six months, and twelve months after surgery (1).
The main outcome parameter evaluated in this study assesses the osseous integration status of Cerasorb® during radiological routine follow-up exams (1). Secondary outcome parameters included postoperative complications, primarily perilesional fractures, as well as local recurrence rates (1). Assessment of osseous integration of Cerasorb®, as well as recurrence status, was performed according to the modified Neer classification, as depicted in **table 5** (1, 169, 170).

**Table 5.** The modified Neer classification (169, 170) of radiological consolidation (1)

| Score | Classification | Description |
|---|---|---|
| I | Complete healing | Complete or almost complete filling of the lesion with radiologic evidence of new bone formation |
| II | Incomplete healing | Incomplete healing and radiolucent areas in less than 50% of bone diameter with enough cortical thickness to prevent fracture |
| III | Persistent lesion | Incomplete healing and radiolucent areas in more than 50% of bone diameter with a thin cortical rim; no increase in the size of the cyst |
| IV | Recurrent lesion | Progressive lesion reappeared in a previously obliterated area or radiolucent area has increased in size |

Surgical complications were reported according to the classification system by Goslings and Gouma (171), as shown in **table 6**, as follows: 0 (no harm), 1 (temporary disadvantage, no reoperation), 2 (recovery after reoperation), 3 (permanent damage/disability), 4 (death), and 5 (unclear as a result of untimely death) (1).

**Table 6.** Classification of surgical complications by Goslings and Gouma (1, 171)

| Severity | Description |
|---|---|
| 0 | no harm |
| 1 | temporary disadvantage, no (re-)operation |
| 2 | recovery after (re-)operation |
| 3 | (probably) permanent damage/disability |
| 4 | death |
| 5 | unclear due to untimely death |

# 3 RESULTS

## 3.1 Patient collective

Between November 2018 and July 2021, 43 patients who had undergone curettage of benign or low-grade malignant bone tumours and filling with the ABGS Cerasorb® were included in the study. Of those, 21 (48.9%) were male and 22 (51.2%) were female. Mean age at the time of surgery was 42 years (range 15-70 years). The average maximum diameter of the bone tumours accounted for 5.4 cm (range 1.2-14.5 cm). The average filling volume applied to the cavities after curettage added up to 40.2 ml (range 5-100 ml).

**Table 7: Table 7** presents an overview of tumour characteristics, tumour locations and histopathological entities, surgical treatments, follow-up intervals, osseous integration status, and complications (1)

| | Age | Sex | Localization | Entity | Maximum diameter | Filling volume | Treatment | Follow-up | Osseous integration | Complications |
|---|---|---|---|---|---|---|---|---|---|---|
| 1 | 54 | M | Distal femur | EC | 3.6 cm | 30 ml | Curettage, Cerasorb® | 7 months | Partial / Neer 2 | - |
| 2 | 48 | F | Distal femur | ACT | 4.8 cm | 20 ml | Curettage, Cerasorb® | 35 months | Partial / Neer 2 | - |
| 3 | 66 | F | Distal femur | ACT | 10.0 cm | 90 ml | Curettage, Cerasorb®, plate | 27 months | Partial / Neer 2 | - |
| 4 | 45 | M | Distal femur | ACT | 11.8 cm | 70 ml | Curettage, Cerasorb®, plate | 24 months | Partial / Neer 2 | - |
| 5 | 15 | M | Proximal humerus | Chondro-blastoma | 2.7 cm | 15 ml | Curettage, Cerasorb® | 11 months | Complete / Neer 1 | - |
| 6 | 49 | F | Proximal fibula | EC | 1.8 cm | 10 ml | Curettage, Cerasorb® | 3 months | Partial / Neer 2 | - |
| 7 | 49 | M | Humerus diaphysis | ACT | 14.5 cm | 50 ml | Curettage, Cerasorb® | 4 months | Partial / Neer 2 | - |
| 8 | 55 | F | Distal femur | ACT | 2.1 cm | 10 ml | Curettage, Cerasorb® | 16 months | Partial / Neer 2 | - |
| 9 | 45 | F | Proximal tibia | Intraoss. ganglion | 4.8 cm | 100 ml | Curettage, Cerasorb® | 29 months | Partial / Neer 2 | - |

| | | | | | | | | | | |
|---|---|---|---|---|---|---|---|---|---|---|
| **10** | 56 | M | Distal femur | EC | 9.0 cm | 90 ml | Curettage, Cerasorb®, plate | 34 months | Partial / Neer 2 | - |
| **11** | 64 | M | Distal femur | EC | 8.4 cm | 90 ml | Curettage, Cerasorb®, plate | 28 months | Partial / Neer 2 | - |
| **12** | 49 | M | Acetabulum | RDD | 2.8 cm | 30 ml | Curettage, Cerasorb® | 19 months | Partial / Neer 2 | - |
| **13** | 29 | F | Proximal femur | FD | 5.5 cm | 40 ml | Curettage, Cerasorb®, allograft | 24 months | Complete / Neer 1 | - |
| **14** | 59 | M | Humerus diaphysis | EC | 5.0 cm | 45 ml | Curettage, Cerasorb® | 3 months | Partial / Neer 2 | - |
| **15** | 40 | F | Distal femur | EC | 6.5 cm | 40 ml | Curettage, Cerasorb®, plate | 14 months | Complete / Neer 1 | - |
| **16** | 50 | F | Proximal humerus | EC | 4.4 cm | 20 ml | Curettage, Cerasorb® | 30 months | Partial / Neer 2 | - |
| **17** | 60 | M | Proximal humerus | EC | 2.5 cm | 20 ml | Curettage, Cerasorb® | 21 months | Partial / Neer 2 | - |
| **18** | 63 | F | Distal femur | EC | 5.0 cm | 100 ml | Curettage, Cerasorb® | 12 months | Partial / Neer 2 | Fracture, plate osteosynthesis |
| **19** | 15 | M | Proximal tibia | Chondro-blastoma | 2.9 cm | 50 ml | Curettage, Cerasorb® | 25 months | Partial / Neer 2 | - |

| | | | | | | | | | | |
|---|---|---|---|---|---|---|---|---|---|---|
| **20** | 26 | M | Proximal humerus | Bone cyst | 2.1 cm | 30 ml | Curettage, Cerasorb® | 12 months | Complete / Neer 1 | - |
| **21** | 34 | F | Distal femur | EC | 4.8 cm | 35 ml | Curettage, Cerasorb® | 25 months | Partial / Neer 2 | Fracture, plate osteosynthesis |
| **22** | 55 | F | Distal femur | ACT | 4.5 cm | 30 ml | Curettage, Cerasorb® | 18 months | Partial / Neer 2 | - |
| **23** | 40 | F | Distal femur | ACT | 5.2 cm | 40 ml | Curettage, Cerasorb®, plate | 20 months | Partial / Neer 2 | - |
| **24** | 15 | M | Distal femur | Bone cyst | 5.2 cm | 40 ml | Curettage, Cerasorb®, plate | 12 months | Partial / Neer 2 | - |
| **25** | 39 | F | Proximal humerus | ACT | 5.3 cm | 45 ml | Curettage, Cerasorb® | 12 months | Partial / Neer 2 | - |
| **26** | 44 | F | Proximal humerus | ACT | 2.6 cm | 15 ml | Curettage, Cerasorb® | 10 months | Partial / Neer 2 | - |
| **27** | 54 | F | Humerus diaphysis | ACT | 13.0 cm | 60 ml | Curettage, Cerasorb® | 12 months | Partial / Neer 2 | - |
| **28** | 22 | M | Distal femur | EC | 3.0 cm | 50 ml | Curettage, Cerasorb®, plate | 13 months | Partial / Neer 2 | - |
| **29** | 15 | M | Proximal tibia | Chondro-blastoma | 3.7 cm | 30 ml | Curettage, Cerasorb® | 12 months | Partial / Neer 2 | - |

| | | | | | | | | | | |
|---|---|---|---|---|---|---|---|---|---|---|
| **30** | 24 | F | Proximal femur | LCH | 2.0 cm | 20 ml | Curettage, Cerasorb®, plate | 17 months | Complete / Neer 1 | - |
| **31** | 34 | M | Proximal femur | Bone cyst | 7.5 cm | 80 ml | Curettage, Cerasorb®, allograft | 12 months | Partial / Neer 2 | - |
| **32** | 43 | F | Proximal humerus | ACT | 2.0 cm | 20 ml | Curettage, Cerasorb® | 10 months | Partial / Neer 2 | - |
| **33** | 19 | M | Femur diaphysis | ACT | 7.3 cm | 30 ml | Curettage, Cerasorb®, plate | 12 months | Partial / Neer 2 | - |
| **34** | 45 | F | Distal femur | EC | 9.0 cm | 30 ml | Curettage, Cerasorb®, plate | 12 months | Partial / Neer 2 | - |
| **35** | 21 | M | Humerus diaphysis | ACT | 11.0 cm | 35 ml | Curettage, Cerasorb® | 5 months | Partial / Neer 2 | Fracture, plate osteosynthesis |
| **36** | 49 | F | Proximal humerus | ACT | 4.1 cm | 40 ml | Curettage, Cerasorb® | 6 months | Partial / Neer 2 | - |
| **37** | 68 | M | Humerus diaphysis | ACT | 6.5 cm | 30 ml | Curettage, Cerasorb® | 8 months | Partial / Neer 2 | Fracture, plate osteosynthesis |
| **38** | 61 | F | Metacarpal bone | ACT | 2.2 cm | 10 ml | Curettage, Cerasorb® | 6 months | Partial / Neer 2 | - |
| **39** | 33 | M | Distal femur | Chondro-blastoma | 2.2 cm | 10 ml | Curettage, Cerasorb® | 6 months | Complete / Neer 1 | - |

| | | | | | | | | | | |
|---|---|---|---|---|---|---|---|---|---|---|
| **40** | 66 | F | Distal femur | ACT | 8.0 cm | 70 ml | Curettage, Cerasorb®, plate | 7 months | Partial / Neer 2 | - |
| **41** | 21 | M | Distal tibia | Bone cyst | 5.0 cm | 30 ml | Curettage, Cerasorb®, plate | 8 months | Partial / Neer 2 | - |
| **42** | 39 | M | Metacarpal bone | EC | 4.2 cm | 20 ml | Curettage, Cerasorb®, plate | 4 months | Partial / Neer 2 | - |
| **43** | 29 | F | Finger | EC | 1.2 cm | 10 ml | Curettage, Cerasorb® | 4 months | Complete / Neer 1 | - |

*F = female, M = male, intraoss. = intraosseous

## 3.2 Tumour localizations

In total, 27 (62.8%) of the 43 lesions studied occurred in the lower extremity, and 16 (37.2%) were observed in the upper extremity.

Most tumours (n=21, 48.9%) were localized in the femur. Amongst those, the majority (n=17, 39.5%) occurred in the distal femur (**figure 15**). One (2.3%) tumour was diagnosed in the femoral diaphysis, and three (7.0%) were located in the proximal femur (**figure 15**). Four (9.3%) lesions were described in the tibia, of which three (7.0%) were localized in the proximal tibia, and one (2.3%) in the distal tibia. One (2.3%) tumour was located in the proximal fibula, and one (2.3%) tumour occurred in the acetabular region (**figure 15**).

Concerning the upper extremity, 13 (30.2%) tumours were located in the humerus, of which eight (18.6%) occurred in the proximal humerus. Five tumours (11.6%) were detected in the humeral diaphysis (**figure 15**). Two (4.7%) lesions were located in metacarpal bones, and one (2.3%) tumour was described in the medial phalanx of the fifth finger (**figure 15**).

The metaphysis was the most commonly affected region concerning bone tumours in the proximal and distal parts of long bones (n=31). However, four tumours were located in the epiphyseal regions of the distal femur, proximal humerus, and proximal tibia, all of which constituted chondroblastomas.

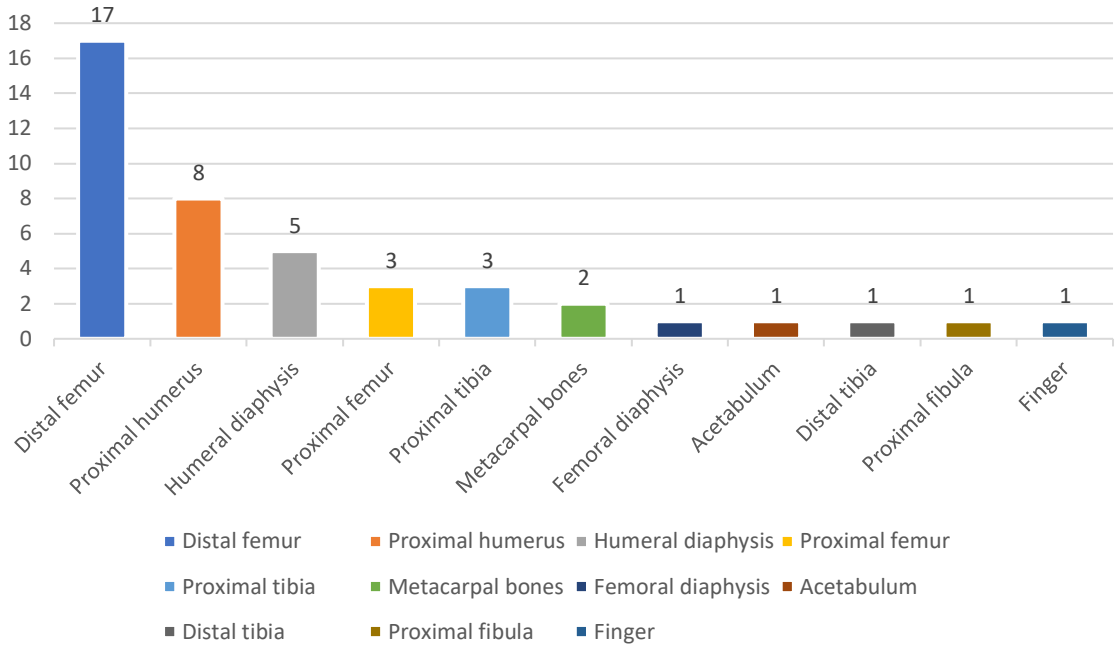


**Figure 15:** A graphical schema of bone tumour localizations (x-axis). The y-axis indicates the absolute number of tumours (n), with the kind permission of Springer Nature, according to figure 1 in "Artificial bone graft substitutes for curettage of benign and low-grade malignant bone tumors: clinical and radiological experience with Cerasorb", Indian Journal of Orthopaedics, published online on June 22nd, 2023 (1).

## 3.3 Histological entities

As outlined in **figure 16**, atypical cartilaginous tumours (n=17, 39.5%) and enchondromas (n=14, 32.6 %) comprised the most frequently diagnosed entities in our study collective. The latter were followed by bone cysts and chondroblastomas, which were diagnosed in four cases (9.3%), respectively. Intraosseous ganglion cysts, fibrous dysplasia, Langerhans cell histiocytosis, and Rosai-Dorfman syndrome were detected in one case (2.3%), respectively (**figure 16**).

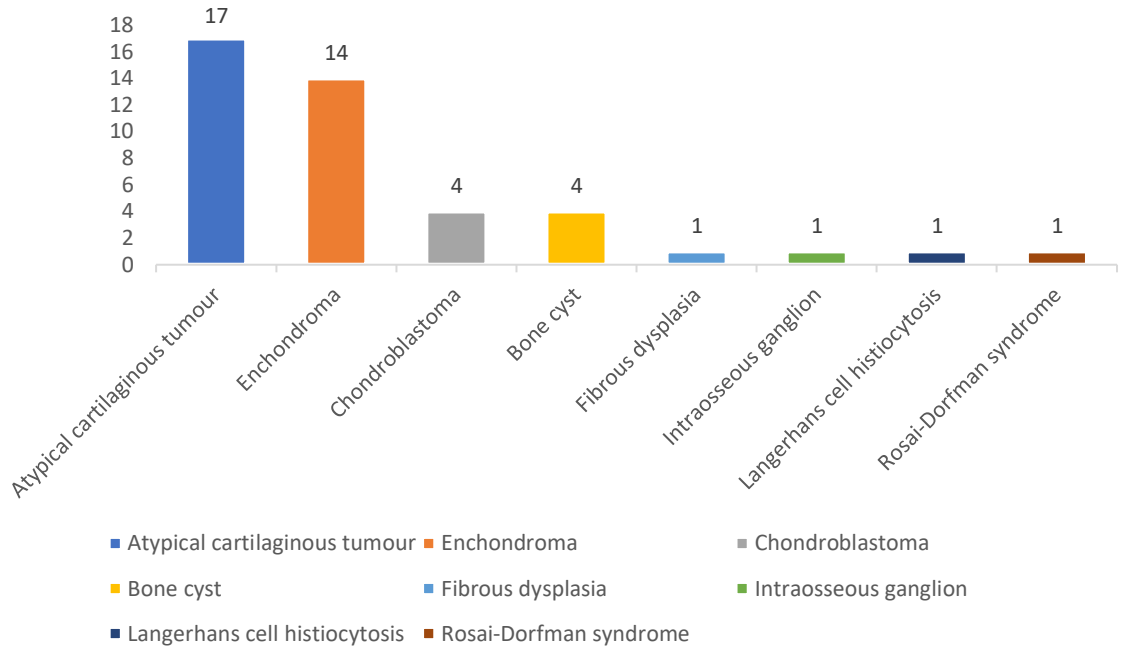


**Figure 16:** Summary of tumour entities treated in our study (n = 43). The y-axis indicates the absolute number of tumours (n), with the kind permission of Springer Nature, according to figure 2 in "Artificial bone graft substitutes for curettage of benign and low-grade malignant bone tumors: clinical and radiological experience with Cerasorb", Indian Journal of Orthopaedics, published online on June 22nd, 2023 (1).

## 3.4 Surgical outcomes and complications

Regarding the assessment of recurrences or residual tumours, we observed no local recurrences after filling with Cerasorb®, and none of the patients required revision surgery due to a local recurrence during the follow-up interval. According to the classification of surgical complications by Goslings and Gouma (171), as shown in **table 8**, none of the patients experienced grade 0, I, III, IV or V complications. Four patients (9.3%) presented with grade II complications (e.g., postoperative fractures), but showed complete recovery after revision surgery.

In these four patients (9.3%), fractures occurred within six weeks after primary surgery. Of these patients, two suffered from a tumour in the distal femur and two had a lesion in the humeral diaphysis. An example of one of these fractures is outlined in **figure**

**17b**. The tumours associated with postoperative fracture after curettage and filling were comparatively large, involving maximum diameters of 4.8 cm and 5.0 cm in the distal femur and 6.0 cm and 11.0 cm in the humeral diaphysis. In all four cases, uneventful revision surgery with plate osteosynthesis was performed, as illustrated in **figure 17c**.


**Figures 17a, 17b and 17c: (17a)** Postoperative x-ray of a 21-year-old male patient one day after curettage and filling of an enchondroma in the left humeral diaphysis, and **(17b)** after a pathologic fracture within the curetted area that occurred after minor trauma five weeks after primary surgery. **(17c)** Follow-up radiograph following plate osteosynthesis in order to stabilize the pathologic fracture five weeks after primary surgery, with the kind permission of Springer Nature, according to figures 5a, 5b and 5c in "Artificial bone graft substitutes for curettage of benign and low-grade malignant bone tumors: clinical and radiological experience with Cerasorb", Indian Journal of Orthopaedics, published online on June 22nd, 2023 (1).

According to the modified Neer classification (169, 171), seven lesions (16.3%) in the present study were grade I lesions, while the other 36 lesions (83.7%) were classified as grade II lesions. No grade III or IV lesions were found in the present study collective.

## 3.5 Clinical and radiological outcomes

After an average follow-up of 14.6 months (range 3-35 months), radiological consolidation of the lesion and surrounding cortex following curettage was observed in all patients.

Cerasorb® was completely resorbed in seven patients (16.3%), as presented in **figures 18a**-**18c**, as well as in **figures 19a**-**19c.** On average, complete osseous integration was observed after 10.1 months (range 3-12 months).

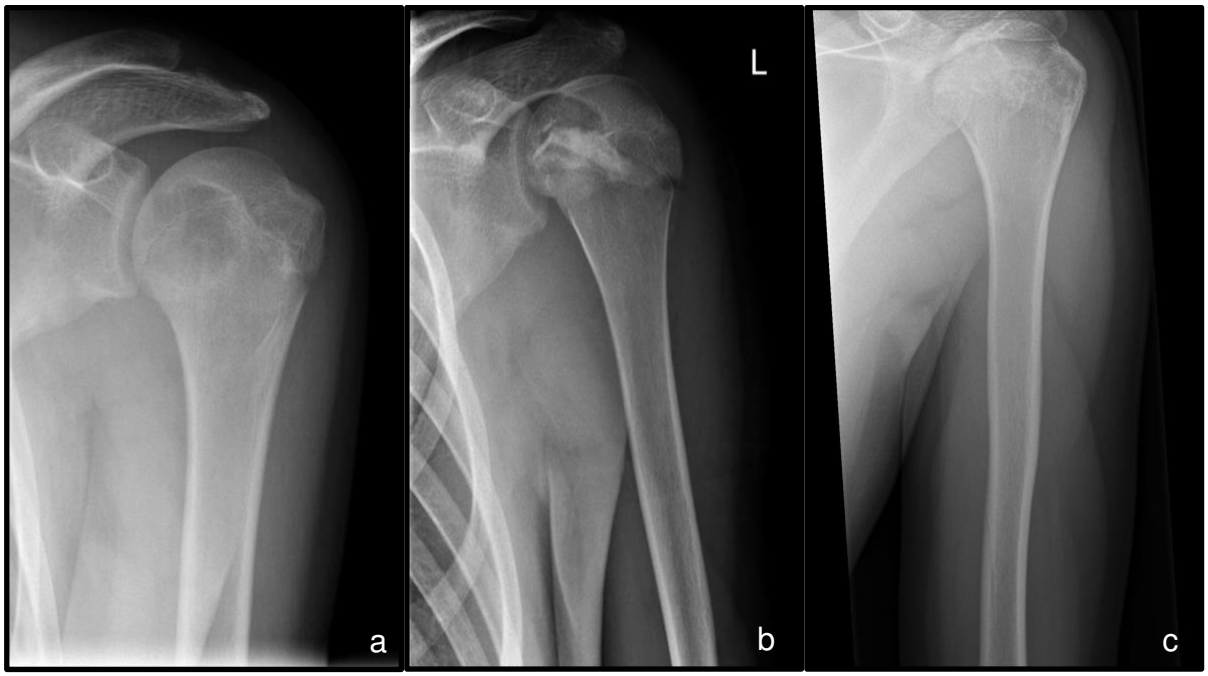


**Figures 18a, 18b and 18c: (18a)** Preoperative and **(18b)** one-day postoperative X-rays of a 15-year-old male patient after curettage and filling of a chondroblastoma in the left proximal humerus. **(18c)** An X-ray twelve months after surgery shows complete osseous integration of the ABGS, with the kind permission of Springer Nature,

according to figures 3a and 3b in "Artificial bone graft substitutes for curettage of benign and low-grade malignant bone tumors: clinical and radiological experience with Cerasorb", Indian Journal of Orthopaedics, published online on June 22nd, 2023 (1).

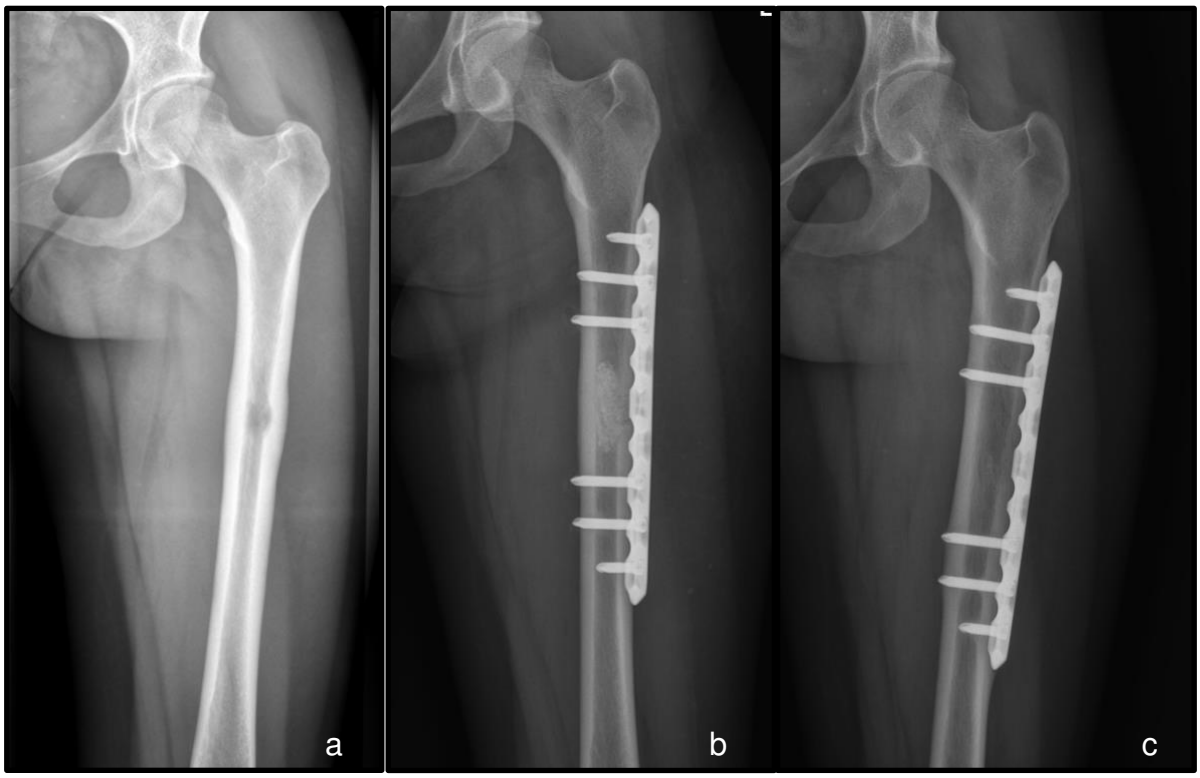


**Figures 19a, 19b and 19c: (19a)** Preoperative and **(19b)** one-day postoperative X-rays of a 24-year-old female patient after curettage and filling as well as protective plate osteosynthesis of LCH in the left femur. **(19c)** An X-ray twelve months after surgery shows complete osseous integration of the ABGS.

Of those seven tumours (16.3%) in which Cerasorb® was completely integrated after a maximum observation time of twelve months, only two measured more than 5 cm. These two bigger tumours were localized in the proximal femur (size: 5.5 cm) and distal femur (size: 6.5 cm), respectively. The sizes of the other five tumours ranged from 1.2 cm to 2.7 cm. Two of these tumours were located in the proximal humerus (size: 2.1 cm, 2.7 cm), one was located in the proximal femur (size: 2.0 cm), one was described in the distal femur (size: 2.2 cm), and the fifth tumour was located in a finger (size: 1.2 cm). On average, regarding the seven tumours with full osseous integration, tumour

size was 3.2 cm (range 1.2-6.5 cm). Consequently, complete osseous integration was observed more frequently in tumours smaller than 2.7 cm. Moreover, the average time until complete osseous integration was shorter in the cohort of lesions smaller than 2.7 cm, in particular nine months compared to twelve months in the cohort of larger lesions. Mean age at the time of surgery was only 28 years (range 15-40 years), which was significantly lower compared to the total patient collective, in which the mean age at surgery was 42 years (range 15-70 years). This finding indicates a potential correlation between a younger age at the time of surgery and faster osseous integration. Altogether, no fractures or other complications were reported in the cohort of the seven tumours with complete osseous integration. Additionally, no correlation between the tumour location and the achievement of complete osseous integration could be observed. Moreover, no link between tumour entity and complete osseous integration was detected. Furthermore, no hint of faster integration in the upper or lower extremity was found. The characteristics of this cohort are summed up in **table 8**.

**Table 8: Table 8** presents an overview of tumour entities, tumour locations, patients' age at the time of surgery, tumour size (in cm), time until complete integration (in months), and complications of the cohort of seven lesions with complete osseous integration.

| | Entity | Location | Age | Size | Time |
|---|---|---|---|---|---|
| 1 | Enchondroma | Distal femur | 15 | 6.5 | 12 |
| 2 | Fibrous dysplasia | Proximal femur | 29 | 5.5 | 12 |
| 3 | Chondroblastoma | Proximal humerus | 40 | 2.7 | 11 |
| 4 | Chondroblastoma | Distal femur | 33 | 2.2 | 6 |
| 5 | Simple bone cyst | Proximal humerus | 26 | 2.1 | 12 |
| 6 | LCH | Proximal femur | 24 | 2.0 | 12 |
| 7 | Enchondroma | Finger | 29 | 1.2 | 4 |

In the remaining 36 patients (83.7%), partial osseous integration was observed, with the ABGS still clearly definable, as shown in **figures 20a-c**. In all tumours filled with

Cerasorb®, incipient integration was observed at the first routine follow-up visit six weeks after surgery. Osseous integration increased with time, but still, in these 36 patients (83.7%), integration remained only partial at the last follow-up visit. Again, no difference between tumours in the upper or lower extremity was found. Regarding the 17 patients in the whole patient collective with tumours of more than 5 cm in size, only two showed complete resorption, while the rest showed partial resorption at the end of follow-up. Still, larger tumour size did not seem to prohibit osseous integration of Cerasorb®, thus, its use seems to be safe also for larger tumour sizes.


**Figures 20a, 20b and 20c: (20a)** Preoperative and **(20b)** one-day postoperative X-rays of a 50-year-old female patient suffering from an enchondroma of the left proximal humerus. **(20c)** An X-ray 30 months after surgery shows partial osseous integration of the ABGS.

In 14 patients (32.6%), the decision to perform an additional plate osteosynthesis in course of the index surgery was made in order to achieve more stable conditions due to the size of the lesion, as outlined in **table 7** and **figures 21a-c**. In two cases (4.7%), an additional structural allograft was added (**table 7**).

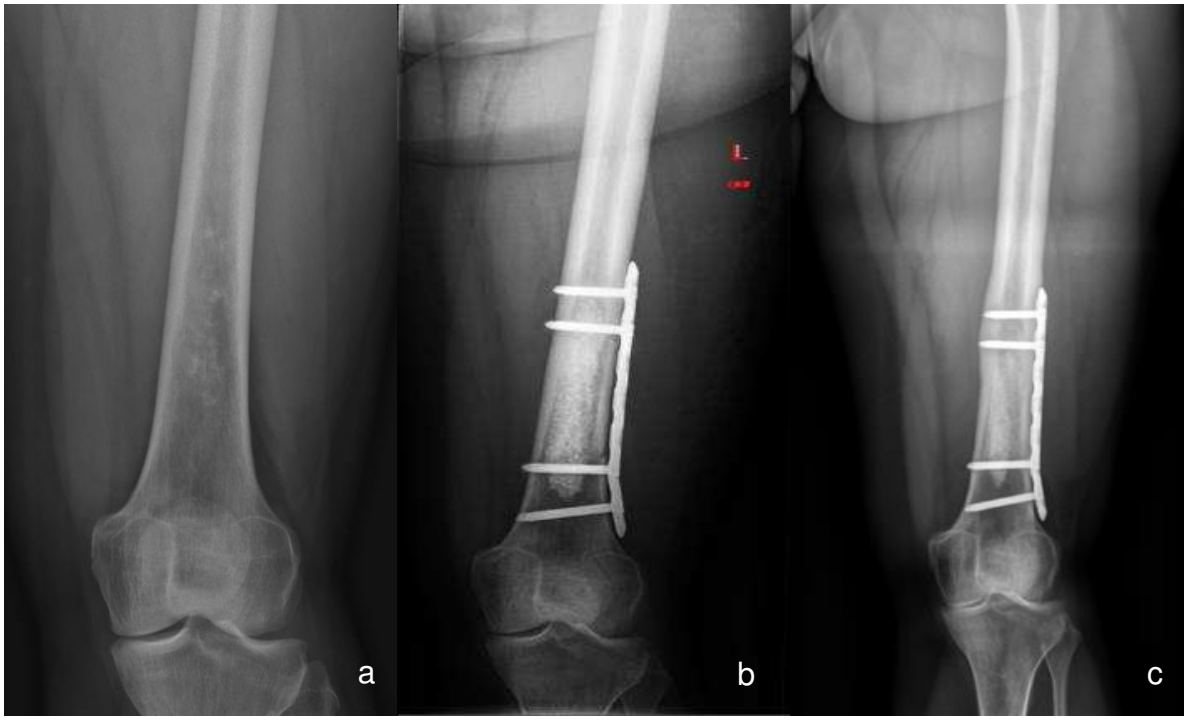


**Figures 21a, 21b and 21c: (21a)** Preoperative and **(21b)** postoperative x-ray one day after surgery of a 40-year-old female patient after curettage and filling of an enchondroma in the left distal femur with additional protective plate osteosynthesis. **(21c)** Follow-up radiograph twelve months after index surgery showing only partial osseous integration of the ABGS, with the kind permission of Springer Nature, according to figures 4a and 4b in "Artificial bone graft substitutes for curettage of benign and low-grade malignant bone tumors: clinical and radiological experience with Cerasorb", Indian Journal of Orthopaedics, published online on June 22nd, 2023 (1).

Altogether, 18 patients (41.9%) received plate osteosynthesis: 14 (32.6%) in course of primary surgery, and four (9.3%) due to secondary fracture. All four patients that suffered a secondary fracture merely received plate osteosynthesis. Repeated filling using the ABGS Cerasorb®, or any other filling material, was not performed. Of the 14 patients with primary protective plate osteosynthesis, twelve suffered from a tumour localized in the femur, while only one tumour was situated in the tibia and one in a metacarpal bone, respectively. Tumours treated with additional primary plate osteosynthesis were mainly larger tumours with an average size of 6.8 cm (range 2.0-11.8 cm). When comparing osseous integration behaviour between patients with

primary and secondary plate osteosynthesis, no major trend was found at last follow-up, as partial osseous integration was observed after a mean follow-up of nine months, respectively. However, two patients in the group of primary plate osteosynthesis showed complete osseous integration.

# 4 DISCUSSION

The aim of the present retrospective study was to investigate the clinical and radiological outcomes, as well as the adverse effects associated with the use of the beta-TCP Cerasorb® in filling bone cavities after curettage of bone tumours. In the following chapter, the results of this thesis will be discussed in the context of the current literature. Furthermore, potential future research questions arising from the results of the present thesis will be pointed out. Moreover, strengths and weaknesses will be analyzed.

## 4.1 Lessons learnt from the use of Cerasorb® in our sample: osseous integration and postoperative complications

We found that Cerasorb® was fully resorbed and integrated in a small proportion of patients (n=7, 16.3%) after 10.1 months, on average (range 3-12 months) (1). Full osseous integration was seen in comparatively small lesions (mean size 3.2 cm, range 1.2-6.5 cm), irrespective of a tumour's location in the upper or the lower extremity (1). Only two tumours in which Cerasorb® was fully integrated, measured more than 5.0 cm in size. The sizes of the other five tumours varied from 1.2 to 2.7 cm (1).

In a large proportion of patients, however, Cerasorb® was not fully resorbed after the observational period of 14.6 months (range 3-35 months) (1). Particularly in larger lesions (mean size 5.7 cm, range 2.0-14.5 cm), we saw an incomplete integration and consolidation at last follow-up (1). Nevertheless, progressive consolidation and integration was observed in all cases (n=36) with most of them showing only small residual defects according to the modified Neer classification (Neer II, n=36) at last follow-up (14.6 months, range 3-35 months) (1). Based on the comparatively small sample size and the short follow up of less than twelve months in 16 cases (37.2%), our data allow no final conclusion regarding the time it takes for Cerasorb® to fully integrate in larger bone defects (1).

In addition, four patients (9.3%) with comparatively large bone tumours (mean 6.8 cm, range 4.8-11.0 cm) suffered from fractures within six weeks after primary surgery (1).

These fractures occurred in equal proportions in the lower extremity (femur: n=2) and the upper extremity (humerus: n=2). In all of these cases, uneventful revision surgery with plate osteosynthesis was performed (1).

According to the instructions for use regarding Cerasorb®, its resilience is supposed to permit immediate weightbearing and an unlimited postoperative mobilization protocol. However, only little is known about stability and fractures after curettage and filling with this ABGS (1, 166-168).

Even though patients with larger bone defects underwent restricted weight-bearing for six weeks postoperatively, fractures in the present study occurred within a few weeks after primary surgery (1). Thus, our findings indicate that Cerasorb® should be accompanied by plate osteosynthesis in larger tumours of the lower as well as upper extremity, especially in long bones (1). Based on our data, we suggest a cut-off of approximately 5 cm, even though these suggestions will require confirmation in a larger sample and/or an experimental setting (1).

Apart from patients who fractured postoperatively, 14 patients (32.6%) underwent plate osteosynthesis in course of their primary surgery: their tumours were mainly located in the femur (n=12), while only one tumour was situated in the tibia and one in a metacarpal bone, respectively (1). These tumours were rather large and had a mean size of 6.8 cm (range 2.0-11.8 cm). Albeit the small number of subjects involved, none of those showed a secondary fracture or other postoperative complications. All of them displayed sufficient osseous integration and consolidation at last follow-up (1).

Otherwise, complication rates associated with Cerasorb® were low, and the ABGS was well-tolerated by the patients: we did not observe any treatment-associated infections or adverse reactions (1).

Also, we did not see any recurrences until the last follow-up (1). However, detection of residual tumours and recurrences might be delayed based on the osseous integration of the ABGS compared to other fillers, for instance bone cement (156-160). Thus, a larger sample and a longer follow-up are required to allow final conclusions regarding detection of recurrences after the use of Cerasorb®.

## 4.2 Fracture risk after curettage of bone tumours

A major complication observed in our sample were fractures occurring within six weeks postoperatively, accounting for a postoperative fracture rate of 9.3%. Previous studies have stated a correlation between tumour biology, its site of occurrence, and the risk of fracture (172-174).

For example, Hirn et al. reported a positive correlation between tumour size and volume and fracture risk (172). The authors investigated a series of 146 benign bone tumours that were curetted and left without filling of the cavity (172). Similar to our data, they stated that the subsequent fracture risk was strongly related to the size of the defect (172): they reported a significantly higher incidence of complications in cysts greater than 60 $cm^3$ (approximately 5 cm in diameter) (172).

Furthermore, Kundu et al. reported a positive correlation between size, volume, and localization of the tumour and postoperative fracture risk (173). In a sample of 42 patients who had undergone curettage of benign bone tumours without filling, the authors showed that the rate of osseous integration, risk of fracture and incidence of complications was related to the size of the tumour (173). They reported that tumours greater than 70 $cm^3$ were associated with a higher risk of complications (173).

Another retrospective study by Perisano et al. focused on the definition of standards for prophylactic osteosynthesis after curettage of benign and low-grade malignant bone tumours localized in the distal femur (174). Consistent with the findings regarding fracture risk in larger tumours of Hirn et al. (172) and Kundu et al. (173), also these authors recommended protective osteosynthesis for comparatively large lesions (>5 cm, >60 $cm^3$), or in patients with high mechanical load, e.g. in obese patients, and/or in patients with high functional requirements (174). Moreover, they suggested plating for all cases in which ABGS were used instead of autologous or allogenic bone grafts (174).

In summary, also other authors reported postoperative fractures after the curettage of larger bone defects, especially those greater than 5 cm and 60 $cm^3$ (172-174). The cut-offs provided in the literature are comparable to those suggested by our data. However, future studies with larger patient collectives and/or experimental designs will be necessary in order to determine stability properties of a lesion in a standardized and reliable manner.

## 4.3 Osseous integration, biomechanical properties and complications of Cerasorb® compared to other bone fillers

To date, extensive literature evaluating the use of the beta-TCP Cerasorb® as a bone filler after curettage of bone tumours of the peripheral skeleton is sparse: in fact, the publication resulting from this thesis was the first to deal with this topic (1). Moreover, except for three comparable studies, in which Cerasorb® was applied for tibial plateau fractures and in dental surgery, no clinical trial with a comparable number of participants regarding Cerasorb® has been published yet (1, 166, 175, 176).

In contrast to the current lack of studies investigating the use of Cerasorb® in the peripheral skeleton, several studies focus on Cerasorb® as a bone filler in periodontal bone defects (166, 175). For example, Horch et al investigated the effect of Cerasorb® on bone regeneration in reconstructive jaw surgery in 152 patients (166). The authors reported that bone regeneration was complete after approximately 12 months, which differs from the complete osseous integration rate of Cerasorb of only 16.3% that we observed in tumours of the extremities in our patient collective (1, 166). However, in the study by Horch et al., Cerasorb® was associated with a low complication rate, similar to the findings of the present thesis (1, 166). Another study by Bokan et al., involving 56 patients with deep intra-bony defects, in which Cerasorb® was added to enamel matrix proteins, showed no clear superiority regarding osseous integration of the composite of Cerasorb® and enamel matrix proteins, compared to enamel matrix proteins alone (175).

Even though Cerasorb® hasn't been studied extensively in the published literature, there are reports dealing with other beta-TCPs: In 2006, Hirata et al. presented a retrospective study in which 53 patients suffering from benign bone tumours underwent curettage and filling with a beta-TCP (177). Although the follow-up interval was comparable to the present study, the authors found higher complete osseous integration rates than in the present study (177). They reported full osseous integration in 23 cases (43.0%), compared to 16.3% of full osseous integration in our series (1, 178). The mean time until complete resorption was 12.7 months (range 5-26 months).

In patients with complete resorption, Hirata et al. reported a statistical correlation between filling volume and time needed for osseous integration (177). This finding might indicate that smaller defects tend to show faster osseous integration. However, the authors did not include information about the average defect size in their patient collective. Moreover, the authors observed no postoperative fractures, which is in contrast to the findings of the present study, which showed a postoperative fracture rate of 9.3% (1, 177).

Apart from beta-TCPs, also other TCPs have been studied in the literature: In 2017, a prospective, non-randomized study analyzing 27 patients who were treated with the alpha-TCP Calcibon (Biomet, Warsaw, IN) in granular form was published by Friesenbichler et al (178). Patients included in the study suffered from benign or low-grade malignant bone tumours and had curettage and filling of the bone defects performed (178). The average postoperative follow-up interval was 26 months. After a mean follow-up of six months, radiological consolidation was observed in 23 patients (178). Nevertheless, complete osseous integration was neither seen at that time point, nor after 32 months of follow-up (178). The authors described no occurrence of local recurrences (178). The results of the study by Friesenbichler et al. were similar to those observed in the present study (1, 178). However, in contrast to Calcibon, for which complete osseous integration was not described in any of the cases, the ABGS Cerasorb® showed complete osseous integration in 16.3% of patients after a mean follow-up of 14.6 months (1, 178). These findings are in line with the product characteristics, as the ABGS Calcibon is a TCP like Cerasorb®, but belongs to the group of alpha-TCPs, which are characterized by a similar degree of solubility, but show a slower biodegradation (1, 178).

Since the 1980s, bone cements, e.g. PMMA, have been the treatment of choice for vertebral body augmentation and as bone fillers after the curettage of bone tumours (179, 180). PMMA offers biomechanical strength and stiffness, but lacks any remodeling potential (179, 180). Consequently, research focused on the development of new materials that have the potential to be resorbed and replaced by new bone, for example calciumsulfate alone or in combination with beta-TCP (181).

A study by Yang et al. tested geneX Paste (Biocomposites, UK), consisting of calcium sulfate and beta-TCP and applied as an injectable paste, in a sheep vertebral body defect model (181). The study demonstrated an improved tissue response compared to PMMA, indicating an improved biological tolerance (181). Moreover, micro-CT and histology showed marked osteoregenerative capacity in comparison to PMMA (181). Additionally, formation of new bone was higher, and bone regeneration was almost complete after 36 weeks (181).

However, adverse reactions following the application of geneX as a bone graft substitute after curettage of benign bone tumours in humans were reported in a study by Friesenbichler et al. (135). Although the authors had intended to include 40 patients, enrollment was stopped after 31 patients due to serious complications (135). These complications included sterile inflammation adjacent to the bone graft substitute with delayed wound healing and pain, furthermore severe skin damage in the area of the scar requiring revision surgery, and the development of inflammatory cysts measuring up to 15 cm (135). The authors concluded that owing to these severe complications, geneX should not be used for filling bony defects after the curettage of benign bone tumours (135). These findings indicate potential differences between the use of bone fillers such as geneX in animals compared to human bone.

Another case report by Harimtepathip et al. (182) reported a serious complication after application of another artificial bone graft substitute consisting of calcium sulfate and calcium phosphate. Two years after application of the composite, progressive femoral neck osteolysis caused by an inflammatory reaction to the composite occurred in a 21-year-old female previously suffering from fibrous dysplasia of the femoral neck.

On the contrary, some studies also reported no negative effects following the use of a composite of calcium sulfate and calcium phosphate. Multani et al. (183) reported the outcome of an injectable calcium sulfate - calcium phosphate composite regarding bone regeneration after intralesional curettage of primary bone tumours and filling with a follow-up of at least four years. However, only 14 patients were included. They reported complete osseous integration at the end of follow-up (mean 68 months, range 50-105 months) in all patients (183). The authors stated that the use of this composite was safe and that no long-term complications were observed (183).

Additionally, a recent study by Razii et al. reported beneficial outcomes after application of GeneX in defects following curettage of benign bone tumours (184). In a patient collective of ten cases, radiographic evidence of healing was demonstrated after a mean follow-up of 24 months (range 20-30 months) in all patients. Furthermore, no tumour recurrences or complications were observed (184). Again, the authors stated that the use of this composite was safe (184).

Also, Evaniew et al. (185) performed a retrospective study including 24 patients with benign primary bone tumours who underwent intralesional curettage followed by reconstruction with a calcium sulfate - calcium phosphate composite bone substitute. The mean follow-up was 23 months. Two patients suffered local tumour recurrences. However, no postoperative fractures occurred, and no complications related to the use of the composite were reported (185).

Moreover, the results of the individual use of the injectable aqueous calciumsulfate BonePlast (Biomet, Warsaw, USA) have been reported as beneficial in the literature (186). In a prospective non-randomized case series by Johnson et al. (186), 46 patients suffering from bone tumours who had received curettage and filling were evaluated clinically and radiologically for a minimum period of twelve months (range 12-85 months). In contrast to our study, in which most patients (83.7%) showed only partial osseous integration after an average follow-up of 14.6 months (1, 186), Johnson et al. report complete bone reconstruction in 83% of patients, and partial integration in 15%, whereas 2% showed no consolidation (1, 186). However, a reliable comparison of both patient collectives is not possible, as tumour sizes are not reported in the study by Johnson et al. (1, 186). Furthermore, another study by Yang et al. comparing calcium sulfate with allografts in the reconstruction of bone defects after curettage of tumours in 50 patients after a mean follow-up of 19.9 months (range 12-55 months) reported no major complications after the application of calcium sulfate (187).

In summary, concerning the combination of calcium sulfate and calcium phosphate, the literature is quite controversial (137, 182-185), whereas calcium sulfate in its individual use seems to be a safe agent (186, 187).

Furthermore, combinations of ABGS with autologous materials have been studied (188): In a randomized prospective clinical trial by Hagel et al., the anterior fusion rates

of cages were studied in 26 patients who suffered from degenerative spine disease (188). Following randomization, patients received either autologous bone grafting from the iliac crest, or the beta-TCP Cerasorb® combined with platelet-rich plasma (188). The aim of the combination with platelet-rich plasma was to accelerate osseous integration and bone regeneration (188). Radiologic control imaging was performed three, six, nine, and twelve months after surgery (188). CT scans were performed twelve months after surgery (188). The authors reported fusion rates of 49% on conventional radiographs, which contrasted with fusion rates of only 28% in CT imaging (188). Of note, none of the cages filled with Cerasorb® showed complete anterior fusion in the CT scans (188). However, in approximately half of the cages filled with cancellous bone from the iliac crest, fusion was proven via CT (188). Consequently, the authors concluded that cages loaded with cancellous bone from the iliac crest were associated with a significantly higher anterior fusion rate compared to cages filled with Cerasorb® combined with platelet-rich plasma (188). As these observations were derived from spinal surgery, and given the lack of data directly comparing the use of autologous bone grafts versus Cerasorb® after the curettage of tumours in the extremities to date, future randomized studies will need to address this aspect.

In this context, a prospective multicentre randomized clinical trial by Szabó et al. compared the histologic and histomorphometric aspects of autologous bone grafts and Cerasorb® in 20 patients with bilateral sinus elevation (189). The authors reported that there were no significant differences regarding osseous integration, indicating that Cerasorb® was equivalent to autologous bone grafts in terms of bone regeneration (189).

Another prospective randomized pilot study by Lerner et al. on 40 patients with a mean follow-up of four years compared the clinical and radiological results of the beta-TCP Vitoss® versus autologous bone grafts harvested from the iliac crest for posterior spinal fusion in scoliosis surgery (190). The authors concluded that beta-TCP and autologous bone grafts showed equivalent results regarding posterior correction of scoliosis and osseous integration (190). They furthermore pointed out that beta-TCP provides the advantage of avoiding donor-site morbidity of the iliac crest (190). In line with these findings, a study by Hernigou et al. published in 2017 comparing beta-TCP

with autologous bone grafts in open-wedge high tibial osteotomies as well as osteonecrosis treatments in 50 patients concluded that beta-TCP might even be superior to autologous bone grafts with respect to fusion rates, pain, and side effects (176).

Finally, several authors suggested to leave the bone cavity empty after curettage instead of using bone fillers (172, 173). In an experimental study by Zheng et al., bone defects were drilled into the distal femurs of rabbits (191). Defects filled with a composite of beta-TCP and collagen were compared with defects which were left unfilled. At the end of the investigation period of six months, significantly better bone healing - regarding both the quantity and the quality of the newly formed bone - was reported for the beta-TCP and collagen composite (191). These results clearly support the use of beta-TCP for filling bone defects instead of leaving the defect unfilled (191).

## 4.4 Strengths and limitations of the present study

This study was conducted at the Medical University of Graz, which is a highly specialized tertiary care centre, providing the resources required to diagnose and treat musculoskeletal tumours in a multi-disciplinary expert team.

One of the main strengths of the current study is that the paper resulting from the current study is the first published report of Cerasorb® applied in humans as a filler for bone tumours of the extremities. Our sample size was comparable to three previously published studies evaluating the application of Cerasorb® in humans, though in other contexts.

On the other hand, there are several limitations associated with the present study: First, data collection was performed retrospectively. Furthermore, the average follow-up period only amounted to 14.6 months, which is a rather short observation period. Also, the patient collective in the present study was rather small and heterogeneous, as many different tumour entities in various localizations were included. Moreover, this retrospective analysis was solely descriptive, as a precise statistical analysis could not be performed due to the heterogeneity of the data. As a consequence of these limitations, information on long-term results and complications cannot be derived from the current series.

As most patients showed incomplete osseous integration at last follow-up, this leads to the question as to whether complete osseous integration can be achieved, and how long the latter would take. In this context, it is furthermore of interest if patient collectives can be identified that show trends of a delayed osseous integration of Cerasorb®. A detailed characterization of these patient collectives will be useful and required to allow final recommendations regarding the application of Cerasorb® in bone tumour patients. To answer these questions, studies observing larger and more homogeneous cohorts over a longer observation period will be required.

## 4.5 Conclusion

In conclusion, based on the present short-term observation, the beta-TCP Cerasorb® is a reliable bone graft substitute with low complication rates. It is a suitable alternative to autologous or allogenic bone grafts, even though there seems to be a tendency towards delayed osseous integration (1). Based on our findings, it can be safely applied in small osseous lesions with a diameter of less than 5 cm. However, our data suggest that protective plate osteosynthesis should be performed in bone defects exceeding 5 cm in their diameter, independent of tumour location in the upper or lower extremity. Final conclusions regarding the time interval to full osseous integration cannot be drawn based on the heterogeneity of our sample and the comparatively short observation period. Thus, final recommendations regarding the application of Cerasorb® in various subgroups of patients will require studies in larger, more homogeneous cohorts, and extended observation periods.

# REFERENCES


1. Wittig US, Friesenbichler J, Liegl-Atzwanger B, Igrec J, Andreou D, Leithner A, Scheipl S. Artificial bone graft substitutes for curettage of benign and low-grade malignant bone tumors: clinical and radiological experience with Cerasorb®. Indian J Orthop. 2023;57(9):1409-1414.

2. Ogilvie CM, Cheng EY. What's new in primary bone tumors. J Bone Joint Surg Am. 2016;98(24):2109-2113.

3. Choi JH, Ro JY. The 2020 WHO classification of tumours of bone: an updated review. Adv Anat Pathol. 2021;28(3):119-138.

4. WHO Classification of Tumours Editorial Board. Soft tissue and bone tumours. Lyon (France): International Agency for Research on Cancer; 2020.

5. Benna C, Simioni A, Pasquali S, et al. Genetic susceptibility to bone and soft tissue sarcomas: a field synopsis and meta-analysis. Oncotarget. 2018;9(26):18607-18626.

6. MacCarthy A, Bayne AM, Brownbill PA, et al. Second and subsequent tumours among 1927 retinoblastoma patients diagnosed in Britain 1951-2004. Br J Cancer. 2013;108(12):2455-2463.

7. Coindre JM, Terrier P, Guillou L, et al. Predictive value of grade for metastasis development in the main histologic types of adult soft tissue sarcomas: a study of 1240 patients from the French Federation of Cancer Centres Sarcoma Group. Cancer. 2001;91(10):1914-1926.

8. Neuville A, Chibon F, Coindre JM. Grading of soft tissue sarcomas: from histological to molecular assessment. Pathology. 2013;46(2):113-120.

9. Enneking WF, Spanier SS, Goodman MA. A system for the surgical staging of musculoskeletal sarcoma. Clin Orthop Relat Res. 1980;153:106-120.

10. Enneking WF. A system of staging musculoskeletal neoplasms. Clin Orthop Relat Res. 1986;204:9-24.

11. Morley N, Omar I. Imaging evaluation of musculoskeletal tumors. Cancer Treat Res. 2014;162:9-29.

12. Umer M, Hasan OHA, Khan D, Uddin N, Noordin S. Systematic approach to musculoskeletal benign tumors. Int J Surg Oncol (N Y). 2017;2(11):e46.

13. Widhe B, Widhe T. Initial symptoms and clinical features in osteosarcoma and Ewing sarcoma. J Bone J Surg Am. 2000;82(5):667-674.
14. Grimer RJ, Briggs TW. Earlier diagnosis of bone and soft-tissue tumours. J Bone Joint Surg Br. 2010;92(11):1489-1492.
15. Malhas AM, Grimer RJ, Abudu A, Carter SR, Tillman RM, Jeys L. The final diagnosis in patients with a suspected primary malignancy of bone. J Bone Joint Surg Br. 2011;93(7):980-983.
16. Adams SC, Potter BK, Mahmood Z, . Consequences and prevention of inadvertent internal fixation of primary osseous sarcomas. Clin Orthop Relat Res. 2009;467(2):519-525.
17. Costelloe CM, Madewell JE. Radiography in the initial diagnosis of primary bone tumors. AJR Am J Roentgenol. 2013;200(1):3-7.
18. Strauss SJ, Frezza AM, Abecassis N, et al. Bone sarcomas: ESMO - EURACAN - GENTURIS - ERN PaedCan Clinical Practice Guideline for diagnosis, treatment and follow-up. Ann Oncol. 2021;32(12):1520-1536.
19. Massengill AD, Seeger LL, Eckardt JJ. The role of plain radiography, computed tomography, and magnetic resonance imaging in sarcoma evaluation. Hematol Oncol Clin North Am. 1995;9(3):571-604.
20. Miller TT. Bone tumors and tumorlike conditions: analysis with conventional radiography. Radiology. 2008;246(3):662-674.
21. Nichols RE, Dixon LB. Radiographic analysis of solitary bone lesions. Radiol Clin North Am. 2011;49(6):1095-1114.
22. Lodwick GS, Wilson AJ, Farrell C, Virtama P, Dittrich F. Determining growth rates of focal lesions of bone from radiographs. Radiology. 1980;134(3):577-583.
23. Benndorf M, Bamberg F, Jungmann PM. The Lodwick classification for grading growth rate of lytic bone tumors: a decision tree approach. Skeletal Radiol. 2022;51(4):737-745.
24. Andreou D, Bielack SS, Carrle D, et al. The influence of tumor- and treatment-related factors on the development of local rrecurrence in osteosarcoma after adequate surgery. An analysis of 1355 patients treated on neoadjuvant Cooperative Osteosarcoma Study Group protocols. Ann Oncol. 2011;22(5):1228-1235.

25. Blay JY, Soibinet P, Penel N, et al. Improved survival using specialized multidisciplinary board in sarcoma patients. Ann Oncol. 2017;28(11):2852-2859.
26. Daley NA, Reed WJ, Peterson JJ. Strategies for biopsy of musculoskeletal tumors. Semin Roentgenol. 2017;52(4):282-290.
27. Singla A, Geller DS. Musculoskeletal tumors. Pediatr Clin North Am. 2020;67(1):227-245.
28. Muramatsu K, Ihara K, Taguchi T. Treatment of giant cell tumor of long bones: clinical outcome and reconstructive strategy for lower and upper limbs. Orthopedics. 2009;32(7):491.
29. WHO Classification of Tumours Editorial Board. Soft tissue and bone tumours. Lyon (France): International Agency for Research on Cancer; 2013.
30. Stomp W, Reijnierse M, Kloppenburg M, et al. Prevalence of cartilaginous tumours as an incidental finding on MRI of the knee. Eur Radiol. 2015;25(12):3480-3487.
31. Hakim DN, Pelly T, Kulendran M, Caris JA. Benign tumours of the bone: a review. J Bone Oncol. 2015;4(2):37-41.
32. Marco RA, Gitelis S, Brebach GT, Healey JH. Cartilage tumors: evaluation and treatment. J Am Acad Orthop Surg. 2000;8(5):292-304.
33. Pansuriya TC, van Eijk R, d'Adamo P, et al. Somatic mosaic IDH1 and IDH2 mutations are associated with enchondroma and spindle cell hemangioma in Ollier disease and Maffucci syndrome. Nat Genet. 2011;43(12):1256-1261.
34. Amary MF, Damato S, Halai D, et al. Ollier disease and Maffucci syndrome are caused by somatic mosaic mutations of IDH1 and IDH2. Nat Genet. 2011;43(12):1262-1265.
35. Damato S, Alorjani M, Bonar F, et al. IDH1 mutations are not found in cartilaginous tumours other than central and periosteal chondrosarcomas and enchondromas. Histopathology. 2012;60(2):363-365.
36. Venneker S, Kruisselbrink AB, Baranski Z, et al. Beyond the influence of IDH mutations: exploring epigenetic vulnerabilities in chondrosarcoma. Cancers (Basel). 2020;12(12):3589.
37. Suijker J, Baelde HJ, Roelofs H, et al. The oncometabolite D-2-hydroxyglutarate induced by mutant IDH1 or -2 blocks osteoblast differentiation in vitro and in vivo. Oncotarget. 2015;6(17):14832-14842.

38. Jin Y, Elalaf H, Watanabe M, et al. Mutant IDH1 dysregulates the differentiation of mesenchymal stem cells in association with gene-specific histone modifications to cartilage- and bone-related genes. PLoS One. 2015;10(7):e0131998.
39. Pansuriya TC, Kroon HM, Bovee JVMG. Enchondromatosis: insights on the different subtypes. Int J Clin Exp Pathol. 2010;3(6):557-569.
40. Flemming DJ, Murphey MD. Enchondroma and chondrosarcoma. Semin Musculoskelet Radiol. 2000;4(1):59-71.
41. Murphey MD, Flemming DJ, Boyea SR, Bojescul JA, Sweet DE, Temple HT. Enchondroma versus chondrosarcoma in the appendicular skeleton: differentiating features. Radiographics. 1998;18(5):1213-1237.
42. Choi BB, Jee WH, Sunwoo HJ, et al. MR differentiation of low-grade chondrosarcoma from enchondroma. Clin Imaging. 2013;37(3):542-547.
43. Altay M, Bayrakci K, Yildiz Y, Erekul S, Saglik Y. Secondary chondrosarcoma in cartilage bone tumors: report of 32 patients. J Orthop Sci. 2007;12(5):415-423.
44. Horvai A, Unni KK. Premalignant conditions of bone. J Orthop Sci. 2006;11(4):412-423.
45. Park HY, Joo MW, Choi YH, Chung YG, Park CJ. Simple curettage and allogeneic cancellous bone chip impaction grafting in solitary enchondroma of the short tubular bones of the hand. Sci Rep. 2023;13(1):2081.
46. Schaller P, Baer W. Operative treatment of enchondromas of the hand: is cancellous bone grafting necessary? Scand J Plast Reconstr Surg Hand Surg. 2009;43(5):279-285.
47. Morii T, Mochizuki K, Tajima T, Satomi K. Treatment outcome of enchondroma by simple curettage without augmentation. J Orthop Sci. 2010;15(1):112-117.
48. Crim J, Layfield LJ. Bone and soft tissue tumors at the borderlands of malignancy. Skeletal Radiol. 2023;52(3):379-392.
49. Crim J, Schmidt R, Layfield L, et al. Can imaging criteria distinguish enchondroma from grade 1 chondrosarcoma? Eur J Radiol. 2015;84(11):2222-2230.
50. Ferrer-Santacreu EM, Ortiz-Cruz EJ, González-López JM, et al. Enchondroma versus low-grade chondrosarcoma in appendicular skeleton: clinical and radiological criteria. J Oncol. 2012;2012:437958.

51. Bui KL, Illaslan H, Bauer TW, et al. Cortical scalloping and cortical penetration by small eccentric chondroid lesions in the long tubular bones: not a sign of malignancy? Skeletal Radiol. 2009;38(8):791-796.
52. Choi BB, Jee WH, Sunwoo HJ, et al. MR differentiation of low-grade chondrosarcoma from enchondroma. Clin Imaging. 2013;37(3):542-547.
53. Douis H, Singh L, Saifuddin A. MRI differentiation of low-grade from high-grade appendicular chondrosarcoma. Eur Radiol. 2014;24(1):232-240.
53. Engel H, Herget GW, Füllgraf H, et al. Chondrogenic bone tumors: the importance of imaging characteristics. Fortschr Röntgenstr. 2021;193:262-274.
54. Verdegaal SH, Bovée JV, Pansuriya TC, et al. Incidence, predictive factors, and prognosis of chondrosarcoma in patients with Ollier disease and Maffucci syndrome: an international multicenter study of 161 patients. Oncologist. 2011;16(12):1771-1779.
55. Gelderblom H, Hogendoorn PC, Dijkstra SD, et al. The clinical approach towards chondrosarcoma. Oncologist. 2008;13(3):320-329.
56. Pretell-Mazzini J, Murphy RF, Kushare I, Dormans JP. Unicameral bone cysts: general characteristics and management controversies. J Am Acad Orthop Surg. 2014;22(5):295-303.
57. Jordanov MI. The "rising bubble" sign: a new aid in the diagnosis of unicameral bone cysts. Skeletal Radiol. 2009;38(6):597-600.
58. Baumhoer D, Smida J, Nathrath M, et al. The nature of the characteristic cementum-like matrix deposits in the walls of simple bone cysts. Histopathology. 2011;59(3):390-396.
59. Mascard E, Gomez-Brouchet A, Lambot K. Bone cysts: unicameral and aneurysmal bone cyst. Orthop Traumatol Surg Res. 2015;101(1 Suppl):S119-127.
60. Rajasekaran RB, Krishnamoorthy V, Gulia A. Unicameral bone cysts: review of etiopathogenesis and current concepts in diagnosis and management. Indian J Orthop. 2022;56(5):741-751.
61. Noordin S, Allana S, Umer M, Jamil M, Hilal K, Uddin N. Unicameral bone cysts: current concepts. Ann Med Surg (Lond). 2018;34:43-49.
62. Gaillard F, Foster T, Knipe H, et al. Intraosseous ganglion. Reference article, Radiopaedia.org (Accessed on 07 Jun 2024).

63. Lao LF, Li QY, Zhong GB, Liu ZD. Intraosseous ganglion of the scaphoid: a case report and review of published reports. Orthop Surg. 2014;6(3):252-254.
64. Jamshidi K, Shooroki KK, Ata Sharifi Dalooei SM, Mirazei A. Intraosseous ganglion cyst of the talus treated with curettage and bone grafting through a medial malleolus osteotomy. Foot Ankle Int. 2023;44(2):118-124.
65. Lui TH. Endoscopic curettage and bone grafting of intraosseous ganglion of the second metatarsal. J Foot Ankle Surg. 2020;59(4):807-812.
66. Bancroft LW, Peterson JJ, Kransdorf MJ. Cysts, geodes, and erosions. Radiol Clin North Am. 2004;42(1):73-87.
67. Guitton TG, van Leerdam RH, Ring D. Necessity of routine pathological examination after surgical excision of wrist ganglions. J Hand Surg. 2010;35(6):905-908.
68. Bahk, WJ. Ganglion Cyst. In: Diagnosis and Management of Primary Bone Tumors. Springer, Singapore; 2023.
69. Buldu H, Kantarci U, Cepel S. Intraosseous ganglions at the same localization in twin sisters. Acta Orthop Traumatol Turc. 2009;43;379-380.
70. Büchler L, Hosalkar H, Weber M. Arthroscopically assisted removal of intraosseous ganglion cysts of the distal tibia. Clin Orthop Relat Res. 2009;467:2925-2931.
71. Sedeek SM, Choudry Q, Garg S. Intraosseous ganglion of the distal tibia: clinical, radiological, and operative management. Case Rep Orthop. 2015;2015:759257.
72. De Mattos CB, Angsanuntsukh C, Arkader A, Dormans JP. Chondroblastoma and chondromyxoid fibroma. J Am Acad Orthop Surg. 2013;21(4):225-233.
73. Ramappa AJ, Lee FY, Tang P, Carlson JR, Gebhardt MC, Mankin HJ. Chondroblastoma of bone. J Bone Joint Surg Am. 2000;82(8):1140-1145.
74. Suneja R, Grimer RJ, Belthur M, Jeys L, Carter SR, Tillman RM, Davies AM. Chondroblastoma of bone: long-term results and functional outcome after intralesional curettage. J Bone Joint Surg Br. 2005;87(7):974-978.
75. Weatherall PT, Maale GE, Mendelsohn DB, Sherry CS, Erdman WE, Pascoe HR. Chondroblastoma: classic and confusing appearance at MR imaging. Radiology. 1994;190(2):467-474.

76. De Silva MV, Reid R. Chondroblastoma: varied histologic appearance, potential diagnostic pitfalls, and clinicopathologic features associated with local recurrence. Ann Diagn Pathol. 2003;7(4):205-213.
77. Behjati S, Tarpey PS, Presneau N, et al. Distinct H3F3A and H3F3B driver mutations define chondroblastoma and giant cell tumor of bone. Nat Genet. 2013;45(12):1479-1482.
78. Baumhoer D, Amary F, Flanagan AM, et al. An update of molecular pathology of bone tumors. Lessons learned from investigating samples by next generation sequencing. Genes Chromosomes Cancer. 2019;58(2):88-99.
79. Presneau N, Baumhoer D, Behjati S, et al. Diagnostic value of H3F3A mutations in giant cell tumour of bone compared to osteoclast-rich mimics. J Pathol Clin Res. 2015;1(2):113-123.
80. Rybak LD, Rosenthal DI, Wittig JC. Chondroblastoma: radiofrequency ablation-alternative to surgical resection in selected cases. Radiology. 2009;251(2):599-604.
81. Bertin H, Moussa MS, Komarova S. Efficacy of antiresorptive agents in fibrous dysplasia and McCune-Albright syndrome, a systematic review and meta-analysis. Rev Endocr Metab Disord. 2023;24(6):1103-1119.
82. Lietman SA, Levine MA. Fibrous dysplasia. Pediatr Endocrinol Rev PER. 2013;10(Suppl 2):389-396.
83. MacDonald-Jankowski D. Fibrous dysplasia: a systematic review. Dentomaxillofac Radiol. 2009;38(4):196-215.
84. Javaid MK, Boyce A, Appelman-Dijkstra N, et al. Best practice management guidelines for fibrous dysplasia/McCune-Albright syndrome: a consensus statement from the FD/MAS international consortium. Orphanet J Rare Dis. 2019;14(1):139.
85. Riminucci M, Collins MT, Fedarko NS, et al. FGF-23 in fibrous dysplasia of bone and its relationship to renal phosphate wasting. J Clin Invest. 2003;112(5):683-692.
86. Hart ES, Kelly MH, Brillante B, et al. Onset, progression, and plateau of skeletal lesions in fibrous dysplasia and the relationship to functional outcome. J Bone Miner Res. 2007;22(9):1468-1474.
87. Burke AB, Collins MT, Boyce AM. Fibrous dysplasia of bone: craniofacial and dental implications. Oral Dis. 2017;23(6):697-708.

88. Parekh SG, Donthineni-Rao R, Ricchetti E, Lackman RD. Fibrous dysplasia. J Am Acad Orthop Surg. 2004;12:305-313.
89. Boyce AM, Collins MT. Fibrous dysplasia/McCune-Albright syndrome: a rare, mosaic disease of Gα s activation. Endocr Rev. 2020;41:345-370.
90. Jour G, Oultache A, Sadowska J, et al. GNAS mutations in fibrous dysplasia: a comparative study of standard sequencing and locked nucleic acid PCR sequencing on decalcified and nondecalcified formalin-fixed paraffin-embedded tissues. Appl Immunohistochem Mol Morphol. 2016;24(9):660-667.
91. Lee SE, Lee EH, Park H, et al. The diagnostic utility of the GNAS mutation in patients with fibrous dysplasia: meta-analysis of 168 sporadic cases. Hum Pathol. 2012;43(8):1234-1242.
92. De Castro LF, Burke AB, Wang HD, et al. Activation of RANK/RANKL/OPG pathway is involved in the pathophysiology of fibrous dysplasia and associated with disease burden. J Bone Miner Res. 2019;34(2):290-294.
93. Riminucci M, Kuznetsov SA, Cherman N, Corsi A, Bianco P, Gehron RP. Osteoclastogenesis in fibrous dysplasia of bone: in situ and in vitro analysis of IL-6 expression. Bone. 2003;33:434-442.
94. Takeuchi T, Yoshida H, Tanaka S. Role of interleukin-6 in bone destruction and bone repair in rheumatoid arthritis. Autoimmun Rev. 2021;20:102884.
95. Guille JT, Kumar SJ, MacEwen GD. Fibrous dysplasia of the proximal part of the femur: long-term results of curettage and bone-grafting and mechanical realignment. J Bone Joint Surg Am. 1998;80:648-658.
96. Enneking WF, Gearen PF. Fibrous dysplasia of the femoral neck: treatment by cortical bone-grafting. J Bone Joint Surg Am. 1986;68:1415-1422.
97. Wang Y, Wang O, Jiang Y, Li M, Xia W, Meng X, Xing X. Efficacy and safety of biphosphonate therapy in McCune-Albright syndrome-related polyostotic fibrous dysplasia: A single-center experience. Endocr Pr. 2019;25(1):23-30.
98. Boyce AM, Kelly MH, Brillante BA, et al. A randomized, double blind, placebo-controlled trial of alendronate treatment for fibrous dysplasia of bone. J Clin Endocrinol Metab. 2014; 99(11):4133-4140.
99. Chapurlat R, Legrand MA. Biphosphonates for the treatment of fibrous dysplasia of bone. Bone. 2021;143:115784.

100. Florenzano P, Pan KS, Brown SM, et al. Age-related changes and the effect of biphosphonates on bone turnover and disease progression in fibrous dysplasia of bone. J Bone Min Res. 2018;34(4):653-660.
101. Majoor BCJ, Papapoulos SE, Sander Dijkstra PD, Fiocco M, Hamdy NAT, Appelman-Dijkstra NM. Denosumab in patients with fibrous dysplasia previously treated with bisphosphonates. J Clin Endocrinol Metab. 2019;104(12):6069-6078.
102. De Castro LF, Michel Z, Pan K, et al. Safety and efficacy of denosumab for fibrous dysplasia of bone. N Engl J Med. 2023;388(8):766-768.
103. Grana N. Langerhans cell histiocytosis. Cancer Control. 2014;21(4):328-334.
104. DiCaprio MR, Roberts TT. Diagnosis and management of Langerhans cell histiocytosis. J Am Acad Orthop Surg. 2014;22(10):643-652.
105. Allen CE, Merad M, McClain KL. Langerhans-cell histiocytosis. N Engl J Med. 2018;379(9):856-868.
106. Khung S, Budzik JF, Amzallag-Bellenger E, Lambilliote A, Soto Ares G, Cotten A, Boutry N. Skeletal involvement in Langerhans cell histiocytosis. Insights Imaging. 2013;4(5):569-579.
107. Huang WD, Yang XH, Wu ZP, et al. Langerhans cell histiocytosis of spine: a comparative study of clinical, imaging features, and diagnosis in children, adolescents, and adults. Spine J. 2013;13(9):1108-1117.
108. Girschikofsky M, Arico M, Castillo D, et al. Management of adult patients with Langerhans cell histiocytosis: recommendations from an expert panel on behalf of Euro-Histo-Net. Orphanet J Rare Dis. 2013;8(1):72.
109. Haupt R, Minkov M, Astigarraga I, et al. Langerhans cell histiocytosis (LCH): guidelines for diagnosis, clinical work-up, and treatment for patients till the age of 18 years. Pediatr Blood Cancer. 2013;60(2):175-184.
110. Filipovich A, McClain K, Grom A. Histiocytic disorders: recent insights into pathophysiology and practical guidelines. Biol Blood Marrow Transplant. 2010;16(1 suppl):S82-S89.
111. Clarke BE. Cystic lung disease. J Clin Pathol. 2013;66(10):904-908.
112. Khung S, Budzik JF, Amzallag-Bellenger E, Lambilliote A, Soto Ares G, Cotten A, Boutry N. Skeletal involvement in Langerhans cell histiocytosis. Insights Imaging. 2013;4(5):569-579.

113. Goyal G, Tazi A, Go RS, et al. International expert consensus recommendations for the diagnosis and treatment of Langerhans cell histiocytosis in adults. Blood. 2022;139(17):2601-2621.
114. Gulati N, Allen CE. Langerhans cell histiocytosis: Version 2021. Hematol Oncol. 2021;39 Suppl 1(Suppl 1):15-23.
115. Alayed K, Medeiros LJ, Patel KP, et al. BRAF and MAP2K1 mutations in Langerhans cell histiocytosis: a study of 50 cases. Hum Pathol. 2016;52:61-67.
116. Rollins BJ. Genomic alterations in Langerhans cell histiocytosis. Hematol Oncol Clin North Am. 2015;29(5):839-851.
117. Héritier S, Emile JF, Barkaoui MA, et al. BRAF mutation correlates with high-risk Langerhans cell histiocytosis and increased resistance to first-line therapy. J Clin Oncol. 2016;34(25):3023-3030.
118. Berres ML, Lim KP, Peters T, et al. BRAF-V600E expression in precursor versus differentiated dendritic cells defines clinically distinct LCH risk groups. J Exp Med. 2014;211(4):669-683.
119. Kriz J, Eich HT, Bruns F, et al. Radiotherapy in Langerhans cell histiocytosis: a rare indication in a rare disease. Radiat Oncol. 2013;8(1):233.
120. Kotecha R, Venkatramani R, Jubran RF, Arkader A, Olch AJ, Wong K. Clinical outcomes of radiation therapy in the management of Langerhans cell histiocytosis. Am J Clin Oncol. 2014;37(6):592-596.
121. Gadner H, Minkov M, Grois N, et al. Therapy prolongation improves outcome in multisystem Langerhans cell histiocytosis. Blood. 2013;121(25):5006-5014.
122. Minkov M, Grois N, Heitger A, et al. Response to initial treatment of multisystem Langerhans cell histiocytosis: an important prognostic indicator. Med Pediatr Oncol. 2002;39(6):581-585.
123. Emile JF, Abla O, Fraitag S, et al. Revised classification of histiocytoses and neoplasms of the macrophage-dendritic cell lineages. Blood. 2016;127(22):2672-2681.
124. Mosheimer BA, Oppl B, Zandieh S, et al. Bone involvement in Rosai-Dorfman disease (RDD): a case report and systematic literature review. Curr Rheumatol Rep. 2017;19(5):29.

125. Bist SS, Varshney S, Bisht M, Pathak VP, Kusum A, Gupta N. Rosai Dorfman syndrome - a rare clinical entity. Indian J Otolaryngol Head Neck Surg. 2007;59(2):184-186.
126. Foucar E, Rosai J, Dorfman RF. Sinus histiocytosis with massive lymphadenopathy (Rosai Dorfman disease): Review of entity. Semin Diagn Pathol. 1990;7:19-73.
127. Goodnight JW, Wang MB, Sercarz JA, Fu YS. Extranodal Rosai Dorfman disease of the head and neck. Laryngoscope. 1996;106:253-256.
128. Demicco EG, Rosenberg AE, Björnsson J, et al. Primary Rosai-Dorfman disease of bone: a clinicopathologic study of 15 cases. Am J Surg Pathol. 2010;34(9):1324-1333.
129. Cai Y, Shi Z, Bai Y. Review of Rosai-Dorfman disease: new insights into the pathogenesis of this rare disorder. Acta Haematol. 2017;138(1):14-23.
130. Abla O, Jacobsen E, Picarsic J, et al. Consensus recommendations for the diagnosis and clinical management of Rosai-Dorfman-Destombes disease. Blood. 2018;131(26):2877-2890.
131. Fatobene G, Haroche J, Hélias-Rodzwicz Z, et al. BRAF V600E mutation detected in a case of Rosai-Dorfman disease. Haematologica. 2018;103(8):e377-379.
132. Richardson TE, Wachsmann M, Oliver D, et al. BRAF mutation leading to central nervous system Rosai-Dorfman disease. Ann Neurol. 84(1):147-152.
133. Foucar E, Rosai J, Dorfman RF. Sinus histiocytosis with massive lymphadenopathy. An analysis of 14 deaths occurring in a patient registry. Cancer. 1984;54:1834-1840.
134. Komp DM. The treatment of sinus histiocytosis with massive lymphadenopathy (Rosai Dorfman disease). Semin Diagn Pathol. 1990;7:83-86.
135. Friesenbichler J, Maurer-Ertl W, Sadoghi P, Pirker-Fruehauf U, Bodo K, Leithner A. Adverse reactions of artificial bone graft substitutes: lessons learned from using tricalcium phosphate geneX(R). Clin Orthop Relat Res. 2014;472(3):976-982.
136. Van Hoff C, Samora JB, Griesser MJ, Crist MK, Scharschmidt TJ, Mayerson JL. Effectiveness of ultraporous beta-tricalcium phosphate (vitoss) as bone graft substitute for cavitary defects in benign and low-grade malignant bone tumors. Am J Orthop. 2012;41(1):20-23.

137. Migliorini F, Cuozzo F, Torsiello E, Spiezia F, Oliva F, Maffulli N. Autologous bone grafting in trauma and orthopaedic surgery: an evidence-based narrative review. J Clin Med. 2021;10(19):4347.
138. Bauer TW, Muschler GF. Bone graft materials. An overview of the basic science. Clin Orthop Relat Res. 2000;371:10-27.
139. Baldwin P, Li DJ, Auston DA, Mir HS, Yoon RS, Koval KJ. Autograft, allograft and bone graft substitutes: clinical evidence and indications for use in the setting of orthopaedic trauma surgery. J Orthop Trauma. 2019;33:203-213.
140. Calori GM, Colombo M, Mazza EL, Mazzola S, Malagoli E, Mineo GV. Incidence of donor site morbidity following harvesting from iliac crest or RIA graft. Injury. 2014;45:S116-S120.
141. Ahlmann E, Patzakis M, Roidis N, Sheperd L, Holtom P. Comparison of anterior and posterior iliac crest bone grafts in terms of harvest-site morbidity and functional outcomes. J Bone Joint Surg Am. 2002;84:716-720.
142. Dimitriou R, Mataliotakis GI, Angoules AG, Kanakaris NK, Giannoudis PV. Complications following autologous bone graft harvesting from the iliac crest and using the RIA: a systematic review. Injury. 2011;42:S3-S15.
143. Marchand LS, Rothberg DL, Kubiak EN, Higgins TF. Is this autograft worth it? The blood loss and transfusion rates associated with reamer irrigator aspirator bone graft harvest. J Orthop Trauma. 2017;31:205-209.
144. Finkemeier CG. Bone-grafting and bone-graft substitutes. J Bone Joint Surg Am. 2002;84:454-464.
145. Myeroff C, Archdeacon M. Autogenous bone graft: donor sites and techniques. J Bone Joint Surg Am. 2011;93:2227-2236.
146. Asmus A, Vogel K, Vogel A, Eichenauer F, Kim S, Eisenschenk A. Pedicled vascularized iliac bone graft for treatment of osteonecrosis of the femoral head. Oper Orthop Traumatol. 2020;32:127-138.
147. Costain DJ, Crawford RW. Fresh-frozen vs. irradiated allograft bone in orthopaedic reconstructive surgery. Injury. 2009;40:1260-1264.
148. Vokov MV, Imamaliyev AS. Use of allogenous articular bone implants as substitutes for autotransplants in adult patients. Clin Orthop Relat Res. 1976;114:192-202.

149. Stevenson S, Li XQ, Martin B. The fate of cancellous and cortical bone after transplantation of fresh and frozen tissue-antigen-matched and mismatched osteochondral allografts in dogs. J Bone Joint Surg Am. 1991;73:1143-1156.
150. Stevenson S. The immune response to osteochondral allografts in dogs. J Bone Joint Surg Am. 1987;69:573-582.
151. Pelker RR, McKay Jr J, Troiano N, Panjabi MM, Friedlaender GE. Allograft incorporation: a biomechanical evaluation in a rat model. J Orthop Res. 1989;7:585-589.
152. Mankin HJ, Hornicek FJ, Raskin KA. Infection in massive bone allografts. Clin Orthop Relat Res. 2005;432:210-216.
153. Zamborsky R, Svec A, Bohac M, Kilian M, Kokavec M. Infection in bone allograft transplants. Exp Clin Transplant. 2016;14(5):484-490.
154. Dziedzic-Goclawska A, Kaminski A, Uhrynowska-Tyszkeiwicz I, Stachowicz W. Irradiation as a safety procedure in tissue banking. Cell Tissue Bank. 2005;6:201-219.
155. Hannink G, Schreurs BW, Buma P. Irradiation has no effect on the incorporation of impacted morselized bone. A bone chamber study in goats. Acta Orthop. 2007;78:31-38.
156. Evaniew N, Tan V, Parasu N, et al. Use of a calcium sulfate-calcium phosphate synthetic bone graft composite in the surgical management of primary bone tumors. Orthopedics. 2014;36(2):e216-222.
157. Johnson LJ, Clayer M. Aqueous calcium sulphate as bone graft for voids following open curettage of bone tumours. ANZ J Surg. 2013;83(7-8):564-570.
158. Kelly CM, Wilkins RM. Treatment of benign bone lesions with an injectable calcium sulfate-based bone graft substitute. Orthopedics. 2004;27(1 Suppl):s131-135.
159. Liu B, Lun DX. Current application of β-tricalcium phosphate composites in orthopaedics. Orthop Surg. 2012;4(3):139-144.
160. Saadoun S, Macdonald C, Bell BA, Papadopoulos MC. Dangers of bone graft substitutes: lessons from using GeneX. J Neurol Neurosurg Psychiatry. 2011;82(8):e3.
161. Lobb DC, DeGeorge Jr BR, Chhabra AB. Bone graft substitutes: current concepts and future expectations. J Hand Surg Am. 2019;44(6):497-505.e2.
162. Shah AM, Jung H, Skirboll S. Materials used in cranioplasty: a history and analysis. Neurosurg Focus. 2014;36(4):E19.

163. Pietrzak WS, Ronk R. Calcium sulfate bone void filler: a review and a look ahead. J Craniofac Surg. 2000;11(4):327-333.
164. Koepp HE, Schorlemmer S, Kessler S, et al. Biocompatibility and osseointegration of beta-TCP: histomorphological and biomechanical studies in a weight-bearing sheep model. J Biomed Mater Res. 2014;70(2):209-217.
165. Xin R, Leng Y, Chen J, Zhang Q. A comparative study of calcium phosphate formation on bioceramics in vitro and in vivo. Biomaterials. 2005;26(33):6477-6486.
166. Horch HH, Sader R, Pautke C, Neff A, Deppe H, Kolk A. Synthetic, pure-phase beta-tricalcium phosphate ceramic granules (Cerasorb®) for bone regeneration in the reconstructive surgery of the jaws. Int J Oral Maxillofac Surg. 2006;35(8):708-713.
167. Fini M, Giavaresi G, Nicoli Aldini N, et al. A bone substitute composed of polymethylmethacrylate and alpha-tricalcium phosphate: results in terms of osteoblast function and bone tissue formation. Biomaterials. 2002;23(23):4523-4531.
168. Zerbo IR, Bronckers AL, De Lange G, Burger EH. Localisation of osteogenic and osteoclastic cells in porous beta-tricalcium phosphate particles used for human maxillary sinus floor elevation. Biomaterials. 2005;26(12):1445-1451.
169. Kaczmarczyk J, Sowinski P, Goch M, Katulska K. Complete twelve month bone remodeling with a bi-phasic injectable bone substitute in benign bone tumors: a prospective pilot study. BMC Musculosket Disord. 2015;16:369.
170. Cho HS, Seo SH, Park SH, Park JH, Shin DS, Park IH. Minimal invasive surgery for unicameral bone cyst using demineralized bone matrix: a case series. BMC Musculoskelet Disord. 2012;13:134.
171. Goslings JC, Gouma DJ. What is a surgical complication? World J Surg. 2008;32:952.
172. Hirn M, de Silva U, Sidharthan S, Grimer RJ, Abudu A, Tillman RM, Carter SR. Bone defects following curettage do not necessarily need augmentation. Acta Orthop. 2009; 80(1):4-8.
173. Kundu ZS, Gupta V, Sangwan SS, Rana P. Curettage of benign bone tumors and tumor like lesions: a retrospective analysis. Indian J Orthop. 2013;47(3):295-301.
174. Perisano C, Barone C, Stomeo D, Di Giacomo G, Vasso M, Schiavone Panni A, Maccauro G. Indications for prophylactic osteosynthesis associated with curettage in

benign and low-grade malignant primitive bone tumors of the distal femur in adult patients: a case series. J Orthopaed Traumatol. 2016;17(4):377-382.
175. Bokan I, Bill JS, Schlagenhauf U. Primary flap closure combined with Emdogain® alone or Emdogain® and Cerasorb® in the treatment of intra-bony defects. J Clin Periodontol. 2006;33:885-893.
176. Hernigou P, Dubory A, Pariat J, et al. Beta-tricalcium phosphate for orthopedic reconstructions as an alternative to autogenous bone graft. Morphologie. 2017;101(334):173-179.
177. Hirata M, Murata H, Takeshita H, Sakabe T, Tsuji Y, Kubo T. Use of purified beta-tricalcium phosphate for filling defects after curettage of benign bone tumours. Int Orthop 2006;30(6):510-513.
178. Friesenbichler J, Maurer-Ertl W, Bergovec M, Holzer LA, Ogris K, Leitner L, Leithner A. Clinical experience with the artificial bone graft substitute Calcibon used following curettage of benign and low-grade malignant bone tumors. Sci Rep. 2017;7(1):1736.
179. Chao B, Jiao J, Yang L, et al. Comprehensive evaluation and advanced modification of polymethylmethacrylate cement in bone tumor treatment. J Mater Chem B. 2023;11(39):9369-9385.
180. Beall DP, Phillips TR. Vertebral augmentation: an overview. Skeletal Radiol. 2023;52(10):1911-1920.
181. Yang HL, Zhu XS, Chen L, Chen CM, Mangham DC, Coulton LA, Aiken SS. Bone healing response to a synthetic calcium sulfate/β-tricalcium phosphate graft material in a sheep vertebral body defect model. J Biomed Mater Res B Appl Biomater. 2012;100(7):1911-1921.
182. Harimtepathip P, Callaway LF, Sinkler MA, Sharma S, Homlar KC. Progressive osteolysis after use of synthetic bone graft substitute. Cureus. 2021;13(11):e20002.
183. Multani I, Schneider P, Baldawi H, Deheshi B, Ghert M. Long-term follow-up of the use of a synthetic bone graft composite in the surgical management of primary bone tumors. Orthopedics. 2018;41(6):e868-e875.
184. Razii N, Docherty LM, Halai M, Mahendra A, Gupta S. Injectable synthetic beta-tricalcium phosphate/calcium sulfate (GeneX) for the management of contained

defects following curettage of benign bone tumours. Curr Oncol. 2023;30(4):3697-3707.
185. Evaniew N, Tan V, Parasu N, et al. Use of a calcium sulfate-calcium phosphate synthetic bone graft composite in the surgical management of primary bone tumors. Orthopedics. 2013;36(2):e216-222.
186. Johnson LJ, Clayer M. Aqueous calcium sulphate as bone graft for voids following open curettage of bone tumours. ANZ J Surg. 2013;83/7-8):564-570.
187. Yang Y, Niu X, Zhang Q, Hao L, Ding Y, Xu H. A comparative study of calcium sulfate artificial bone graft versus allograft in the reconstruction of bone defect after tumor curettage. Chin Med J (Engl). 2014;127(17):3092-3097.
188. Hagel A, Zeh A, Hein W, Held A, Wohlrab D. Comparison of anterior lumbar fusion rates after circumferential fusion using β-tricalcium phosphate (Cerasorb®) versus autologous iliac crest spongiosa. Z Orthop Unfall. 2007;145:488-492.
189. Szabó G, Huys L, Coulthard P, Maiorana C, et al. A prospective multicenter randomized clinical trial of autogenous bone versus beta-tricalcium phosphate graft alone for bilateral sinus elevation: histologic and histomorphometric evaluation. Int J Oral Maxillofac Implants. 2005;20(3):371-381.
190. Lerner T, Bullmann V, Schulter TL, Schneider M, Liljenqvist U. A level-1 pilot study to evaluate of ultraporous β-tricalcium phosphate as a graft extender in the posterior correction of adolescent idiopathic scoliosis. Eur J Spine. 2009;18:170-179.
191. Zheng H, Bai Y, Shih MS, Hoffmann C, Peters F, Waldner C, Hübner WD. Effect of a beta-TCP collagen composite bone substitute on healing of drilled bone voids in the distal femoral condyle of rabbits. J Biomed Mater Res B Appl Biomater. 2014;102(2):376-383.